# JOURNAL OF APPLIED PHYSICS

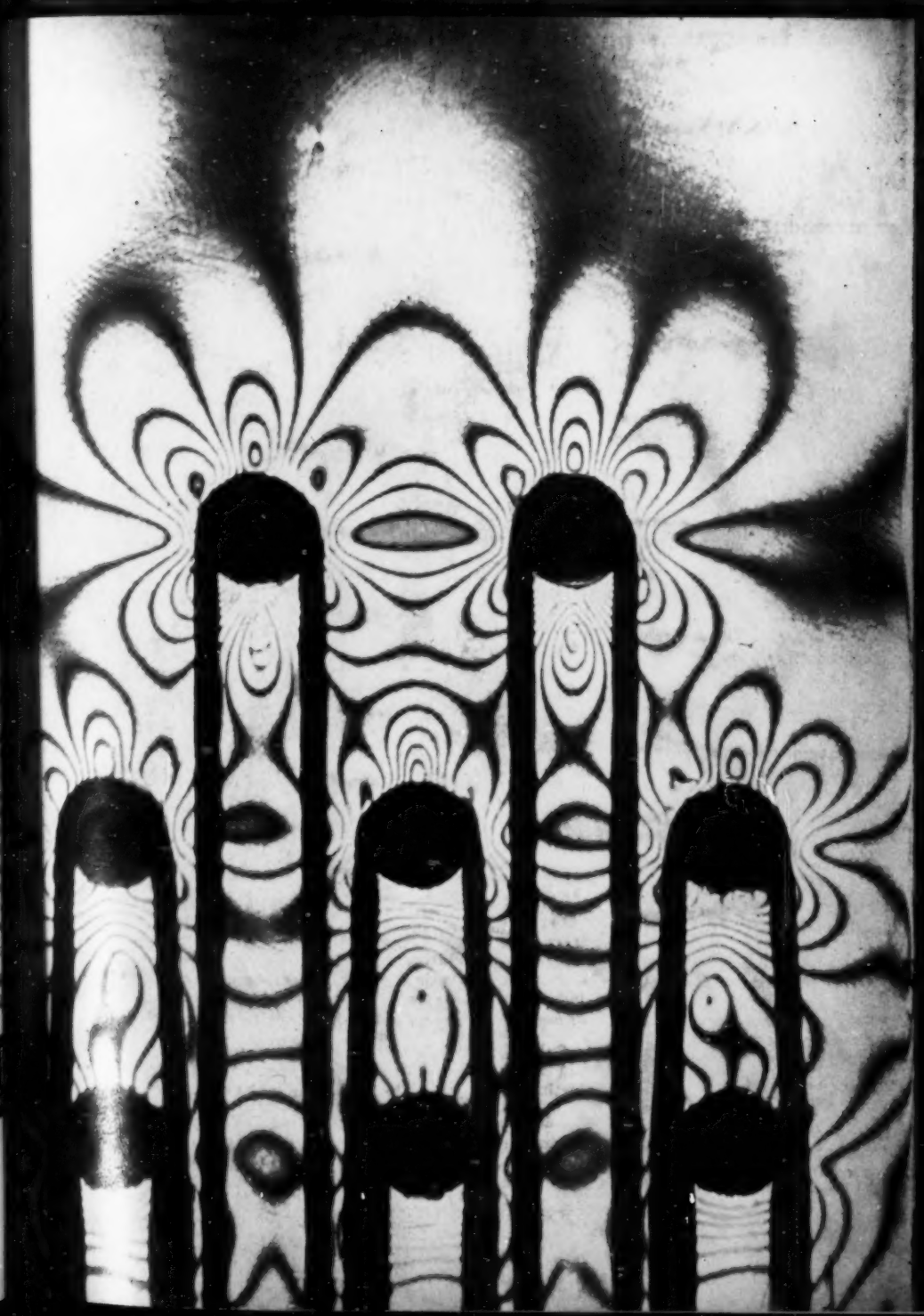

APRIL
1939
Vol. 10 No.

JOURNAL OF APPLIED

# PHYSICS

APRIL, 1939 Vol. 10, No. 4

## *In This Issue*

*Page*

**Deeper Understanding Needed** THE EDITOR 207

**Survey of Crystal Optics. With Emphasis on the Parts Finding Application in Photoelasticity** JOSEPH VALASEK 209

**Review of the Photoelastic Method of Stress Analysis. I** RAYMOND D. MINDLIN 222

**Direct Optical Measurement of Individual Principal Stresses** J. H. A. BRAHTZ AND J. E. SOEHRENS 242

**Isopachic Stress Patterns** MAX M. FROCHT 248

**Operational Calculus. II.** LOUIS A. PIPES 258

### *In Every Issue*

**Resumes of Recent Research** 265

**Letter to the Editor** 266

**Here and There** 267

**New Books** 269

**Contributors to this Issue** 270

**Innovations in Instruments** viii

**Recent Booklets on Instruments and Materials** xii

**Index to Advertisers** xvi

**BOARD OF EDITORS**

ELMER HUTCHISSON, *Editor*

*Associate Editors*

F. BITTER
W. E. FORSYTHE
L. A. JONES
W. F. MEGGERS
B. E. WARREN
J. B. WHITEHEAD
V. K. ZWORYKIN

**Publication of the American Institute of Physics**

**ADMINISTRATIVE STAFF**

HENRY A. BARTON, *Director*

MADELINE M. MITCHELL, *Publications Manager*

WILLIAM C. COPP, *Advertising Manager*

**GOVERNING BOARD**

JOHN T. TATE, *Chairman*
KARL T. COMPTON
E. C. CRITTENDEN
WHEELER P. DAVEY
FLOYD A. FIRESTONE
HARVEY FLETCHER
ARTHUR C. HARDY
PAUL E. KLOPSTEG
MELVIN MOONEY
FREDERIC PALMER, JR.
R. L. PEEK, JR.
GEORGE B. PEGRAM
W. B. RAYTON
F. K. RICHTMYER
WALLACE WATERFALL

THE JOURNAL OF APPLIED PHYSICS, published monthly at Prince and Lemon Sts., Lancaster, Pa., is devoted to physics in its role as the science basic to other natural sciences and to the arts and industries. Previous to 1937 this publication was known as PHYSICS. It aims to be of service not only in physical laboratories, but also in the laboratories of industrial, chemical, geological, geophysical, meteorological, radio, and similar concerns. THE JOURNAL OF APPLIED PHYSICS publishes editorials, news of physicists and reviews, as well as technical papers of applied physics.

SUBSCRIPTION PRICE

| | U. S., POSS. AND CANADA | FOREIGN |
|---|---|---|
| To members of scientific societies | $5.00 | $5.70 |
| To all others | 7.00 | 7.70 |

**Manuscripts** should be submitted to Elmer Hutchisson, Editor, University of Pittsburgh, Pittsburgh, Pennsylvania.

**Changes of address,** proofs, and complaints of failure to receive the JOURNAL OF APPLIED PHYSICS should be addressed to the Publications Manager. New copies can be sent free only if notice of nondelivery is received within three months of date of issue.

**Subscriptions** and orders for back numbers should be addressed to Prince and Lemon Streets, Lancaster, Pa. or to the American Institute of Physics, 175 Fifth Avenue, New York, N. Y.

**Advertising rates** supplied on request. Orders, advertising copy and cuts should be sent to the American Institute of Physics.

Entered as second class matter at the Post Office at Lancaster, Pennsylvania, under the Act of March 3, 1897. Accepted for mailing at the special rate of postage provided for in the Act of February 28, 1925, authorized May 2, 1932.

Copyright 1939, by the American Institute of Physics.

| DATE | RESISTANCE AT 25°C | % CHANGE FROM ORIGINAL VALUE |
|---|---|---|
| 2-24-19 | 100.004 | −.001 |
| 12-10-19 | 100.003 | −.002 |
| 11-15-20 | 100.003 | −.002 |
| 5-12-21 | 100.003 | −.002 |
| 2-17-22 | 100.003 | −.002 |
| 1-10-23 | 100.003 | −.002 |
| 7-14-23 | 100.003 | −.002 |
| 8-29-24 | 100.004 | −.001 |
| 10- 1-25 | 100.003$_5$ | −.001$_6$ |
| 2- 9-27 | 100.003$_2$ | −.001$_8$ |
| 3-26-28 | 100.003$_5$ | −.001$_6$ |
| 4- 9-29 | 100.002$_8$ | −.002$_4$ |
| 8-16-30 | 100.003$_2$ | −.001$_8$ |
| 8-28-31 | 100.003$_5$ | −.001$_5$ |
| 11-20-32 | 100.003$_1$ | −.001$_9$ |
| 1- 3-33 | 100.003$_4$ | −.001$_6$ |
| 3-10-34 | 100.003$_2$ | −.001$_8$ |
| 4- 5-35 | 100.003$_6$ | −.001$_5$ |
| 4-24-36 | 100.003$_6$ | −.001$_4$ |
| 4- 8-37 | 100.003$_5$ | −.001$_5$ |
| 5-10-38 | 100.003$_5$ | −.001$_5$ |

# 19 YEAR RECORD OF A REFERENCE STANDARD OF RESISTANCE

Typical of the constancy with which these NBS Type Standards hold their resistance is our Laboratory Tool No. 357. Used as a reference standard against which our working standards are compared, it is sent to the National Bureau of Standards about once a year for checking. Only once in the last 21 checks listed above has its resistance varied more than 2 one-thousandths of one per cent. In the last eight years, it has varied over a range of *only 5 ten-thousandths of one per cent.*

The performance of this resistor, which for the last eight years has maintained a constancy of 20 times the guaranteed limit of error, is representative. All these NBS Type Standards hold their initial resistance to well within the guaranteed limit of error and, if checked regularly, can be used for even finer work than the guaranteed limits would indicate. Traditional L&N workmanship assures long service . . . permits full advantage to be taken of the increasing stability of resistance which accompanies age.

***Write for Catalog E-53***

**LEEDS & NORTHRUP COMPANY, 4978 STENTON AVE., PHILA., PA.**

**LEEDS & NORTHRUP**

**MEASURING INSTRUMENTS · TELEMETERS · AUTOMATIC CONTROLS · HEAT-TREATING FURNACES**

Jrl Ad 4-53(2)

# PHOTOELASTICITY POLARISCOPES

*for*
*Stress Analysis*

**Strain Free Optics • Large Nicol Prisms • Clear Undistorted Images**
**For use with Camera or Projection Screen • Sodium, Mercury, or Carbon Arc, or Tungsten Lamp**

***Descriptive Bulletin on Request***

## THE GAERTNER SCIENTIFIC CORPORATION

**1212 WRIGHTWOOD AVENUE • CHICAGO • U. S. A.**

*Two Proven Texts in Physical Science*

## Survey of Physical Science for College Students

**By Paul McCorkle, Ph.D., Professor of Physics and Physical Science, State Teachers College, West Chester, Pa.**

273 Illus. 471 Pages. Washable Fabric $2.75

This text is intended for a three hour year course for freshmen. It presents the subject with clarity and definiteness avoiding extended philosophical discussions. Laboratory experiments are provided at the end of each chapter, suitable for classroom demonstration or for individual laboratory work.

## The Physical World

**By L. M. Heil, Ph.D., Associate Professor of Education, University of Chicago.**

426 Illus. 566 Pages. Washable Fabric $2.75

This book was prepared for college students who desire some knowledge of physical science but do not intend to major in science. It combines physics, chemistry and astronomy into a one-year course emphasizing physics. The clear, concise style and diction, and the large number of illustrations are genuinely helpful in establishing fundamental principles.

**P. Blakiston's Son & Co., Inc. Philadelphia**

*At* POLYTECHNIC INSTITUTE OF BROOKLYN

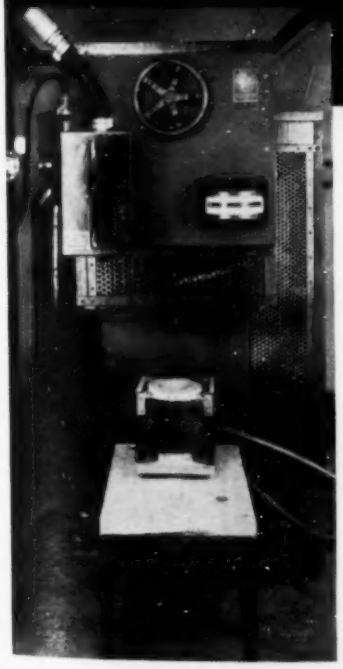

# AJAX-NORTHRUP FURNACES

"We have used our Ajax induction furnace for making high sulphur, high silicate and high manganese alloy steels. Also to experiment with the effect of numerous fluxing agents on the fluidity of metals and alloys. An interesting accessory to the induction furnace has been developed in which the metal may be melted and cast under vacuum.

"The furnace has also been used in a number of instances by Seniors in connection with their theses work; also to produce alloys, the structural properties of which were subsequently studied under the microscope."

AJAX ELECTROTHERMIC CORPORATION

AJAX PARK
TRENTON, N. J.

AJ-14-B

IRC RESISTORS

FOR HIGH FREQUENCIES

*Rating from ½ Watt to 10 KW. (Water-Cooled)*

Makers of Resistance Units of More Types in More Shapes for More Applications than Any Other Manufacturer in the World. Catalog of any type sent on request.

The superior high frequency characteristics of IRC Type F and MP Metallized Resistors are a natural consequence of the design and structure of the resistors:

1. *The ceramic base is the best low loss material available.*
2. *The resistance coating is a homogeneous thin film*
3. *The specific resistance of the coating is high.*
4. *The capacitance between terminals is very low, less than ½ uuf.*

As a result, these units have proved satisfactory for use up to 200 megacycles, depending upon value of the resistor. Standard units now available from stock. Special units utilizing these same proved principles can be made to order.

*Write for IRC High Frequency Engineering Data Bulletin II.*

INTERNATIONAL RESISTANCE COMPANY

419 NORTH BROAD STREET, PHILADELPHIA, PENNA.

*from* 0.1 gram to 1110 grams

WITH THE WELCH 4040 BALANCE

greater capacity :: more accuracy :: acute sensibility

*Special folder sent on request*

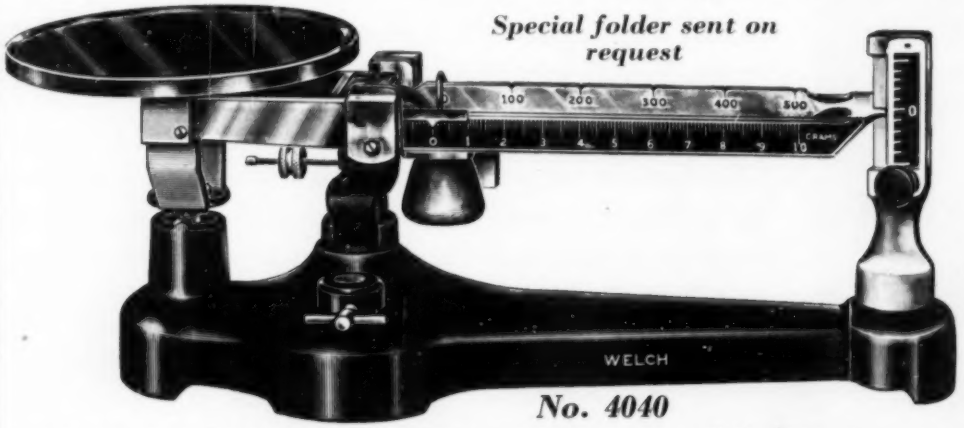


*No. 4040*

*Catalogue lists over 10,000 items for science laboratories*

*Write for it.*

W. M. Welch Scientific Company

Established 1880

1515 Sedgwick Street Chicago, Illinois, U.S.A.

WELCH

# *Important* McGRAW-HILL *BOOKS*

## *Smith's* ELEMENTS OF PHYSICS

By ALPHEUS W. SMITH, Ohio State University. *Fourth edition.* 775 pages, 6 x 9. $3.75

The new edition of this outstanding textbook shows a sustained record of adoption which again places it in the position of leadership it has held for so long. Teachers comment particularly on the way in which the author utilizes the wide range of familiar things to illustrate essential principles. Other well-liked features are the wealth of excellent illustrations and the unusually large amount of problem material.

## *Burington and Torrance's* HIGHER MATHEMATICS. With Applications to Science and Engineering

By RICHARD S. BURINGTON and CHARLES C. TORRANCE, Case School of Applied Science. 838 pages, 6 x 9. $5.00

Designed primarily to meet the growing needs of students interested in the applications of mathematics to physics and engineering, this new book emphasizes physical meanings of the various notations and relationships encountered in the subject. The precise mathematical nterpretations of the concepts studied here have also been stressed.

i

## *Frank's* INTRODUCTION TO MECHANICS AND HEAT. *New second edition*

By NATHANIEL H. FRANK, Massachusetts Institute of Technology. 382 pages, 6 x 9. $3.00

As before, the author of this text gives a systematic elementary treatment of the fundamentals of mechanics and heat, characterized by a close-knit structure and a logical, unified presentation. In the revision the material has been rearranged to make the exposition clearer and more useful from the standpoint of the teacher. The chapters on Kinematics of Linear Motion and Statics of Elasticity have been completely rewritten, and a large number of new problems has been added.

## *Reich*—THEORY AND APPLICATIONS OF ELECTRON TUBES

By HERBERT J. REICH, University of Illinois. 670 pages, 6 x 9. $5.00

The purpose of this book is to give the student a sufficiently thorough grounding in the fundamental principles of electron tubes and associated circuits to enable him to apply electron tubes to the solution of new problems. The book is exceptionally complete, including a wealth of material assembled and coordinated in a uniquely logical presentation.

## *Harnwell*—PRINCIPLES OF ELECTRICITY AND ELECTROMAGNETISM

By GAYLORD P. HARNWELL, University of Pennsylvania. *International Series in Physics.* 619 pages, 6 x 9. $5.00

This text, designed for advanced undergraduate or graduate instruction, emphasizes the experimental and scientific rather than the mathematical or engineering aspects of the subject. Vector notation is used and a unification is achieved by the consistent use of absolute practical units and the electromagnetic approach to magnetism.

***Send for copies on approval***

## McGRAW-HILL BOOK COMPANY, Inc.

330 West 42nd Street New York, N. Y.

# A HIGHLY EFFICIENT SOURCE OF ULTRA-VIOLET RADIATION

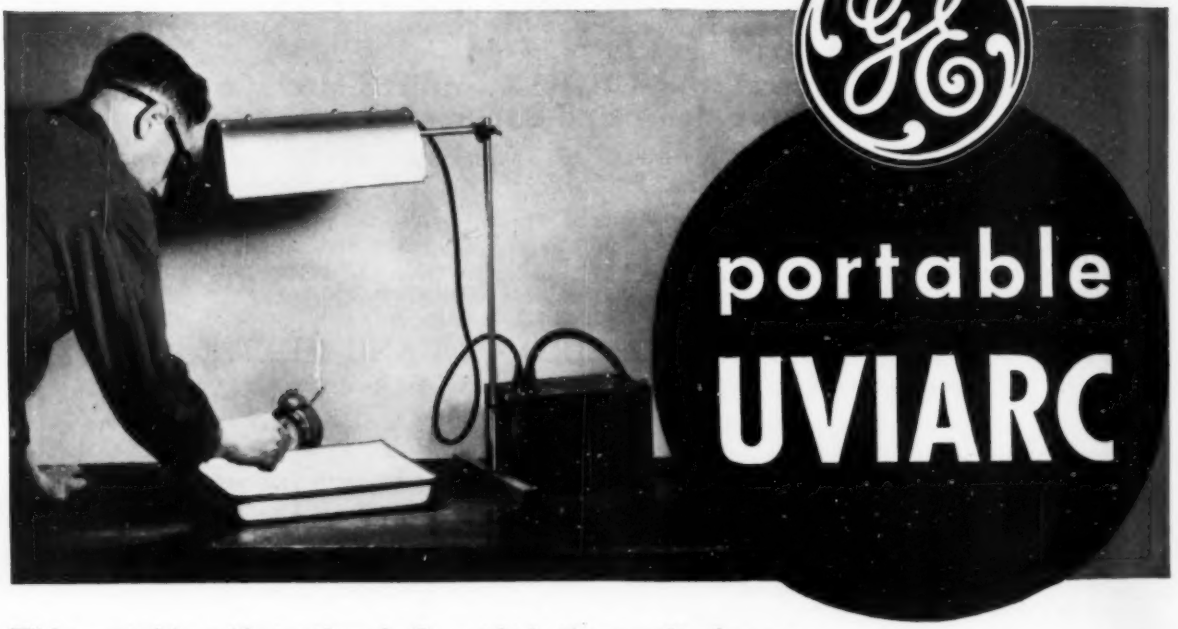


This portable self-starting A. C. outfit is the result of years of experience with mercury-pool cathode quartz lamps. The Uviarc utilizes the same "hot cathode" construction responsible for the efficiency and dependability of General Electric Type H lamps which are widely used throughout industry. » » » The reflector hood concentrates the radiation of the Uviarc within a 90° angle and is designed to accommodate standard 6½ x 6½ in. filters. The outfit draws 410 watts from 115 or 220 volt 60 cycle supply. Full efficiency is obtained in a vertical, horizontal or angular position. » » » Write for a copy of descriptive bulletin. General Electric Vapor Lamp Co., 835 Adams Street, Hoboken, New Jersey.

*Radiation characteristics, spectral analysis and other technical and mechanical data are contained in this Uviarc bulletin.*

**GENERAL ELECTRIC VAPOR LAMP COMPANY**

930U

HARVARD COLLEGE
APR 5 1939
LIBRARY

Journal of Applied

Physics

Volume 10 April, 1939 Number 4

# Deeper Understanding Needed

AS TIME goes on civilization demands more and more from the engineer. As competition increases, the engineer must produce stronger and better materials; he must know better how stresses are distributed; by improved design he must economize on material and weight, and yet with all this there must be no lessening in the degree of safety. There is only one way for the engineer to meet these increased demands—that is in the acquisition of a deeper understanding of the laws of nature. The days of the so-called "handbook engineer" are already past. The good engineer of the future must not only be thoroughly trained in mathematics, physics and engineering but he must also have a wide knowledge and keen appreciation of the results of modern scientific research.

The kindling of a spark of appreciation for research must take place in colleges. Colleges should provide themselves with teachers who themselves are taking part in the continuous transformation of delicate laboratory processes and techniques into rugged engineering practice. Such men will be able to instill into students that feeling for research which will make leaders in the engineering fields.

This plea for more teachers in our colleges who are actually engaged in the making of the engineering of tomorrow is really a plea for more emphasis on applied physics. For instance, no more effective way of helping students visualize the stresses in beams exists than by the use of the methods of photoelasticity. As the student studies the cause of the colorful interference patterns produced with polarized light he gains respect for the powerful tool which physicists have placed in the hands of the engineer. As he compares the mathematical analysis of the stress distribution in relatively simple cases with the observed patterns obtained with polarized light he gains an increased respect for the fundamental reasoning which is the basis of modern engineering. Engineers trained by such methods will really have a deeper understanding of the laws of nature and will be able to meet better the increasing demands of civilization.

*For May*

*A New Million-Volt X-Ray Outfit by* E. E. CHARLTON, W. F. WESTENDROP, L. E. DEMPSTER and G. HOTALING

*A Review of the Photoelastic Method of Stress Analysis, II, by* R. D. MINDLIN

*Operational Calculus, III, by* L. A. PIPES

*The Application of Hardening Resins in Three-Dimensional Photoelastic Studies, by* M. HETENYI

*Physics of Flames and Explosions of Gases, by* B. LEWIS and G. VON ELBE

*Physics and Geologic Structures, by* M. DOBRIN

*Original Research Papers*

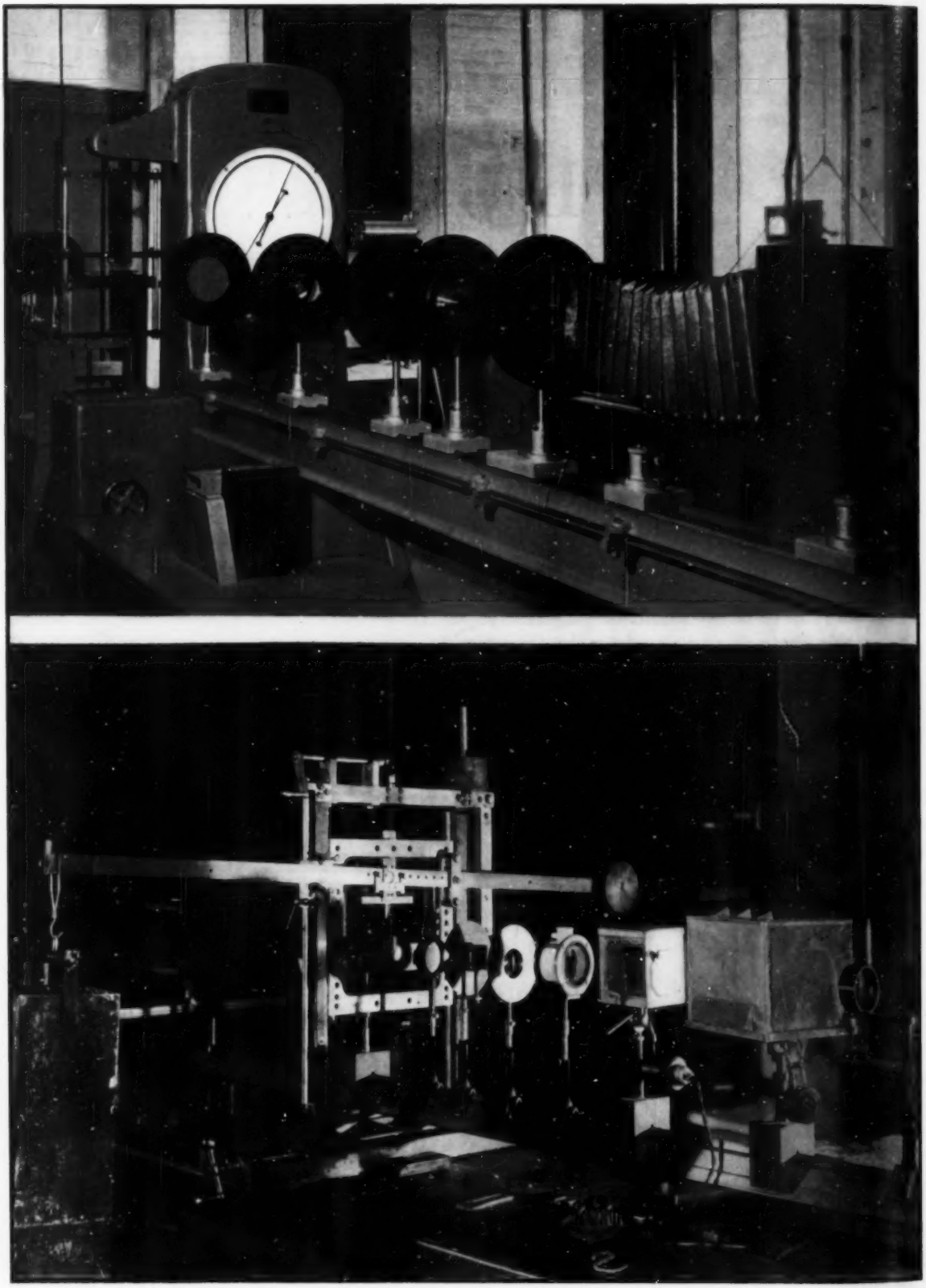

Typical photoelastic installations. The upper photograph is from Cornell University and the lower one is from the Carnegie Institute of Technology. (For complete description see paper by R. Mindlin, page 222.)

# A Survey of Crystal Optics

## With Emphasis on the Parts Finding Application in Photoelasticity

BY JOSEPH VALASEK

*Department of Physics, University of Minnesota, Minneapolis, Minnesota*

WHILE it is impossible to present any simple physical picture of the nature of light, there is no doubt that the propagation of light resembles that of transverse waves. That is to say, the laws of reflection, refraction, interference, diffraction and polarization are formally the same as those for any other kind of transverse wave. The waves one assumes to represent light are electromagnetic in character, since light is certainly one member of a family of radiations which includes long waves from oscillating circuits, as well as waves of much shorter period. The greatly different nature of the interaction of these waves with matter is largely due to the enormous range of frequencies in the electromagnetic spectrum. This interaction can be represented by optical constants which will be defined in this paper but which it will not be necessary to analyze. The electromagnetic theory of light is not only completely adequate for the purpose of this discussion, but also provides the simplest approach to the subject.

A wave is characterized by its amplitude, period or frequency, and state of polarization. The equation for a simple harmonic, plane wave may be written in the form:

$$s = s_0 \sin\left[\frac{2\pi}{T}\left(t - \frac{lx+my+nz}{V}\right)+\epsilon\right].$$

In practice one can never obtain one simple harmonic plane wave, but it can be approximated, and actual waves can always be represented as a sum of such waves. The amplitude $s_0$ may be identified with either the electric field, the dielectric displacement, or the magnetic field. The dielectric displacement is equal to the electric field plus $4\pi$ times the polarization, the latter quantity being the electric dipole moment per cubic centimeter. Usually the dielectric displacement is chosen as the light vector for then the equations for light propagation inside a crystal have the same form as those first given by Fresnel. In free space, and in isotropic media, the dielectric displacement is not only proportional to the electric field but is in the same direction. In these cases the equations for light propagation have the same form regardless of the choice of light vector. It is in such media that the waves are finally observed.

A plane wave of ordinary light may be resolved into a superposition of numerous elementary wave trains having the above form, in which $s_0$ assumes all possible directions normal to the direction of propagation. If however, the vector $s_0$ remains constantly in one plane, the light is said to be plane-polarized. The plane of polarization is defined as the plane perpendicular to the dielectric displacement. This plane is being gradually replaced in the literature by the vibration plane which contains the light vector. It should be noted that the vibrations, like any vector, may always be resolved into two orthogonal components having an orientation most convenient for the problem being discussed. If the light is unpolarized, they will always be equal, while if it is polarized, they will be sine and cosine components of the light vector.

The quantity $T$ in the above equation is the period, or time for one complete oscillation at any given point. Its reciprocal is the frequency, or number of vibrations per second, and it is related to the wave-length by the equation $\lambda = VT$, where $V$ is the velocity of propagation of the wave. Since $V$ depends on the transmitting medium, while $T$ does not, the wave-length corresponding to any color will also depend on the medium. Hence whenever colors are designated by their wave-length, the transmitting medium should also be specified. If this is not given, it is assumed that the wave-length is measured in free space. Since the velocity of

light in air is only 0.03 percent smaller than in free space, the wave-length in air will likewise be that much smaller, and the difference, being very small, may frequently be neglected. The visible spectrum extends from about 3800A to 7600A in wave-length, where $1A=10^{-8}$ cm. The human eye is most sensitive to a wave-length of 5550A which may be taken as the effective wave-length of white light. For purposes of exact optical measurements, light of as nearly a single wave-length as possible must be used. Such light may be obtained from sodium or mercury vapor lamps with the use of filters to remove the undesired spectrum lines. The wave-lengths used most frequently are: mercury 5461A, and sodium 5893A, a green and a yellow line, respectively.

The quantity

$$\frac{2\pi}{T}\left(t-\frac{lx+my+nz}{V}\right)+\epsilon$$

is called the phase of the wave. The locus of points in $xyz$ space at which the phase is constant is called a wave front. In this case it is a plane $lx+my+nz=$a constant, the values of $l$, $m$ and $n$ being the cosines of the angles made by the wave normal with the $x$, $y$ and $z$ axes, respectively. The quantity $V$ is the velocity of advance of the wave in the direction of its normal, as can be readily seen by considering the ratio of the distance of propagation to the corresponding change in time for any given value of the phase. The phase constant, $\epsilon$, is only needed when one has to compare the phases of two waves, for otherwise one may merely change the time origin and incorporate $\epsilon$ within $t$.

When $V$ is independent of the direction of the light vector $s_0$, the medium is said to be isotropic. The wave fronts are then at right angles to the direction of energy flow which is defined as the light ray. The ordinary laws of refraction hold when light passes from one such medium into another. The rays and wave normals all lie in the plane of incidence defined by the normal to the surface and the normal to the incident wave. The angles $\phi_1$ and $\phi_2$ that the wave normals in the two media make with the normal to the surface are related by the equation:

$$\frac{\sin\phi_1}{\sin\phi_2}=\frac{V_1}{V_2}=\text{a constant},$$

which is known as Snell's law. The constant is called the index of refraction of the second medium with respect to the first and is equal to the ratio of $n_2/n_1$, where $n_2$ and $n_1$ are the indices of refraction of the two media with respect to a vacuum.

When $V$ depends on the direction of the light vector, the medium is said to be anisotropic. Such media are crystals, with the exception of those belonging to the cubic system, all transparent media subjected to stresses, and colloidal materials with oriented fibrous or lamellar micelles. The materials in the second group are of especial interest in photoelasticity. The laws of propagation of light in such materials will provide the major part of the following discussion.

The properties of these materials are usually studied by means of interference effects observed in polarized light. Interference phenomena result from the mere superposition of two waves, each traveling as if the other one were not present. Thus the resultant wave is the simple sum:

$$s=s_1+s_2=A_1\sin\left[\frac{2\pi}{T}\left(t-\frac{d_1}{V_1}\right)+\epsilon_1\right]+A_2\sin\left[\frac{2\pi}{T}\left(t-\frac{d_2}{V_2}\right)+\epsilon_2\right],$$

in which it is assumed that $A_1$ and $A_2$ are in the same plane. By expanding these expressions and collecting terms, the result can be put in the form:

$$s=A\sin\left(\frac{2\pi}{T}t-\delta\right),$$

where $A^2=A_1^2+A_2^2+2A_1A_2\cos\Delta$, in which $\Delta$ is the phase difference:

$$\Delta=\frac{2\pi}{T}\left(\frac{d_1}{V_1}-\frac{d_2}{V_2}\right)+(\epsilon_2-\epsilon_1)=\frac{2\pi}{\lambda}(n_1d_1-n_2d_2)+(\epsilon_2-\epsilon_1).$$

The expression $n_1d_1-n_2d_2$ is the difference in optical path measured along the two wave normals. Frequently the two values of $d$ are practically the same and one may then write the path difference in the form $(n_1-n_2)d$. When

the two waves are from different sources, or even from different points in the same source, the phase constants $\epsilon_1$ and $\epsilon_2$ change very frequently by arbitrary amounts and the waves are said to be not coherent. In this case one can only observe the time average of $A^2$ which is equal to $A_1^2+A_2^2$. Since the intensities of all kinds of waves are proportional to the square of their amplitudes, this result shows that the resultant intensity is just the sum of the two individual intensities. It will be convenient to consider the constant of proportionality between the square of the amplitude and the intensity to be unity, as it will be if one uses appropriate units.

If the cross product in the expression for $A^2$ is not to average out, the two waves must preserve a constant phase difference at all times, that is to say, the waves must be coherent. In the case of light, such coherent waves are only obtained by the division of a single wave into two parts which are reunited after traveling along paths which differ by the amount $(n_1-n_2)d$. The difference between the phase constants $\epsilon_1$ and $\epsilon_2$ will be either 0 or $\pi$ in all cases in which we are interested. The union of such coherent waves will produce amplitudes, and therefore intensities, which depend greatly and in a characteristic manner, on the value of $\Delta$. In particular, the intensity will be greatest when $\Delta$ is some integral multiple of $2\pi$ and will in this case be even greater than the sum of the two separate intensities, since:

$$A^2=A_1^2+A_2^2+2A_1A_2.$$

In this case the resulting amplitude is the simple sum of $A_1$ and $A_2$. On the other hand, when $\Delta=(m+\frac{1}{2})2\pi$, one finds that

$$A^2=A_1^2+A_2^2-2A_1A_2,$$

the amplitude being the difference between $A_1$ and $A_2$. Now the intensity is less than the sum of the separate intensities, but the average intensity in the two cases is still equal to the sum of the two intensities. In all interference phenomena there are regions in which there is an excess of energy and others where there is a deficiency, but of such an amount that the total energy is conserved. There is no absorption of light necessarily associated with interference.

The specific cases given above are just those for which the intensity has a maximum or a minimum value. Intermediate results are included in the original formula for $A^2$, the value of which may also be found by a vector diagram which is suggested by the similarity of the formula to the cosine law of trigonometry. The results apply to unpolarized light as well as to light which is polarized in a single plane. The combination of two waves with their vibration planes at right angles to each other will be discussed after the topic of double refraction.

Anisotropic media are those in which the speed and direction of propagation depend on the direction of vibration of the light vector. These exhibit the phenomenon of double refraction first observed by Bartolinus in 1669, which consists of the separation of any incident ray of light into two refracted rays. The laws of double refraction are derivable from a study of the propagation of light waves inside a crystal.

For a given direction of the light vector inside the crystal there is only one possible direction of propagation and a single corresponding wave speed. The equation for this wave velocity is:

$$L^2a^2+M^2b^2+N^2c^2=V^2.$$

The quantities $a$, $b$ and $c$, are the principal wave velocities in three mutually perpendicular directions in which the ray direction coincides with the wave normal or in which the dielectric displacement is in the same direction as the field strength. This is the definition of the principal crystal axes. The quantities $L$, $M$ and $N$, are the cosines of the angles made by the light vector, the dielectric displacement, with these three respective axes. The polar coordinate plot of $V$ as a function of direction gives a cartesian ovaloid, which is called the polarization ovaloid. The principal axes of this three-dimensional figure are $a$, $b$ and $c$, and it is customary to let $a$ represent the largest, and $c$ the smallest of the three principal wave velocities. Any anisotropic medium has three corresponding principal indices, $\alpha$, $\beta$ and $\gamma$, which are equal to the quotient of the velocity of light in space and the respective principal velocities. In terms of the principal indices, the above equation becomes:

$$\frac{L^2}{\alpha^2}+\frac{M^2}{\beta^2}+\frac{N^2}{\gamma^2}=\frac{1}{n^2},$$

where $n$ is the index of refraction of the material for the direction of the light vector given by $L$, $M$ and $N$. When $n$ is plotted in polar coordinates one obtains an ellipsoid which is called the index ellipsoid.

For any given direction of the wave normal defined by the direction cosines $l$, $m$ and $n$, there are two possible vibration directions in the crystal which are perpendicular to each other. The corresponding speeds are given by the semi-major and semi-minor axes of the oval resulting from the intersection of the polarization ovaloid

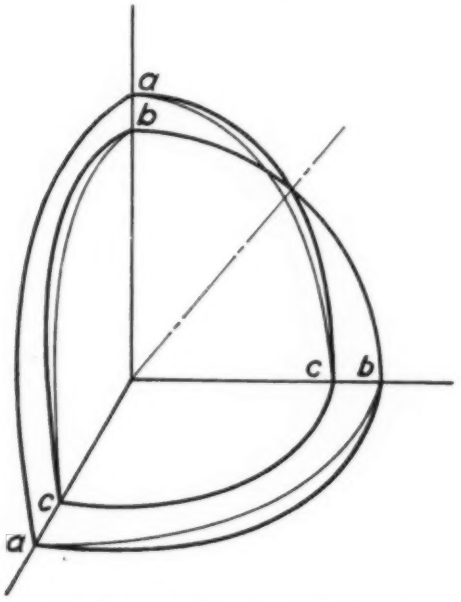


FIG. 1. The heavy outline describes the wave normal velocity surface. The curves represent circles and ovals with radii and axes indicated. To describe the ray velocity surface, the finer lines, ellipses, replace the adjacent ovals, the remainder of the figure being the same.

by the plane wave front passing through the origin. This gives two velocities corresponding to any wave normal which, plotted in polar coordinates, give a surface of two sheets. The equation of this double surface was first given by Fresnel and has the form:

$$\frac{l^2}{a^2-V^2}+\frac{m^2}{b^2-V^2}+\frac{n^2}{c^2-V^2}=0.$$

The heavy lines in Fig. 1 show the intersections of this surface with the coordinate planes. The curves are circles and ovals with radii and semi-axes given by the principal wave velocities as indicated. There are two directions of equal wave velocity in the $yz$ plane and these are called the optic axes. This so-called wave velocity surface describes the velocity relations for the general case of a biaxial anisotropic material. When $a\neq b=c$ there is only one optic axis and the material is said to be negatively uniaxial. Then there is one spherical wave velocity surface which lies wholly within an ovaloid of revolution whose semi-minor axis is equal to the radius of the sphere. Calcite is a familiar example of a negative uniaxial crystal. Most materials become negatively uniaxial when subjected to a compression, the optic axis being in the direction of the force. When $a=b\neq c$ the substance is said to be positively uniaxial, the best known example being quartz. Biaxial materials are frequently termed positive or negative according to which of these cases they approach most closely. When $a=b=c$ the substance is isotropic and there is no double refraction, the ordinary laws of refraction applying as in amorphous materials, glasses, liquids and cubic crystals.

The above discussion in terms of wave velocities is easily translated into one in terms of indices of refraction. It is only necessary to replace each velocity by the reciprocal of the corresponding index of refraction. In the graphical representation, circles remain circles, but ovals become ellipses and vice versa.

Rays of light are defined as the directions of the energy flow. In the electromagnetic theory, this is given by the direction of Poynting's vector: $(c/4\pi)E\times H$, which is at right angles to both $E$ and $H$, the electric and magnetic fields. The relation between the directions of $E$, $H$, $D$, the wave normal $N$, and the light ray $S$ is shown in Fig. 2. The dielectric displacement $D$ is the light vector and represents the direction of the vibrations in a wave of plane-polarized light. The wave normal $N$ is at right angles to both $D$ and $H$. The light ray $S$ is at right angles to $E$ and $H$, but makes some angle $\xi$ with $N$ whenever the direction of the dielectric displacement does not coincide with the direction of the electric field in the crystal. Since the principal axial system is defined in terms of such a coincidence, the directions of $D$ and $E$, and of $N$ and $S$ will be the same when light is traveling in these special directions.

The two possible wave velocities which correspond to a given direction of the wave normal,

$l, m, n$, are conveniently expressed in terms of the quantities defined by the following set of equations:

$$I=l^2(b^2+c^2); \quad J=m^2(c^2+a^2); \quad K=n^2(a^2+b^2);$$
$$R=l^2(b^2-c^2); \quad S=m^2(c^2-a^2); \quad T=n^2(a^2-b^2).$$

The two values of $V$ can then be obtained from:

$$2V^2=I+J+K\pm(R+S-T)^2-4RS.$$

Equations from which the wave velocities are sometimes more readily calculated are obtained if one expresses the above result in terms of the angles $g_1$ and $g_2$ which the wave normal makes with the two optic axes. The positive directions of these axes are chosen as those which make an acute angle with the positive direction of the $z$ axis. Their direction cosines are:

$$l_1=+\left(\frac{a^2-b^2}{a^2-c^2}\right)^{\frac{1}{2}}; \quad m_1=0; \quad n_1=+\left(\frac{b^2-c^2}{a^2-c^2}\right)^{\frac{1}{2}}$$

and

$$l_2=-\left(\frac{a^2-b^2}{a^2-c^2}\right)^{\frac{1}{2}}; \quad m_2=0; \quad n_2=+\left(\frac{b^2-c^2}{a^2-c^2}\right)^{\frac{1}{2}}.$$

The angles between the wave normal $l, m, n$, and

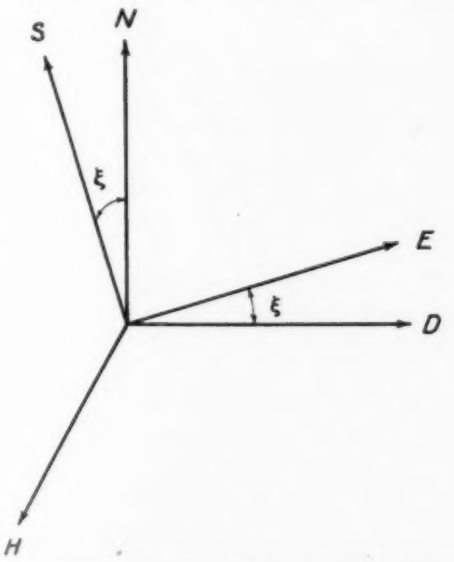


FIG. 2. The wave normal $N$ is perpendicular to the dielectric displacement $D$ and to the magnetic field $H$. The ray direction $S$ makes an angle $\xi$ with $N$ and is normal to the electric field $E$ and to $H$.

these axes are then given by the usual equations:

$$\cos g_1=ll_1+mm_1+nn_1$$

and

$$\cos g_2=ll_2+mm_2+nn_2.$$

In terms of these angles the two roots of the wave velocity equation are:

$$2V_1^2=(a^2+c^2)+(a^2-c^2)\cos(g_1-g_2)$$
$$2V_2^2=(a^2+c^2)+(a^2-c^2)\cos(g_1+g_2).$$

By replacing velocities by reciprocals of indices of

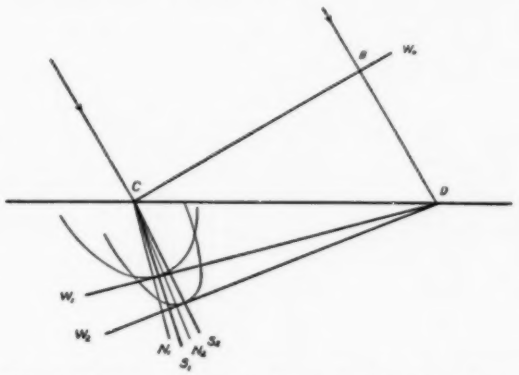


FIG. 3. Huygens' principle is applied to the refraction of a plane wave at a biaxial crystal. $W_0$ is the incident wave, $W_1$ and $W_2$ are the two refracted waves, whose normals are $N_1$ and $N_2$. The corresponding rays are $S_1$ and $S_2$.

refraction, one obtains the corresponding equations for the two indices of refraction associated with a given wave normal.

To each of the two values of $V$ there will correspond only one direction of the light vector, $D$. The two sets of direction cosines are given by the ratios:

$$L_1 : M_1 : N_1=\frac{l}{a^2-V_1^2} : \frac{m}{b^2-V_1^2} : \frac{n}{c^2-V_1^2}$$

and

$$L_2 : M_2 : N_2=\frac{l}{a^2-V_2^2} : \frac{m}{b^2-V_2^2} : \frac{n}{c^2-V_2^2}.$$

The exact values of $L, M, N$, are found with the aid of the requirement that $L^2+M^2+N^2=1$. It can be readily proved that the two vibration directions are at right angles to each other. In the case of uniaxial substances one of them is in the plane of the wave normal and the optic axis while the other is at right angles to this so-called principal plane. In the case of biaxial materials, the wave normal defines a plane with each optic axis. In this case the $D$ vibrations lie in the two bisecting planes. These planes also contain the rays which correspond to the respective vibrations. It should be noted that these statements and equations apply only to the propagation of

light wholly inside an anisotropic medium. Thus the two values of $V$ and their associated vibration directions and light rays are in general not the two observed when light passes from air into the medium, for in the general case of double refraction by a crystal there are obtained two waves of different $l$, $m$ and $n$. In the above discussion it is assumed that the same wave normal applies to both waves. In the case of passage of light from one medium to another, this is only true if the angle of incidence is zero.

It was noted before that the directions of energy flux, the light rays, are in general not the same as the wave normals. It will therefore be necessary to distinguish between the velocity of propagation of light in the direction of the ray, $U$, from the normal velocity of the wave, $V$, the relation being $U = V/\cos \xi$, where $\xi$ is the angle between the light ray and the wave normal. The ray velocity associated with any given wave velocity is accordingly always greater than the latter, still, strangely enough, when one plots $U$ on the same polar diagram as $V$, the former surface lies within, or at most touches the latter. The equation for $U$ as a function of the direction cosines of the ray, $f$, $g$ and $h$, is as follows:

$$\frac{f^2}{1/a^2-1/U^2}+\frac{g^2}{1/b^2-1/U^2}+\frac{h^2}{1/c^2-1/U^2}=0.$$

The surface described by this equation is qualitatively very similar to the wave velocity surface but the ovals are replaced by ellipses, the light lines in Fig. 1. Accordingly, it has the same shape as the index surface.

The ray velocity surface is of particular importance in that it gives a picture of the manner in which light spreads out in all directions from a point inside a crystal. Thus it gives the form of the Huygens' wavelets in an anisotropic medium and its principal use is in the determination of the reflected and refracted rays and waves resulting from the passage of light through an interface between two media where one or both of them is anisotropic.

The application of Huygens' principle to the general case of oblique refraction at the surface of a biaxial substance is illustrated in Fig. 3. The wavelet from the point $C$ spreads out as shown during the time that the incident wave is traveling from $B$ to $D$. The incident wave is assumed to be perpendicular to the paper. The two refracted waves are also perpendicular to the paper, or plane of incidence, and are respectively tangent to the two sheets of the wave surface. The corresponding wave normals $N_1$ and $N_2$ lie in the plane of incidence. The two rays are found by drawing lines from the point $C$ to the points of tangency of the two refracted waves with the wave surface. In general the rays will not lie in the plane of incidence, though it is impossible to show this in a two-dimensional diagram. If the refracted wave is traveling in the direction of an optic axis in the crystal, it will touch the outer wave surface at an infinite number of points lying on a circle around one of the depressions in the wave surface. There will then be an infinite number of refracted rays lying on a cone and because of this the phenomenon is called internal conical refraction.

In photoelastic and many other studies it is customary to have the light strike the surface perpendicularly. This always results in two refracted waves whose normals coincide and are also normal to the surface. The rays, however, may be at various angles with the normal.

If there exist any special relations between the principal velocities $a$, $b$ and $c$, this fact simplifies the problem. If any two of the principal velocities are equal, the wave surface consists of a sphere and a spheroid which are tangent to each other at two points which define the direction of the single optic axis. The spheroid is prolate or oblate depending on whether the crystal is positively or negatively uniaxial.

Two applications of Huygens' principle to refraction at the interface between an isotropic and a uniaxial material are shown in Fig. 4. The optic axis is assumed to lie in the plane of incidence. The directions of the rays are given by the lines from $C$ to the points of tangency, and the wave normals $N_e$ and $N_o$ are by definition the perpendiculars to the two waves. The ray and wave normal belonging to the wave determined by the spherical wavelet coincide. For this wave the same laws of refraction hold as for isotropic media, and for this reason the corresponding ray is called the ordinary ray though it is polarized. The other, extraordinary, ray is not in the direction of the corresponding wave normal and

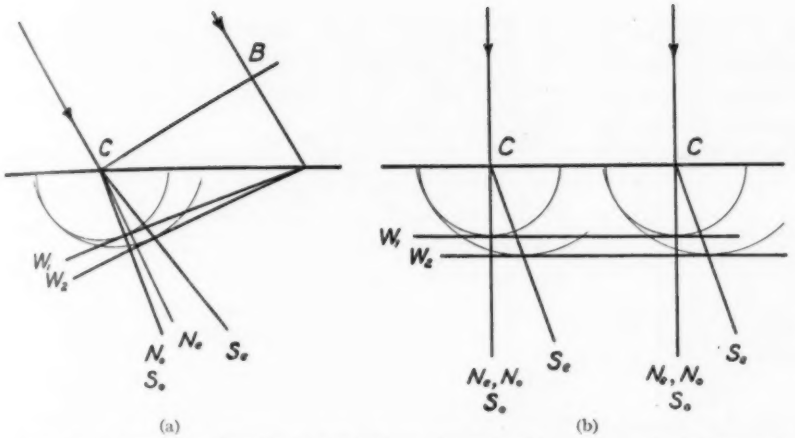


FIG. 4. Huygens' principle is applied to the refraction at a uniaxial crystal; (a) oblique incidence, (b) normal incidence. $N_0$ and $N_e$ are the normals to the ordinary and extraordinary waves, and $S_0$ and $S_e$ are the associated rays.

does not obey the ordinary laws of refraction. This ray is also polarized. The $D$ or $E$ vibrations associated with the ordinary ray are normal to the principal plane defined by the ordinary ray and the optic axis. The $D$ vibrations associated with the extraordinary ray are perpendicular to the extraordinary wave normal and lie in the principal plane formed by this wave normal and the optic axis. When the optic axis lies in the plane of incidence, the extraordinary and ordinary vibration directions are exactly at right angles to each other. This is also true for any case of normal incidence such as is illustrated in Fig. 4(b). The two directions are in this case called the principal vibration directions of the plate. The one for the extraordinary ray is given by the projection of the optic axis on the surface of the uniaxial plate. Any incident plane-polarized wave is resolved into components vibrating in this direction and at right angles to it.

The incident plane-polarized light can be obtained in a variety of ways. One convenient method is by the use of polarizing filters in sheet form recently introduced under the name of Polaroid.[7] These plates contain a layer of oriented microscopic crystals of herapathite between glass plates. Herapathite is an iodosulphate of quinine which is dichroic, meaning that it not only resolves an incident vibration into two orthogonal components, but absorbs one of them much more strongly than the other. In a thickness great enough to absorb one component almost completely, the other transmitted component is also reduced appreciably. Moreover the degree of polarization falls off at both ends of the visible spectrum.

A method by which one may obtain a polarized beam of large cross section with the least expense is by the use of a reflecting glass plate at the polarizing angle. This employs the discovery made by Malus and Brewster that the light reflected by any isotropic insulator is plane-polarized when the tangent of the angle of incidence is equal to the index of refraction of the substance. The reflecting power of a glass plate at this angle, which is about 57° for ordinary glass, is only 14 percent for the component reflected. Surface films and imperfections diminish the degree of polarization. The reflected electric vibrations are normal to the plane of incidence.

The most efficient method for producing plane-polarized light is still the Nicol prism or one of its modifications. The Nicol prism is made of calcite the ends of which are ground to make the angles shown in Fig. 5. This is then cut diagonally at such an angle that when cemented together by Canada balsam, the ordinary ray is totally reflected at the balsam and absorbed in the blackened mount of the prism. The extraordinary ray which vibrates in the principal plane that it makes with the optic axis is alone transmitted. This plane of vibration is parallel to the short diagonal of the rhombic cross section of the prism. In order that the conditions for total reflection of the ordinary ray are satisfied, the direction of the incident light must not deviate too much from the direction of the long axis of the Nicol prism. This limits the usable aperture to about 29°. Of the other similar forms of polarizing prism,[8] the most common is that of Glan-Thompsom which has perpendicular ends and a square cross section. It is somewhat more efficient as a polarizer but has a smaller field of view.

In photoelastic studies it is necessary to produce wide beams of polarized light and to have the rays incident normally on the specimen. If a

Nicol prism is used alone as a polarizer, this would require one of very large cross section, the cost of which would be prohibitive. Hence an arrangement of lenses similar to that shown in Fig. 6 is used to accomplish the same result with

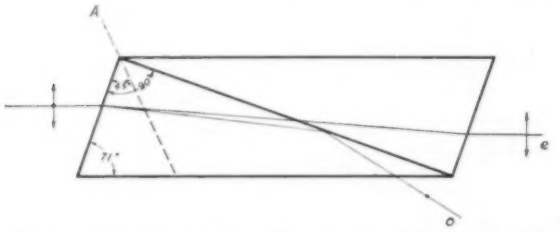


FIG. 5. The Nicol prism. The optic axis is in the plane of the paper and is indicated by the dashed line $A$. The extraordinary ray $e$ vibrates in the plane of the optic axis and the ray, while the ordinary ray vibrates at right angles to this.

a small polarizing prism. The diverging lenses $L_3$ and $L_4$ are used to keep the rays which pass through the relatively small Nicol prism well within its aperture. In fact the rays are practically parallel and thus assure that the vibration direction is the same over the entire field of view. If they were not parallel, one can see that, as a consequence of the different principal planes for each different direction, the vibrations associated with each ray would be in a somewhat different direction.

A plane polariscope consists of two polarizing filters, e.g. Nicol prisms, mounted on a common axis. These are called the polarizer and analyzer, respectively. When one of them is rotated with respect to the other, the transmitted light intensity varies as the square of the cosine of the angle between the vibration planes of the polarizer and analyzer. This follows from the vector type of resolution of amplitudes in double refraction and the fact that the intensity is proportional to the square of the amplitude. It will be noted in particular that when the angle $\theta = 90°$ or some odd multiple thereof, the light is completely extinguished. If now one places a plate of anisotropic material between the polarizer and analyzer, some of the original light intensity is restored unless the light happens to be traveling along an optic axis or unless either one of the principal vibration directions of the plate coincides with the principal plane of the polarizer or analyzer. If monochromatic light is not used, there will be a change in the color of the transmitted light. Since this color is caused by a superposition of effects for the different wave-lengths, it is logical to consider monochromatic light first.

When polarized light of wave-length $\lambda$ enters the doubly refracting plate, its two components in the principal vibration directions of the plate are propagated with different speed so that they emerge with a phase difference:

$$\Delta = (2\pi/\lambda)(n_1 - n_2)d.$$

Their amplitudes will be, respectively, $a' \cos \phi$ and $a'' \cos \phi$ where $a'$ and $a''$ are the products of the incident amplitude and the amplitude transmission coefficients of the plate for the two vibrations. Reflection losses at the two surfaces are included in these factors. Since for normal incidence on transparent media, the losses due to both causes are very nearly equal, we can put $a' = a'' = a$ for all practical purposes. The resultant of two perpendicularly vibrating polarized

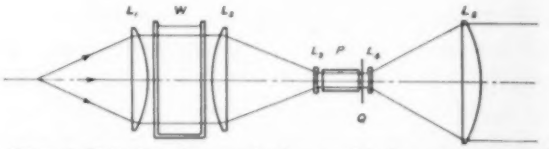


FIG. 6. Polarizer for producing a wide beam of polarized light. $L_1$, $L_2$, $L_3$, $L_4$ and $L_5$ are lenses, $W$ is a water cell, $P$ is a polarizing prism, and $Q$ is a quarter-wave plate which is inserted when circularly-polarized light is desired.

waves with amplitudes $a \cos \phi$ and $a \sin \phi$ and phase difference $\Delta$ is in general an elliptical vibration, the intensity of which is independent of $\phi$ and $\Delta$. However, when this light is passed through the analyzer only the coplanar components of $a \cos \phi$ and $a \sin \phi$ which lie in the principal plane of the polarizer are transmitted. These still have the phase difference $\Delta$ since they both travel with the same speed over the same distance except in the doubly refracting plate. The amplitudes of the transmitted wave components are obtained by a vector diagram of the type shown in Fig. 7, where $A$ represents the principal plane of the analyzer, $P$, that of the polarizer, while $x$ and $y$ denote the principal vibration directions of the plate being examined. If the principal planes of the polarizing filters are at right angles to each other as shown in Fig. 7, the transmitted wave components have the amplitudes:

$$a_1 = a \cos \phi \sin \phi$$
$$a_2 = -a \sin \phi \cos \phi.$$

They are equal numerically, the minus sign indicating a reversal in phase which can be either used as it stands or regarded as a change in $\Delta$ by the amount $\pi$. In either case, the resultant of the two waves is a plane wave whose amplitude is given by

$$A^2 = a^2(2 \cos^2 \phi \sin^2 \phi - \cos^2 \phi \sin^2 \phi \cos \Delta)$$
$$= a^2 \sin^2 2\phi \sin^2 \tfrac{1}{2}\Delta.$$

If the polarizing filters are parallel, the equation is similar except that the cosine of half the phase difference is replaced by the sine. In photoelastic investigations it is customary to use crossed Nicols, and in this case the above equation applies. It shows how the intensity of the light transmitted by a plane polariscope depends on the orientation of the specimen and on the phase difference which it introduces. Note in particular that regardless of the value of $\Delta$, $A^2$ is zero when $\phi = 0, \pi/2, \pi, 3\pi/2$; that is to say, the intensity is zero when either vibration direction of the plate coincides with the principal plane of the

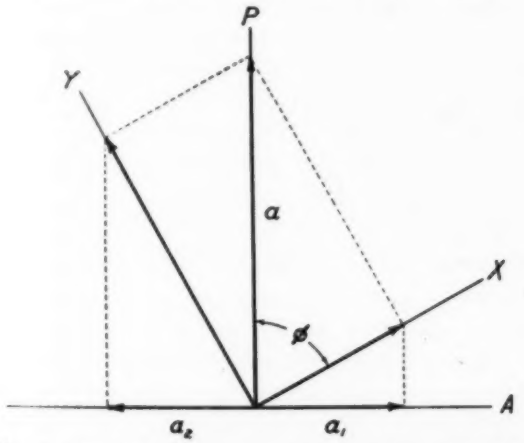


FIG. 7. Amplitude components $a_1$ and $a_2$ transmitted by a plane-polarizing polariscope. The principal planes of the polarizer analyzer and are represented by $P$ and $A$, respectively. The vibration axes of the anisotropic material are in the direction of $x$ and $y$.

polarizer or of the analyzer, these being at right angles. By looking for this condition while rotating the analyzer and polarizer together so as to preserve the 90° setting, one may thus find the principal vibration directions of the material in the polariscope. This procedure is used in photoelastic studies to find the orientation of the stress ellipsoid, since its axes coincide with the principal vibration directions. The lines of zero intensity observed with any setting of the polarizing prisms are called isoclinics.

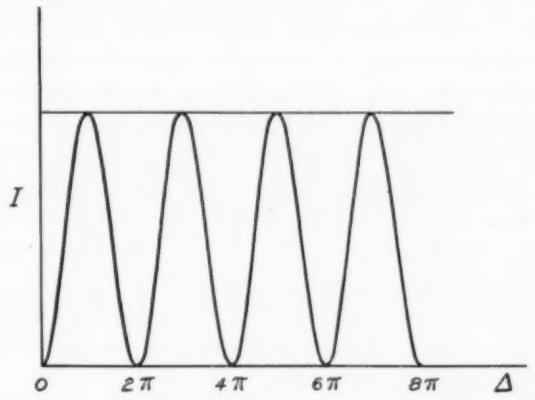


FIG. 8. Intensity variation due to the interference of two waves having a difference in phase of amount $\Delta$.

For any given value of $\phi$, the intensity depends on $\Delta$ as shown in Fig. 8. Complete darkness occurs when $\Delta = m2\pi$, where $m$ is any integer and is called the "order" of the interference. If the value of $\Delta$ varies over the surface of a plate, there will be dark bands called interference fringes in the field of view. Along any one band the value of $\Delta$ is constant for the given wave-length, and therefore $(n_1 - n_2)d$ is constant. If the thickness, $d$, is uniform, these interference fringes are loci of constant birefringence, $(n_1 - n_2)$; this in photoelastic applications is proportional to the difference between the principal stresses in the plane of the plate. Accordingly, this is uniform along any one fringe and varies from fringe to fringe by a constant increment which depends on the stress-optical constant of the material employed.

It has been assumed above that monochromatic light of a definite wave-length is being used. If white light is used, it is primarily due to the variation in the magnitude of the wave-length itself, and secondarily due to the dispersion in the birefringence, that the values of $\Delta$ differ for the various spectral colors. Thus in the transmitted light some wave-lengths will be in phase and some in opposite phase, producing a considerable variation in intensity throughout the spectrum. This selective interference will cause the transmitted light to be colored except where

the birefringence is zero. Here the value of $\Delta$ is the same, zero, for all wave-lengths and the band is achromatic, being perfectly black when the polarizing filters are crossed and white if they are parallel. The loci of points of the same color are called isochromatic lines. Due to the maximum sensitivity of the eye to light of a yellow-green color, the complementary purple locus is quite well defined in several orders. The colored bands fade out as $\Delta$ becomes large, and in any case they are not as sharp as the interference fringes in monochromatic light, and hence do not lend themselves readily to quantitative work. The principal value of white light is that it facilitates the location of the fringe of zero order which shows where the difference between the principal stresses is zero.

The light vector in polarized light may not vary in a simple harmonic manner in one plane, as in plane-polarized light, but may rotate with or without a change in magnitude. When this is the case, the light is said to be circularly or elliptically polarized. Such light may be considered to be a resultant of two simple harmonic vibrations at right angle to each other with some phase difference between them. This is how it is usually produced. When plane-polarized light passes through any anisotropic medium, two orthogonally polarized waves emerge, as was pointed out above. These two waves may be represented by the equations:

$$x=a_1 \sin\left[\frac{2\pi}{T}\left(t-\frac{z}{V_1}\right)+\epsilon\right],$$

$$y=a_2 \sin\left[\frac{2\pi}{T}\left(t-\frac{z}{V_2}\right)+\epsilon\right],$$

where $a_1=a \sin \phi$ and $a_2=a \cos \phi$ are the two amplitudes and $x$ and $y$ denote the components of the light vector in the corresponding principal vibration directions of the plate. If $z$ is measured from the front surface of the plate, its value at emergence will be equal to the thickness of the plate, and due to the difference between $V_1$ and $V_2$ there will be a phase difference given by the usual equation. After that the phase difference remains constant, though the phase itself is a function of $z$ and $t$. At any given point, $z$, there are two simple harmonic vibrations of the type:

$$x=a_1 \sin \omega t,$$
$$y=a_2 \sin (\omega t+\Delta).$$

The resultant vibration of which $x$ and $y$ are components is, in general, no longer plane-polarized, since the instantaneous values of $x$ and $y$ are related by the equation:

$$\frac{x^2}{a_1^2}-\frac{2xy}{a_1 a_2}\cos\Delta+\frac{y^2}{a_2^2}=\sin^2\Delta,$$

which is readily obtained from the above equations by eliminating the time, $t$. This equation shows that the end of the light vector, the point $x$, $y$, describes an ellipse. The presence of the $xy$ product term shows that in general the ellipse is inclined with respect to the $x$ and $y$ directions. There are several important special cases.

When $\Delta=0,\ 2\pi,\ 4\pi,\ \cdots m2\pi$, the equation reduces to that of a straight line with the slope $a_2/a_1$ which is the same as that of the original vibration. On the other hand, when $\Delta=\pi,\ 3\pi,\ 5\pi,\ \cdots(m+\frac{1}{2})2\pi$, the slope is $-a_2/a_1$ and the vibration direction makes an angle equal to $2\tan^{-1} a_2/a_1$ with its original direction. A plate of such a thickness that $\Delta=\pi$ is called a half-wave plate and is frequently used to rotate a plane of vibration through any desired angle for a particular color. The values of $a_1$ and $a_2$ are sine and cosine components of the incident light vector and can therefore be varied at will by rotating the half-wave plate.

When $\Delta=\pi/2,\ 3\pi/2,\ 5\pi/2,\ \cdots(m+\frac{1}{2})\pi$, the vibration equation reduces to that of an ellipse:

$$\frac{x^2}{a_1^2}+\frac{y^2}{a_2^2}=1,$$

the axes of which coincide with the $x$ and $y$ directions and have the values $2a_1$ and $2a_2$. A plate for which $\Delta=\pi/2$ is called a quarter-wave plate. As before, the values of $a_1$ and $a_2$ can be given any relative value by rotating the plate, that is by changing the azimuth angle $\phi$. In this way the eccentricity of the ellipse can be given any desired value. In particular, if $\phi$ is equal to 45°, $a_1=a_2$, and the above equation of the form of the vibration reduces to that of a circle. The electric vector at any point simply rotates about the wave normal with no change in its magnitude. This kind of light is said to be circularly polarized.

The equations of the two traveling waves which make up circularly polarized light can be written as follows for any pair of orthogonal axes:

$$x = a \cos \frac{2\pi}{T}\left(t - \frac{z}{V}\right),$$

$$y = \pm a \sin \frac{2\pi}{T}\left(t - \frac{z}{V}\right).$$

The waves have equal amplitudes and their phase difference is constantly some odd multiple of 90° at any fixed point, $z$=constant. The resultant of which $x$ and $y$ are components is always a vector of magnitude $a=(x^2+y^2)^{\frac{1}{2}}$ but its azimuth varies with the time at any fixed point, and from point to point at any fixed time. In the latter case, the ends of the light vector describe a spiral which may be right-, or left-handed according to the sign of $y$. The equal amplitudes are obtained by orienting the quarter-wave plate so that its axes make angles of plus or minus 45° with the plane of vibration of the incident light. In the case illustrated by the above equations, the $x$ direction would be called the "fast" direction of the quarter-wave plate. If this direction is 45° clockwise of the direction of the incident vibration as seen by an observer toward whom the light is traveling, the positive sign applies to $y$ and the resultant rotates in a counterclockwise direction. This is called right-hand circularly-polarized light since the sense of rotation is related to the direction of advance of the wave as the rotation and advance of a right-handed screw. Conversely, if the fast axis is 45° counterclockwise of the original plane of vibration, the light is said to be left-hand circularly polarized. The advantages of circularly-polarized over plane-polarized light in photoelastic studies will be discussed further on.

The Babinet compensator is useful in measuring phase differences caused by double refraction. It is made of two wedges of quartz with their optic axes at right angles to each other and in the directions of the length and width of the two respective wedges. One of the wedges can be displaced by means of a calibrated screw as shown in Fig. 9. At some point such as $A$, where the thicknesses of the wedges are equal, the phase difference will be zero. It will increase linearly in both directions from $A$. This will result in the transmission of any desired ellipticity including circularly- and plane-polarized light at various points along the wedge. At regularly spaced intervals, the phase difference changes by an increment of $2\pi$ which means that the original vibration is transmitted. Between crossed Nicols,

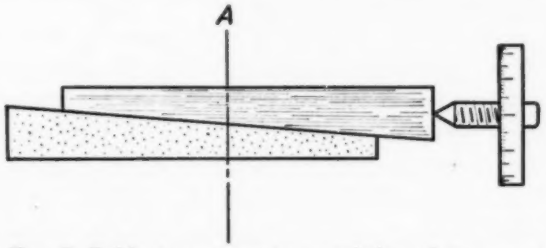


FIG. 9. Babinet compensator consisting of two quartz wedges with optic axes at right angles to each other indicated by the dots and lines.

this light is extinguished so that one sees a set of equally spaced dark bands. The screw rotation required to displace the bands by one space i.e., change the phase difference by $2\pi$, gives the required information for translating a fringe shift of any magnitude into the corresponding phase difference. If the axes of the compensator coincide with the axes of the incident elliptically polarized light, the phase difference observed will be just $\pi/2$. This fact is often applied to the finding of the orientation of the axes in elliptically polarized light. In the general measuring of phase differences, the axes of the compensator must be aligned with the vibration components between which the phase difference is desired. The screw rotation required to displace the zero-order band to its original location at $A$ gives a measure of the phase difference.

In a Soliel-Babinet compensator, the two wedges have their principal planes parallel to each other and are combined with a parallel plate having its principal plane at right angles to this and with a thickness equal to that of the combined wedges in their zero position. The effect is then equivalent to that of a doubly-refracting plate of uniform but variable thickness. Consequently no bands are seen, the intensity being uniform, but undergoing periodic variations as one slides one wedge over the other. In white light, naturally, one obtains colors which run through the various orders of the Newton color scale.

The Babinet compensator measures only the difference between the phases of the two com-

ponents transmitted by any anisotropic plate. From this one obtains the relative retardation, $(n_1-n_2)d$, or the birefringence, $(n_1-n_2)$, when this is divided by the thickness of the plate. The actual retardation $n_1d$ and $n_2d$ for either one of the rays is not obtained except by the use of some form of interferometer.

One typical form of interferometer is that of Jamin, which is illustrated in Fig. 10. The light is separated into two beams of approximately equal intensity at the half-silvered, or, better, aluminized, surface $H_1$. After traveling along the paths as indicated, the light is reunited in the focal plane of the telescope $T$. If one of the mirrors is inclined slightly, the waves arriving at the telescope will give rise to interference fringes of the nature explained in the discussion of interference. If two identical plates $P_1$ and $P_2$ of some material of index $n_0$ and thickness $d$ are placed in the two beams as shown, there will be no change in the difference between the two optical paths and the interference fringes will not be displaced. If now the refractive index of one of the plates is changed by some external agency, such as an applied stress, the interference bands will be displaced by an amount which depends on the phase difference $\Delta$ produced by this change in refractive index, where

$$\Delta=(2\pi/\lambda)(n-n_0)d.$$

To measure this, it is necessary to calibrate the interferometer by measuring the interval $s_0$ between successive fringes by means of cross-wires and a micrometer. This corresponds to a change in phase of just $2\pi$. Any shift in the fringes $s$, is to the fringe interval $s_0$, as the phase shift causing it is to $2\pi$, or

$$\Delta=s/s_0 2\pi.$$

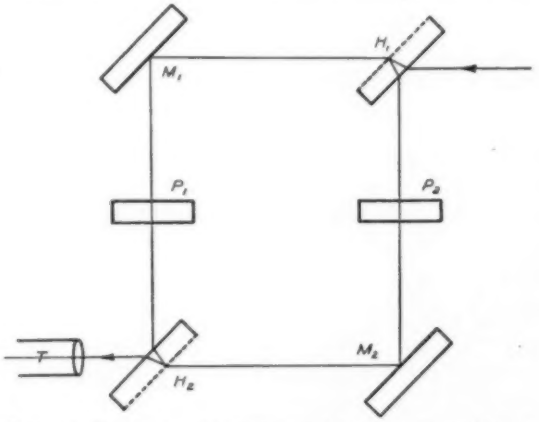


FIG. 10. Jamin interferometer. $M_1$, $M_2$, $H_1$ and $H_2$ are mirrors, $H_1$ and $H_2$ being half-silvered. $P_1$ and $P_2$ are plates of material being examined. Interference bands are observed in the telescope $T$.

If polarized light is used to illuminate the interferometer, it should vibrate in the plane of incidence or at right angles to it in order that it remain plane-polarized. Using such light one finds that the change in phase is different for light vibrating in the two respective vibration directions of the plate. The difference between the two changes in phase is equal to that measured by means of a polariscope equipped with a Babinet compensator. The interferometer is invaluable in studies in which it is required to measure the separate phase retardations instead of just their difference.

It is often of advantage to examine anisotropic materials with the aid of a circularly-polarizing polariscope. A quarter-wave plate is placed in front of the plane-polarizer with its fast axis at $\pm 45°$ with the direction of the incident plane polarized light. A clockwise rotation, Fig. 11, gives right-hand circularly-polarized light, and the combination of quarter-wave plate and Nicol prism is called a right-hand circular polarizer. A similar combination in the reverse order is used at the other end of the polariscope as a right-hand circular analyzer. The circularly-polarized light transmitted by the polarizer may be represented by the equations

$$x=a\cos\omega t=a\sin(\omega t+\pi/2),$$
$$y=a\sin\omega t.$$

Suppose that these waves strike a right-hand circular analyzer which has been rotated so that all corresponding vibration directions are at right angles to those of the polarizer. The slow axis of the analyzing quarter-wave plate will then be in the $x$ direction so that the components it transmits will be

$$x=a'\sin(\omega t'+\pi/2-\pi/2),$$
$$y=a'\sin\omega t'.$$

Their resultant is in the original direction $P$, as can be verified by examining Fig. 11. Therefore the light is not transmitted by the analyzing Nicol prism which is at right angles to $P$.

If now a doubly refracting plate is placed

between the polarizer and analyzer of such a circular polariscope it will transmit two waves vibrating in the directions of its principal axes which may make any angle $\phi$ with $P$. To find these waves, one must first take the components of the circularly-polarized light which is incident on the plate. These are given by the same equations as those given above except that now $x$ and $y$ refer to the principal axes of the substance being examined. Circularly-polarized light has similar components for any mutually perpendicular axes. These components are transmitted by the substance with a slight reduction in amplitude and with the introduction of a relative phase retardation $\Delta$ so that they can be represented by

$$x' = a'' \sin(\omega t'' + \pi/2 + \Delta/2 + \Delta/2),$$
$$y' = a'' \sin(\omega t'' + \Delta/2 - \Delta/2).$$

The double prime on $t$ takes care of the absolute phase retardation in the plate, and those on $a$ take care of the reflection and absorption losses which are small. When light is incident normally these losses are the same for both components if the substance is not dichroic, and consequently the primes may be dropped. The phase retardation $\Delta$ has been split into halves in order to make it easier to show that $x'$ and $y'$ represent a right- and a left-hand circularly-polarized wave traveling together. To do this, these quantities are expanded by the trigonometric formulas for the sine of the sum and of the difference of two angles, as follows:

$$x' = a \sin(\omega t + \pi/2 + \Delta/2) \cos \Delta/2 + a \cos(\omega t + \pi/2 + \Delta/2) \sin \Delta/2,$$
$$y' = a \sin(\omega t + \Delta/2) \cos \Delta/2 - a \cos(\omega t + \Delta/2) \sin \Delta/2.$$

The first terms of $x'$ and $y'$ together represent waves of equal amplitude with a phase difference of $\pi/2$ and therefore make up a right-hand circularly-polarized wave having an amplitude equal to $a \cos \Delta/2$. Similarly, the remaining terms represent a left-hand circularly-polarized wave of amplitude $a \sin \Delta/2$. Since a right-hand circular analyzer set for extinction as defined before, transmits only the latter, the transmitted light will have an intensity which is proportional to $\sin^2(\Delta/2)$. It is important to note that this is independent of $\phi$. Thus the intensity is the same

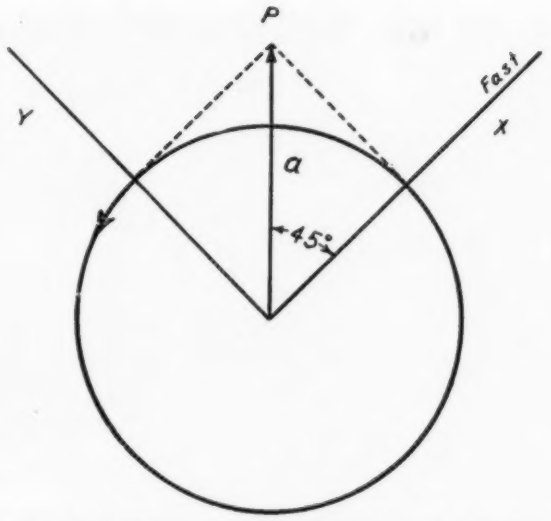


FIG. 11. Illustrating the production of right-hand circularly-polarized light by means of a quarter-wave plate with its vibration axes in the direction of $x$ and $y$, the fast axis being 45° clockwise of the vibration direction of the incident light $P$.

regardless of the orientation of the principal axes of the plate, but otherwise depends on the phase difference $\Delta$ in exactly the same way as the light transmitted by a plane polariscope with its Nicols crossed. In the latter case the variation of $\Delta$ is obscured when the values of $\phi$ approach 0° or 90°. This happens when the principal vibration directions, or stresses in photoelastic applications, coincide or are near the principal planes of the polarizer and analyzer. In a circularly-polarizing polariscope on the other hand, a given difference between the stress components in the plane of the figure produces exactly the same effect regardless of how the stresses are oriented. Naturally, this is of particular value in photoelastic investigations.

### *Bibliography*


1. E. G. Coker and L. N. G. Filon, *Photoelasticity* (Cambridge University Press, 1931), pp. 1–92.
2. L. N. G. Filon, *A Manual of Photoelasticity for Engineers* (Cambridge University Press, 1936), pp. 1–29.
3. F. A. Jenkins and H. E. White, *Fundamenials of Physical Optics* (McGraw-Hill Book Company, 1937).
4. F. Pockels, *Lehrbuch der Kristalloptik* (Teubner, 1906).
5. Wien-Harms, *Handbuch der Experimental Physik*, Vol. 18 (Akademische Verlagsgesellschaft, 1928), pp. 366–615.
6. E. Gehrcke, *Handbuch der Physikalischen Optik* (Johann Ambrosius Barth, 1927), Vol. I, pp. 813–900.
7. M. Grabau, "Polarized Light," J. App. Phys. 9, 215–225 (1938).
8. S. P. Thompson, Proceedings of the Optical Convention of 1905, p. 216+.

# A Review of the Photoelastic Method of Stress Analysis. I*

BY RAYMOND D. MINDLIN

*Department of Civil Engineering, Columbia University, New York, New York*

*Introduction*

A DETAILED knowledge of the stress distributions in structural elements and machine parts is of great importance to designers in many branches of engineering. The mathematical methods of the theory of elasticity have been applied successfully to the solution of many stress problems involving relatively simple boundary conditions, but innumerable cases arise for which the mathematical tools are inadequate. Recourse must then be had to experimental procedures and one of the most useful of these has been the photoelastic method. This method is based upon the fact that when transparent materials are stressed, their optical properties undergo changes which can be measured and related quantitatively to the state of stress.

In applying the photoelastic method, the engineer chooses a suitable transparent material (Section 12) and fashions from it a model (Section 13) of the same shape as the structure or machine part under investigation. The model is loaded (Section 14) in a manner similar to the loading of the prototype and resulting optical effects (Section 8) are measured in a variety of manners (Sections 15, and 26 to 28) many of which have been borrowed from the field of physical optics, while some have been developed especially for photoelasticity. The optical properties are then translated into terms of stress (Sections 9, 11 and 15 to 19), and the latter are interpreted by means of the fundamental ideas of the theory of elasticity and strength of materials (Sections 1 to 7, and 10). The stress distribution in the model is then converted to the analogous stress system for the prototype (Section 13) and the engineer uses this knowledge in his design.

It is found that the optical observations which are most easily made are not sufficient to completely determine the state of stress in all cases. Supplementary methods (Sections 20 to 31) have therefore been developed for securing the additional measurements which are required. Some of these are optical, but others are graphical, numerical or mechanical.

The photoelastic method has been applied to a wide variety of stress problems in many branches of engineering and applied physics (Sections 32 to 38), and a large number of research papers have appeared in technical and scientific

*This paper is the first half of a comprehensive review of the principles of photoelasticity by Dr. R. D. Mindlin of Columbia University. In the present installment are treated:*

*I. Principles of Stress, Strain and Optics*
*II. Materials, Models and Loading Machines*
*III. Measurement of the Difference between and the Directions of the Principal Stresses*

*In the second installment which will be published next month the main section headings are:*

*IV. Independent Determination of the Principal Stresses*
*V. Special Developments and Applications*
*VI. Bibliography for the Period 1930–1938*

*The second installment will also contain acknowledgments to those who have assisted in the preparation of the manuscript and to those who have contributed photographs of apparatus and fringe patterns.*

THE EDITOR

* Publication assisted by the Ernest Kempton Adams Fund for Physical Research of Columbia University.

journals. Much of the theory, technique and application has been described in the monumental "Treatise on Photo-Elasticity" by E. G. Coker and L. N. G. Filon, published in 1931. Insofar as theory is concerned, only a few advances have been made since that time; but it is inevitable, in a field which is developing so rapidly, that substantial improvements in technique and widening of fields of application should appear in an interval of almost a decade.

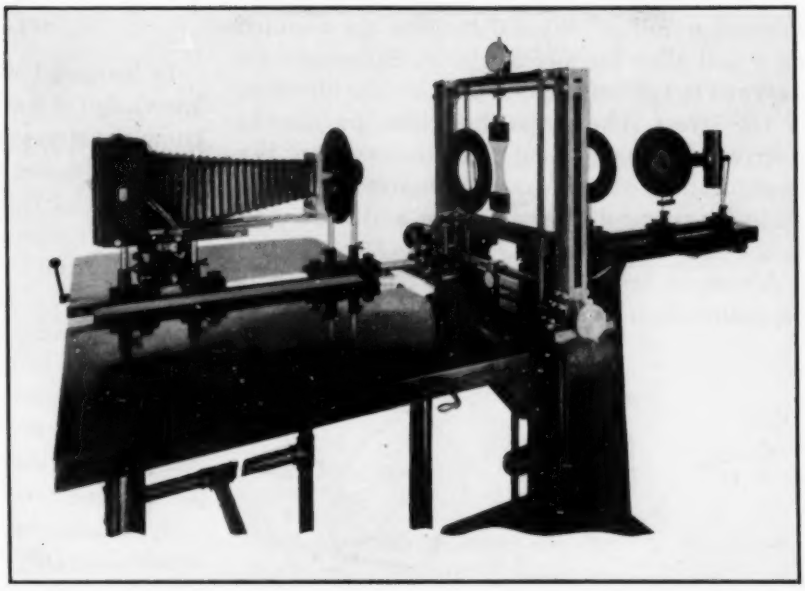

The photoelastic polariscope and loading machine at Columbia University.

It is the purpose of this paper to review the fundamental principles upon which the photoelastic method is based and to describe the techniques, apparatus and some of the applications which have appeared, especially in the last ten years.

### *Part I. Principles of Stress, Strain and Optics*

#### 1. Definition of Stress

When a system of forces acts on a body, each part of the material exerts an action on an adjacent part. The mutual interaction of neighboring parts of the body is one aspect of the concept of stress. For example, in a bar of cross-sectional area $A$ under a longitudinal pull $P$ (Fig. 1.1), the material on one side of a normal section $n-n$ exerts a tensile stress on the material on the other side. The magnitude of the stress is defined as the quotient $P/A$ and the direction of the stress is parallel to the axis of the bar. In more complicated stress situations, the stress on a small sectional area $\delta A$ through a point $O$ in the body (Fig. 1.2(a)) is not necessarily normal to the section and, furthermore, both the magnitude and direction of the stress may vary from point to point through the material. A complete analysis of stress should include a description of the state of stress on every plane through each point of the body.

Consider an element of area $\delta A$ containing a point $O$ in a body acted upon by a system of forces (Fig. 1.2(b)). A normal $N$ drawn to one side of the area serves to specify the orientation of the small section. The material on one side exerts a force $\delta P$ on the material on the other side and the direction of $\delta P$ is in general inclined to $N$. If we now shrink the area $\delta A$ in such a way that it always includes $O$, the magnitude of $\delta P$ will also diminish and will approach zero as $\delta A$ approaches zero. The limit of the ratio $\delta P/\delta A$ as $\delta A$ approaches zero is called the *stress* at $O$ across the plane normal to $N$ and the limiting direction of $\delta P$ is the direction of the stress. If the limiting direction does not coincide with $N$, the stress can always be resolved into a component normal to the plane and a component parallel to the plane. The former is called a normal stress and the latter a shearing stress.

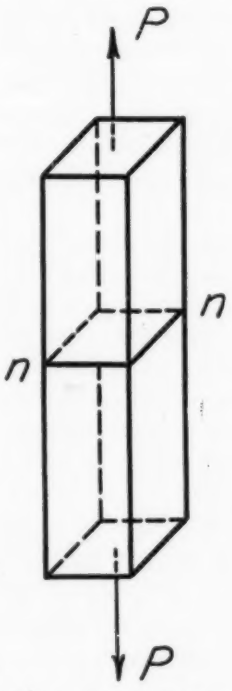


Fig. 1.1. Prismatic bar under tension.

#### 2. Notation

In the system of symbols known as the "con-

tinental notation" normal stresses are denoted by $\sigma$ and shearing stresses by $\tau$. Subscripts are assigned to each of these to indicate the direction of the stress. The stress directions are usually referred to an orthogonal coordinate system. For example, in rectangular coordinates the three mutually perpendicular axes $x$, $y$, and $z$ are used as the axes of reference.

A normal stress acting on a plane which is perpendicular to the $x$ axis is denoted by $\sigma_x$ and

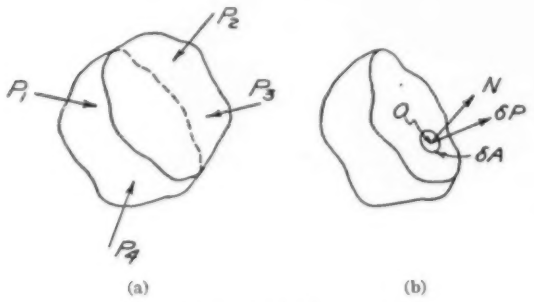


FIG. 1.2. Stress on an interface.

parallel to the other two axes we have $\sigma_y$ and $\sigma_z$ as the normal stresses acting on planes perpendicular to the $y$ and $z$ axes, respectively. A normal stress is considered positive when it produces a tension on the part of the body under consideration. Thus, in Fig. 2.1, we consider a small rectangular parallelepiped with its edges parallel to the coordinate axes. The normal stresses, $\sigma_x$, $\sigma_y$, $\sigma_z$, are represented in Fig. 2.1 by arrows pointing in the directions of positive stresses.

Two subscripts are required to identify a shearing stress. The first specifies the normal to the plane on which the shearing stress acts and the second indicates the direction of the stress in the plane. Thus, the symbol $\tau_{xy}$ represents a shearing stress acting in a plane normal to the $x$ axis and directed parallel to the $y$ axis. In Fig. 2.1, all the shearing stresses are drawn in their positive directions.

The quantities $\sigma_x$, $\sigma_y$, $\sigma_z$, $\tau_{yz}$, $\tau_{zy}$, $\tau_{zx}$, $\tau_{xz}$, $\tau_{xy}$, $\tau_{yx}$ are called the *components of stress*. If we consider the moments of the stresses about the $x$ axis, we find that $\tau_{zy}=\tau_{yz}$. Similarly, by taking moments about axes $y$ and $z$, we find $\tau_{zx}=\tau_{xz}$ and $\tau_{xy}=\tau_{yx}$. Hence only six of the nine components of stress are independent quantities.

## 3. Specification of Stress

In Section 1 we observed that for a complete knowledge of a stress situation, it is necessary to know the stress across every plane through each point of the material. Let $O$, Fig. 3.1, be such a point, and let $N$ be the normal to a plane through $O$. Another plane, with the same normal $N$, but distant $h$ from $O$, will intersect an $x$, $y$, $z$ system of axes at $B$, $C$ and $D$. Since we may take $h$ as small as we wish, the two planes with the normal $N$ may be brought to coincidence and any properties associated with one plane will apply equally well to the other. We are at present interested in investigating the stress across the plane whose normal is $N$.

By considering the equilibrium of the small tetrahedron $OBCD$, we find that the normal component of the stress on plane $BCD$ may be expressed in terms of the six components of stress by

$$\sigma_N=\sigma_x l^2+\sigma_y m^2+\sigma_z n^2 +2\tau_{yz}mn+2\tau_{zx}nl+2\tau_{xy}lm, \quad (3.1)$$

where $l$, $m$, $n$ are the cosines of the angles between the direction $N$ and the $x$, $y$, $z$ axes, respectively.

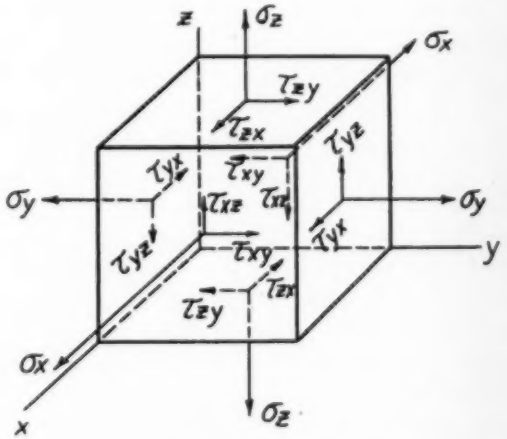


FIG. 2.1. Components of stress on the faces of a small rectangular parallelepiped.

The resultant stress on $BCD$ will in general have a component parallel to the plane. The component of this shearing stress in any direction $S$ determined by the direction cosines $l'$, $m'$, $n'$, is given by

$$\tau_{NS}=\sigma_x ll'+\sigma_y mm'+\sigma_z nn'+\tau_{yz}(m'n+mn')$$
$$+\tau_{zx}(n'l+nl')+\tau_{xy}(l'm+lm'). \quad (3.2)$$

Equations (3.1) and (3.2) show that the normal component of stress on any plane through $O$ and the shearing component in any direction in this plane are completely determined if the six components of stress at $O$ are known.

## 4. Principal Stresses and Principal Planes of Stress

If we examine the variation of $\sigma_N$ in Eq. (3.1) as the direction $N$ is varied, we find that there are always three mutually perpendicular directions for which $\sigma_N$ has stationary values, i.e., it is a maximum, a minimum, or a minimax. The three directions are called the *principal axes* of stress and they are the normals to three mutually perpendicular planes known as the *principal planes* of stress. Furthermore, we find that there are no shearing stresses on the principal planes,

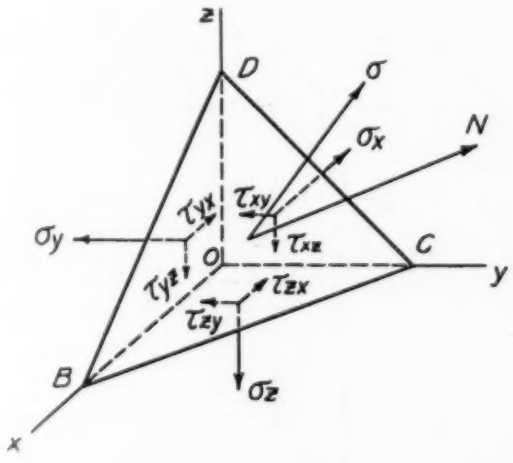


Fig. 3.1. Stresses on a small tetrahedron.

i.e., the resultant stress on a principal plane is purely normal.

Hence, around any point $O$, we can always construct a small cube (Fig. 4.1) so oriented that the stresses on its six faces are purely normal. We denote these three principal stresses by the symbols $\sigma_3$, $\sigma_2$, $\sigma_1$ and we take their magnitudes to be in the order $\sigma_3>\sigma_2>\sigma_1$.

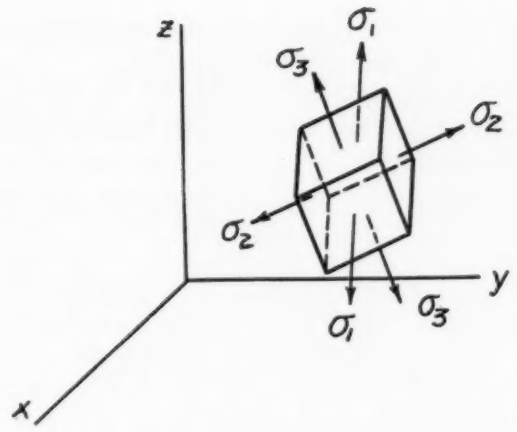


Fig. 4.1. Stresses on a small rectangular parallelepiped with its faces parallel to the principal planes of stress.

## 5. Small Strain and Components of Strain

In a stressed body, a very small element of volume in the shape of a rectangular parallelepiped in general deforms, to a first approximation, into a skew parallelepiped. In Fig. 5.1(a) the element is shown before distortion with its edges $PA$, $PB$, $PC$ parallel to the coordinate axes $x$, $y$, $z$, respectively. After distortion, $A$, $B$, $C$, $P$ occupy new positions $A'$, $B'$, $C'$, $P'$ (Fig. 5.1(b)) so that in general the edges of the element do not meet at right angles and acquire new lengths $P'A'$, $P'B'$, $P'C'$. The change in length per unit of length of any edge of the element is called a unit elongation, and is denoted by the symbol $\epsilon$ with a subscript to denote the direction of the edge. Thus

$$\frac{P'A'-PA}{PA}=\epsilon_x$$

is the component of unit elongation in the $x$ direction.

For small strains, the change in angle between two adjacent edges of the deformed element is called a *component of shearing strain* and is denoted by the symbol $\gamma$ with appropriate subscripts to identify the plane in which the two edges originally lie. Thus $\gamma_{xy}$ is the change in angle between the edge $PA$ originally parallel to $x$, and the edge $PB$, originally parallel to $y$.

The six components of strain $\epsilon_x$, $\epsilon_y$, $\epsilon_z$, $\gamma_{yz}$, $\gamma_{zx}$, $\gamma_{xy}$ are the necessary and sufficient quantities required to completely determine the new shape

and size of the element; hence, they specify the state of strain in the body.

From the geometry of Fig. 5.1 we find that, for small strains, the unit elongation in direction $PN$ is given by

$$\epsilon_N=\epsilon_x l^2+\epsilon_y m^2+\epsilon_z n^2+\gamma_{yz}mn+\gamma_{zx}nl+\gamma_{xy}lm, \quad (5.1)$$

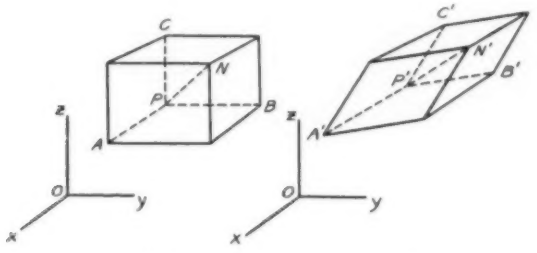


(a) (b)

FIG. 5.1. Deformation of a small rectangular parallelepiped.

in which $l$, $m$, $n$ are the cosines of the angles between $PN$ and $x$, $y$, $z$, respectively.

## 6. Analogy Between Stress and Small Strain

If, in Eq. (5.1) we replace $\epsilon$ by $\sigma$ and $\gamma$ by $2\tau$ we have Eq. (3.1) which expresses the corresponding relation between the normal stress in any direction $l$, $m$, $n$ in terms of the components of stress. Similarly, if, in Eq. (3.2) we replace $\sigma$ by $\epsilon$ and $\tau$ by $\gamma/2$ we obtain

$$\gamma_{NS}=2\epsilon_x ll'+2\epsilon_y mm'+2\epsilon_z nn'+\gamma_{yz}(m'n+mn')+\gamma_{zx}(n'l+nl')+\gamma_{xy}(l'm+lm') \quad (6.1)$$

which expresses the shearing strain between the perpendicular directions $N$ and $S$ in terms of the components of strain and the direction cosines $l, m, n$ of the direction $N$ and the direction cosines $l', m', n'$ of the direction $S$.

There is thus a complete analogy between the specification of stress and the specification of strain. The conclusions drawn for stress in Section 4 apply equally well for strain. It is only necessary to substitute $\epsilon$ for $\sigma$ and $\gamma/2$ for $\tau$. Thus, corresponding to the principal stresses and principal axes of stress, there are three principal strains $\epsilon_3$, $\epsilon_2$, $\epsilon_1$ in three mutually perpendicular directions for which the unit elongations have stationary values while the shearing strains vanish.

## 7. Stress-Strain Relations

An *elastic* solid has two distinguishing properties. First, in such a solid, the components of strain vary linearly with the components of stress and, second, the strains vanish when the stresses are removed. If, furthermore, the solid is isotropic, i.e., at each point its properties are the same in all directions, the principal axes of stress and strain will coincide at each and every point in the body. The stress-strain relations then assume the well-known form

$$\left.\begin{aligned}\epsilon_1&=\frac{1}{E}\sigma_1-\frac{\nu}{E}(\sigma_2+\sigma_3)\\ \epsilon_2&=\frac{1}{E}\sigma_2-\frac{\nu}{E}(\sigma_3+\sigma_1)\\ \epsilon_3&=\frac{1}{E}\sigma_3-\frac{\nu}{E}(\sigma_1+\sigma_2)\end{aligned}\right\}, \quad (7.1)$$

in which $E$ is Young's modulus and $\nu$ is Poisson's ratio, both of which are constants if the elastic

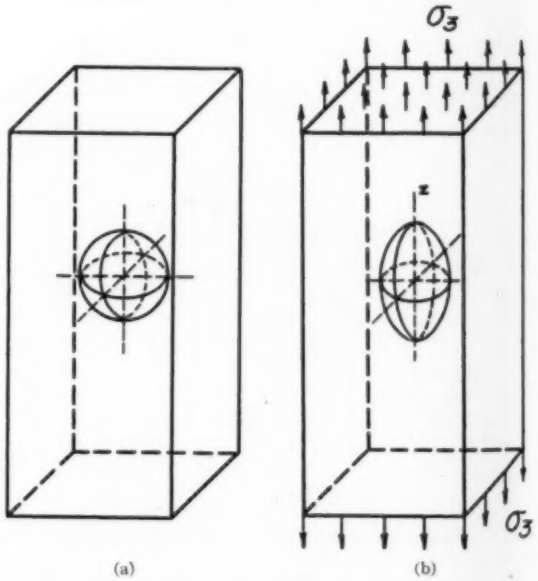


FIG. 7.1. Deformation of a sphere to an ellipsoid in a simple tension field.

material is homogeneous, i.e., has identical elastic properties at each point.

If a simple tension bar is subjected to an axial stress $\sigma_3$, the resulting state of strain is, from Eq. (7.1),

$$\epsilon_3=\sigma_3/E, \quad \epsilon_2=-\nu\sigma_3/E, \quad \epsilon_1=-\nu\sigma_3/E.$$

If we take the $z$ axis parallel to the axis of the bar (Fig. 7.1(a)) and denote the coordinates of any point before strain by $x$, $y$, $z$ and after strain by $x_1$, $y_1$, $z_1$, we have

$$x_1=x\left(1-\frac{\nu\sigma_3}{E}\right), \quad y_1=y\left(1-\frac{\nu\sigma_3}{E}\right),$$

$$z_1=z\left(1-\frac{\sigma_3}{E}\right). \quad (7.2)$$

We may write the equation of a spherical surface

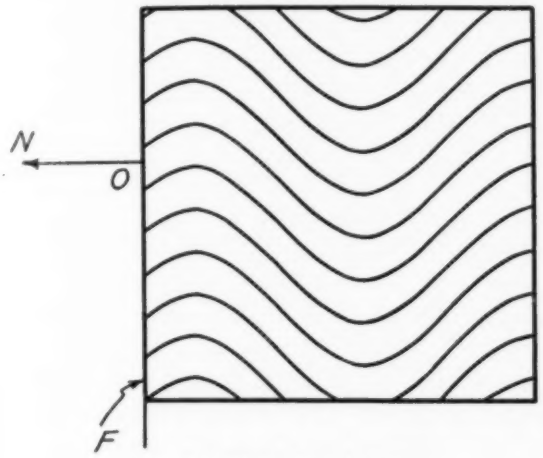


FIG. 8.1. Wave disturbance.

of radius $a$ in the undeformed bar as

$$x^2+y^2+z^2=a^2.$$

Using Eq. (7.2), we see that the sphere deforms into an ellipsoid (Fig. 7.1(b))

$$\frac{x_1^2}{a^2(1-\nu\sigma_3/E)^2}+\frac{y_1^2}{a^2(1-\nu\sigma_3/E)^2}+\frac{z_1^2}{a^2(1+\sigma_3/E)^2}=1. \quad (7.3)$$

## 8. Propagation of Light in Isotropic and Crystalline Media

Optical wave theories describe light as a transverse wave motion. The wave front $F$ (Fig. 8.1) of an optical disturbance advancing through a transparent medium is considered to be plane in the neighborhood of any point, $O$, in the medium. In an isotropic medium there is only one wave velocity and it is the same regardless of the direction of travel of the light. That is, the velocity is independent of the direction of the wave normal $N$. In a crystalline medium there are, in general, two wave velocities for each wave normal and these two velocities are different for wave normals through $O$ in different directions. This is the phenomenon of *double refraction.*

There are thus two waves ($W$ and $W'$, Fig. 8.2) associated with each wave normal, $N$, and, since the waves have different velocities, there will be two parallel wave fronts ($F$ and $F'$) for each wave normal. Furthermore, each of the waves is *plane-polarized*; that is, the vibration corresponding to each of the waves lies in a plane (planes $AOO'$ and $A'O'O$). Finally the vibration directions ($OA$ and $O'A'$) of the two waves are perpendicular to each other and to the wave normal.

All of these optical properties of a crystalline medium may be visualized in terms of the geometry of the *index ellipsoid* (Fig. 8.3). The center of the ellipsoid is placed at point $O$ and the orientations of the principal axes $OA$, $OB$, $OC$ of the ellipsoid are fixed with respect to the medium. Any radius $ON$ from the center of the ellipsoid then represents a possible direction for the wave normal. The plane through $O$ perpendicular to $ON$ is parallel to the wave fronts and intersects the ellipsoid in an ellipse $DE$. The semi-axes $OD$, $OE$ of this ellipse are proportional to the indices of refraction $n_1$ and $n_2$ of the two

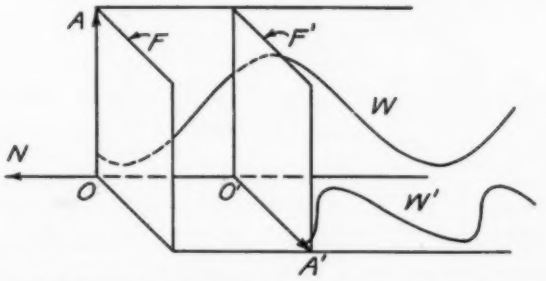


FIG. 8.2. Wave propagation in a doubly refracting medium.

waves and the directions $OD$ and $OE$ are the vibration directions.

As the direction $ON$ is varied, the stationary values of $n_1$ and $n_2$ are $n_a$, $n_b$ and $n_c$. The latter are the *principal indices of refraction;* their directions $OA$, $OB$, $OC$ are the *principal axes of optical symmetry*, and the planes $AOB$, $BOC$,

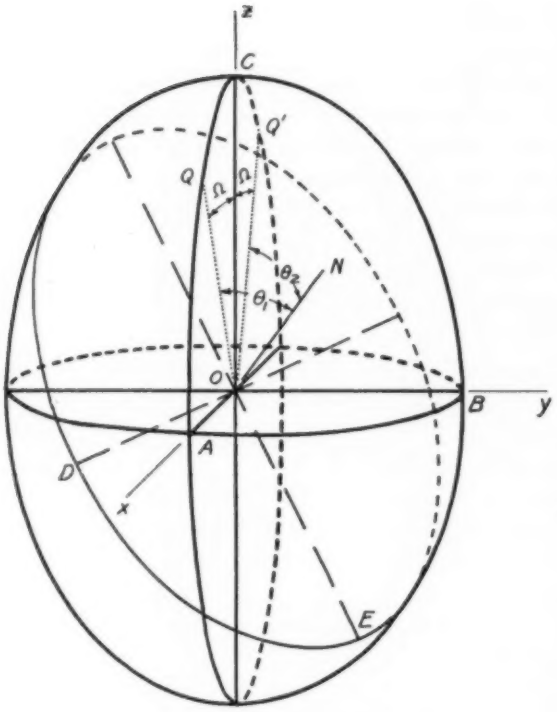


FIG. 8.3. Index ellipsoid.

*COA* are the *principal planes of optical symmetry*. These are analogous to the corresponding terms in the specification of stress and strain.

If light of wave-length $\lambda$ is passed at normal incidence through a crystalline plate of thickness $d$, the two resulting plane-polarized waves undergo *phase retardations*, $\Delta_1$ and $\Delta_2$, with respect to an unimpeded wave, given by

$$\left.\begin{aligned}\Delta_1&=\frac{2\pi d}{\lambda}(n_1-n)\\ \Delta_2&=\frac{2\pi d}{\lambda}(n_2-n)\end{aligned}\right\}, \tag{8.1}$$

where $n$ is the index of refraction of the medium outside the plate and $\Delta_1$ and $\Delta_2$ are measured in radians. Their relative phase difference, $\Delta$, is

$$\Delta=\Delta_1-\Delta_2=\frac{2\pi d}{\lambda}(n_1-n_2). \tag{8.2}$$

## 9. The Photoelastic Effect

It was discovered by Brewster in 1816 that glass, when stressed or strained, becomes optically doubly refracting, and it has since been found that this property is common in some degree to almost all transparent materials. Whether the phenomenon depends upon the stress or the strain is a matter of some difficulty which has not yet been satisfactorily settled. For the present we may observe that, as long as the stress and strain are linearly related, it is immaterial to which we refer the optical effect.

Maxwell observed[104] that, for a glass bar under simple tension (Fig. 7.1), the refracting properties of the material correspond to an index ellipsoid which is a prolatate spheroid. He determined, experimentally, that the axis of revolution of the spheroid is parallel to the direction of the tension and the ellipticity is proportional to the load. Thus we see that the principal axes of stress coincide with the principal axes of optical symmetry, and the principal stresses are linearly related to the principal indices of refraction. Hence, the relation between stress and double refraction is similar to that between stress and strain, with the exception that, whereas the components of strain vanish with removal of stress, the indices of refraction return to the original index, $n_0$, of the unstressed material. The optical properties which an originally isotropic material assumes on the application of stress may be visualized by imagining that the index ellipsoid is the result of the deformation of a sphere of radius $n_0$ subjected to a homogeneous field of principal stresses applied parallel to the principal axes of the ellipsoid. We may then write, by analogy with Eq. (7.1),

$$\left.\begin{aligned}n_a-n_0&=C_1\sigma_1+C_2(\sigma_2+\sigma_3)\\ n_b-n_0&=C_1\sigma_2+C_2(\sigma_3+\sigma_1)\\ n_c-n_0&=C_1\sigma_3+C_2(\sigma_1+\sigma_2)\end{aligned}\right\}, \tag{9.1}$$

in which $C_1$ and $C_2$ are the *stress-optical coefficients*.

Equations (9.1) are the fundamental relations connecting stress and optical effect.

The state of stress at any point may therefore be calculated if we can determine the principal indices of refraction and the directions of the principal axes of optical symmetry. In the general case, the experimental measurement of these data presents great difficulties; with the result that the photoelastic method has been confined, for the most part, to a state of stress for which, of the six required quantities (the magnitudes

and directions of the three principal stresses), three are known *a priori*. We proceed to study this special case in some detail.

## 10. Stresses in a Plane

In Eq. (3.1) the direction $N$ was unrestricted and we found three mutually perpendicular directions for which $\sigma_N$ has stationary values. Suppose, now, that we restrict $N$ so as to lie always in one plane. We can then show that there will always be two perpendicular directions in this plane for which $\sigma_N$ has stationary values and the shearing stress vanishes. These are the principal stresses and principal axes of stress for the particular plane under consideration. They coincide with two of the true principal stresses when the plane is a principal plane. Principal stresses in a plane other than a principal plane are called *secondary principal stresses*.

Let the plane under consideration be the plane of $x$, $y$, and let the direction $N$ in this plane make an angle $\theta$ with the positive $x$ axis; $\theta$ being measured positive in the counterclockwise direction from $x$ to $N$ (Fig. 10.1). Then, in Eq. (3.1), $l=\cos\theta$, $m=\sin\theta$, $n=0$ and we have

$$\sigma_N=\tfrac{1}{2}(\sigma_x+\sigma_y)+\tfrac{1}{2}(\sigma_x-\sigma_y)\cos 2\theta + \tau_{xy}\sin 2\theta. \quad (10.1)$$

Similarly, from Eq. (3.2), putting $l'=-\sin\theta$, $m'=\cos\theta$, $n'=0$,

$$\tau_{NS}=\tfrac{1}{2}(\sigma_y-\sigma_x)\sin 2\theta+\tau_{xy}\cos 2\theta. \quad (10.2)$$

To find the directions for which $\sigma_N$ has stationary values, differentiate Eq. (10.1) with respect to $\theta$ and set the result equal to zero, obtaining

$$(\sigma_x-\sigma_y)\sin 2\theta=2\tau_{xy}\cos 2\theta \quad (10.3)$$

as the equation for determining the values of $\theta$ for stationary values of $\sigma_N$. Note also that Eq. (10.3) is the condition for vanishing $\tau_{NS}$ (see Eq. (10.2)). To find the roots of Eq. (10.3), substitute

$$\cos 2\theta=\pm(1-\sin^2 2\theta)^{\frac{1}{2}}$$

and obtain

$$\sin 2\theta=\pm\frac{2\tau_{xy}}{[(\sigma_x-\sigma_y)^2+4\tau_{xy}^2]^{\frac{1}{2}}}. \quad (10.4)$$

Similarly

$$\cos 2\theta=\pm\frac{\sigma_x-\sigma_y}{[(\sigma_x-\sigma_y)^2+4\tau_{xy}^2]^{\frac{1}{2}}}. \quad (10.5)$$

The upper signs in Eqs. (10.4) and (10.5) give one value of $\theta$ which we shall call $\phi$. The lower signs give $\phi+\pi/2$. Hence $\phi$ and $\phi+\pi/2$ give the directions of the secondary principal stresses in the $x$, $y$ plane and

$$\sin 2\phi=\frac{2\tau_{xy}}{[(\sigma_x-\sigma_y)^2+4\tau_{xy}^2]^{\frac{1}{2}}},\qquad \cos 2\phi=\frac{\sigma_x-\sigma_y}{[(\sigma_x-\sigma_y)^2+4\tau_{xy}^2]^{\frac{1}{2}}}. \quad (10.6)$$

To find the magnitudes of the secondary principal stresses, substitute Eq. (10.6) in Eq. (10.1). Calling $p$ the stress obtained for $\phi$ and $q$ the stress for $\phi+\pi/2$, we have

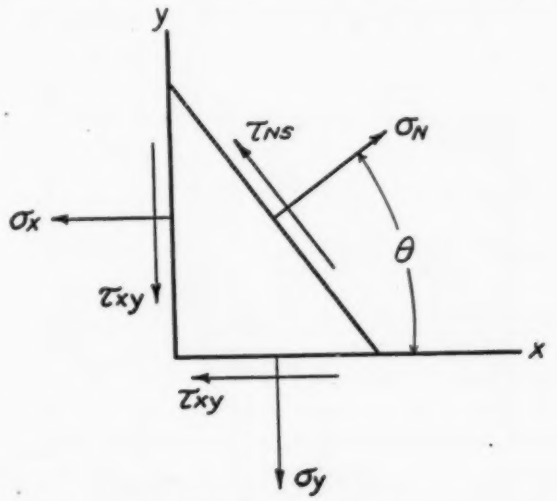


Fig. 10.1. Stresses in a plane.

$$p=\tfrac{1}{2}(\sigma_x+\sigma_y)+\tfrac{1}{2}[(\sigma_x-\sigma_y)^2+4\tau_{xy}^2]^{\frac{1}{2}}, \quad (10.7)$$

$$q=\tfrac{1}{2}(\sigma_x+\sigma_y)-\tfrac{1}{2}[(\sigma_x-\sigma_y)^2+4\tau_{xy}^2]^{\frac{1}{2}}. \quad (10.8)$$

Hence, the angle $\phi$ is identified with the algebraically larger secondary principal stress.

From Eqs. (10.6), (10.7) and (10.8),

$$\tau_{xy}=\tfrac{1}{2}\sin 2\phi[(\sigma_x-\sigma_y)^2+4\tau_{xy}^2]^{\frac{1}{2}} =\tfrac{1}{2}(p-q)\sin 2\phi. \quad (10.9)$$

Hence, the shearing stress in the $x$, $y$ plane is a maximum in directions bisecting the angles between the secondary principal axes, and its

magnitude is given by

$$\tau_{max}=\tfrac{1}{2}[(\sigma_x-\sigma_y)^2+4\tau_{xy}^2]^{\frac{1}{2}}=\tfrac{1}{2}(p-q). \quad (10.10)$$

Furthermore, the shearing stress $\tau_{xy}$ (Eq. (10.9)) vanishes when $\phi=0,\ \pi/2$ so that there is no shearing stress in the $x$ or $y$ directions on the planes across which the secondary principal stresses act. There may, in general, be shearing stresses $\tau_{xz}$, $\tau_{yz}$, but these, too, vanish in the important case of plane stress. This is a state of stress which is approximated in a thin plate loaded only by forces acting in the plane of the plate. Taking the $x$, $y$ plane as the middle plane of a plate of small thickness $d$, the components of stress $\sigma_z$, $\tau_{xz}$ and $\tau_{yz}$ must, of course, vanish when $z=\pm d/2$. If the thickness of the plate is very small in comparison with a representative linear dimension of the plate in the $x$, $y$ plane, it

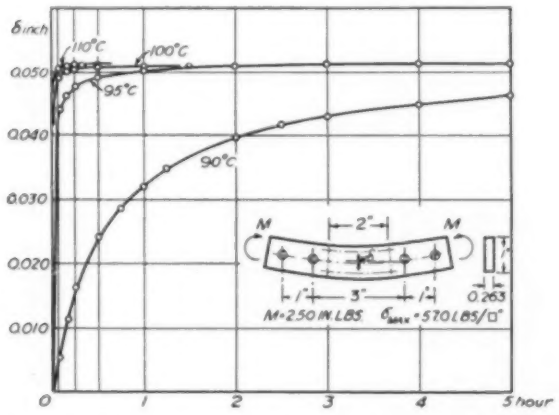


FIG. 12.1. Time-deflection curves for Bakelite BT 61-893 at elevated temperatures. See M. Hetényi, reference 78.

is found that it is reasonable to assume that $\sigma_z$, $\tau_{yz}$ and $\tau_{zx}$ vanish throughout the plate and that the variations of $\sigma_x$, $\sigma_y$ and $\tau_{xy}$ with the $z$ coordinate may be neglected.

## 11. Stress-Optical Relations for Two-Dimensional Photoelasticity

At each point in a plate loaded in its plane, at least one of the principal stresses has zero magnitude and its direction is normal to the plate. One principal plane of stress therefore coincides with the plane of the plate at each point. The two principal stresses in this plane may be $\sigma_3$ and $\sigma_2$ or $\sigma_2$ and $\sigma_1$ or $\sigma_3$ and $\sigma_1$; but, in any case, the two are denoted by $p$ and $q$, respectively.

Similarly, one principal plane of optical symmetry coincides with the plane of the plate. For light at normal incidence to the plate, the indices $n_1$ and $n_2$ of the two resulting waves are principal indices, and these may be $n_c$ and $n_b$ or $n_b$ and $n_a$ or $n_c$ and $n_a$.

With these conventions, Eqs. (9.1) reduce to

$$\left.\begin{aligned} n_1-n_0&=C_1p+C_2q\\ n_2-n_0&=C_1q+C_2p\end{aligned}\right\}. \quad (11.1)$$

Hence, if we measure the absolute phase retardations, $\Delta_1$ and $\Delta_2$ (Eqs. (8.1)), we can calculate the principal stresses $p$ and $q$ from Eqs. (11.1). On the other hand, if we measure the relative phase retardation, $\Delta$ (Eq. (8.2)), we can calculate the *principal stress difference* $p-q$; for, from Eqs. (8.2) and (11.1) we have

$$\Delta=\frac{2\pi dC}{\lambda}(p-q), \quad (11.2)$$

in which $C=C_1-C_2$ is the *relative stress optical coefficient*.

Finally, if we determine the directions of the principal axes of optical symmetry, we shall have the directions of the principal stresses.

It should be noted that at an unloaded boundary of the plate, two of the three principal stresses vanish, namely, the one normal to the plane of the plate and the one normal to the boundary. Furthermore, the third principal stress acts parallel to the boundary. At such a boundary, then, measurement of the *relative* phase difference (Eq. (11.2)) gives directly all the data necessary for complete specification of stress.

The coefficient $C$ in Eq. (11.2) has the same dimensions as the reciprocal of a stress. It is usually expressed in units of $10^{-13}$ cm$^2$/dyne, one such unit being called a brewster.* For a given material $C$ is found to vary with the wave-length and the temperature.

## *Part II. Materials, Model and Loading Machines*

## 12. Photoelastic Materials

The first step in a photoelastic analysis is the selection of a suitable material from which to fashion the model. Among the desirable properties listed by Filon,[6] Carleton,[43] and Solakian[145]

* See reference 5, page 185.

for an ideal material are: (1) High stress-optical coefficient, (2) good machinability, (3) linear stress-strain relation, (4) high modulus of elasticity, (5) physical and optical homogeneity, (6) absence or easy removal of initial double refraction, (7) absence of creep, (8) absence of permanent set and residual double refraction, (9) absence of "edge effect" and (10) high transparency.

The materials which have been used most often are glass, Celluloid (nitrocellulose), Bakelite BT 61-893 (glycerine phthallic anhydride), Phenolite and Trolon (phenol-formaldehyde resins). Glass was the first material to be used in photoelastic experiments. It is difficult to cut to prescribed shapes and has a very low value of $C$, but it possesses the remaining desirable qualities to such a high degree that it is often used to great

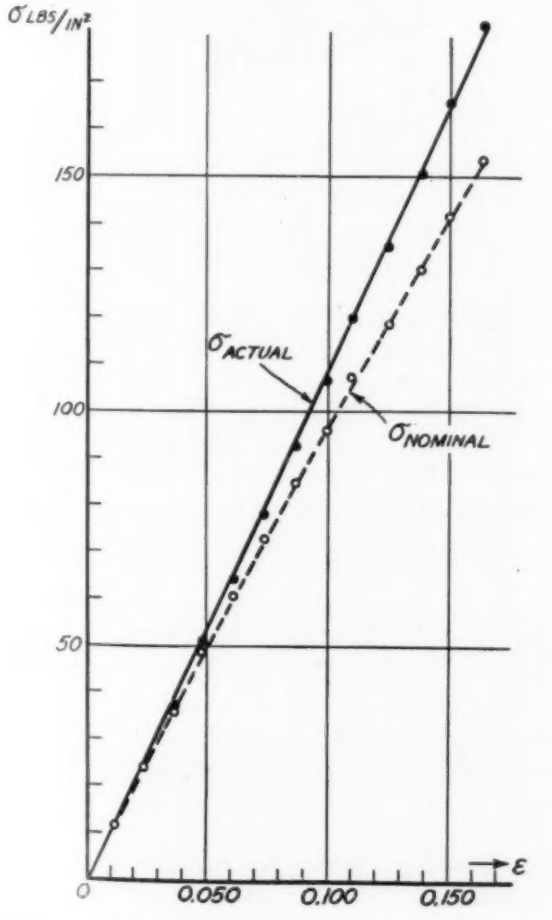


FIG. 12.2. Stress-strain curve for Bakelite at 115°C. See M. Hetényi, reference 78.

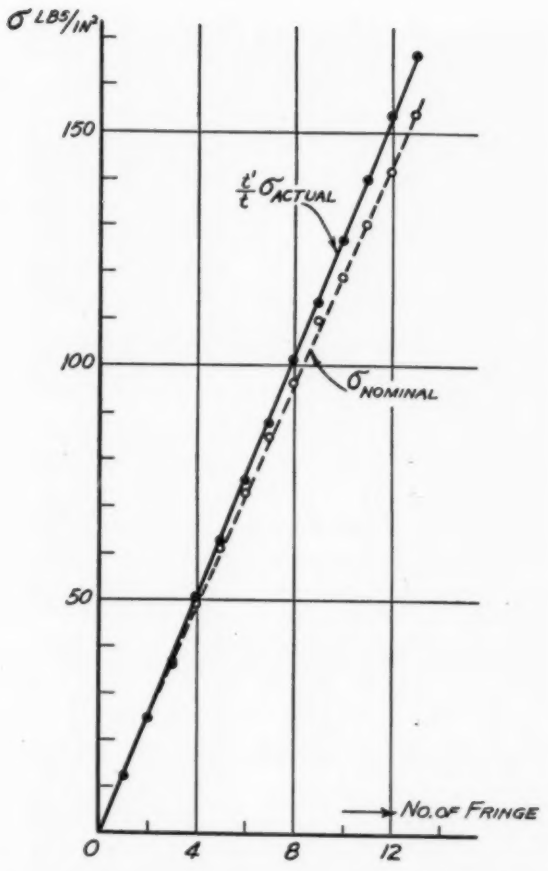


FIG. 12.3. Stress-fringe-order curve for Bakelite at 115°C. See M. Hetényi, reference 78.

advantage in precision experiments. It is especially useful for some of the modern interferometer techniques (see Section 27). Celluloid, with a stress-optical coefficient about five times that of glass, and with good machinability, was the standard photoelastic material from 1906 to 1923, when a phenolic Bakelite resin, with a stress-optical coefficient five times that of Celluloid, was used by Arakawa.[20] In the last fifteen years the materials with high optical sensitivity have gradually displaced the others in the majority of photoelastic experiments.

Carleton[49] gives (Table I) the values of the relative stress optical coefficient ($C$) in brewsters (for $\lambda = 5461$A) for thirteen materials which have been used in photoelasticity. These values are all approximate, the variations for any one material depending upon the temperature and the previous thermal and chemical history. The effect of temperature has been investigated for glass by

Harris;[75] for Celluloid by Harris and Seth;[76] for five varieties of Bakelite and for Marblette by Lee and Armstrong;[96] for Bakelite by Hetényi;[77, 78] and for Trolon by Kuske.[93]

Carleton[43] pointed out the great influence on the stress-optical coefficient of the degree of polymerization of the synthetic resins. The principles underlying this phenomenon have been better understood as the result of the work of Hetényi[77, 78] and Kuske.[93] Hetényi's experiments on Bakelite BT–61–893, and his interpretations of them in the light of the diphase theory of hardening resins, have done much to clarify our ideas of initial and residual double refraction, temperature effects, creep, elastic properties and edge effect.

According to the diphase theory, the hardened resin used in photoelastic tests is composed of two constituents, an infusible three-dimensional skeleton embedded in a fusible matrix. The infusible part constitutes only a small portion of the total volume. It was originally formed from the fusible part by the chemical action called polymerization which continues at a very slow rate.

At room temperatures the fusible part has a high viscosity coefficient and carries most of the load applied to the model; but at elevated temperatures the viscosity coefficient decreases so that the fusible part flows and gradually transfers the load to the infusible skeleton. The deformation under constant load therefore approaches a limiting value which is determined by the percentage of polymerized material and its elastic properties. The higher the temperature, the higher will be the creep rate of the fusible part and the more rapidly will the limiting deformation be reached, as is indicated in Hetényi's experimental curves, Fig. 12.1. At a temperature of 115°C, the limiting deformation is reached almost instantaneously for Bakelite BT–61–893.

TABLE I.

| | |
|---|---|
| Phenolite (Japan) | 56.8 |
| Bakelite (U.S.A.) | 50.2 |
| Bakelite (England) | 46.4 |
| L'Orca (France) | 39.3 |
| Celluloid | 12.8 |
| Cellulose acetate | 19.5 |
| Pollopas | 17.5 |
| Charmoid | 20.6 |
| Vinylite | 18.0 |
| Glyptal | 28–1000 |
| Glass (plate) | 2.7 |
| Rubber (soft) | 2000 (approx.) |
| Rubber (hard) | 106 |

That the polymerized skeleton is linearly elastic is demonstrated by Hetényi's stress-strain data at 115°C shown in Fig. 12.2. The linearity of the optical effect is illustrated in Fig. 12.3.

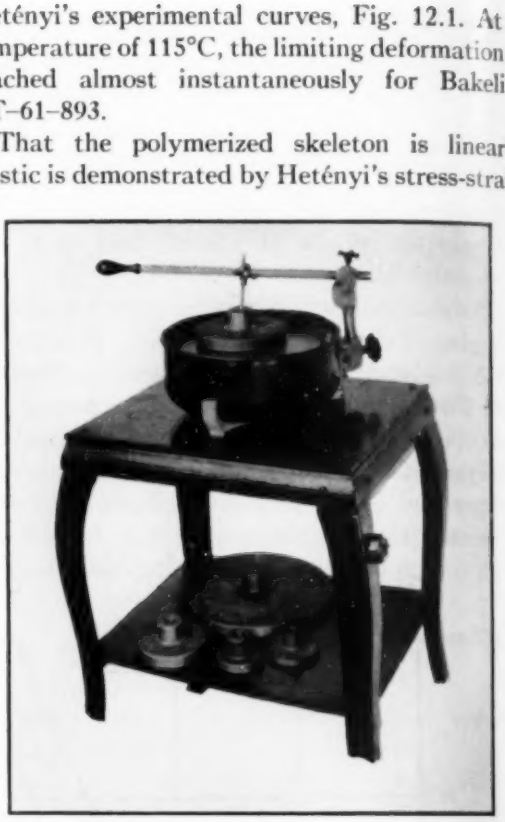

FIG. 13.1. Optical polishing machine.

The application of these phenomena to the photoelastic analysis of three-dimensional stress systems will be discussed in Section 34.

Concerning the explanation of the photoelastic effect from the atomic physics viewpoint, reference should be made to the work of Mueller.[115]

## 13. THE MODEL

In the last few years Bakelite BT–61–893 has become the standard model material in this country. It is supplied in the form of rectangular plates about 6″ by 12″ and in thicknesses ranging from ¼″ to 1″. It has become customary to cut models from those portions of the plate which are free of initial double refraction rather than to attempt annealing. For a recent discussion of the annealing process, see a paper by Kuske.[94]

The faces of the model are first made approximately plane and parallel by hand surfacing with

emery cloth, or by milling, or by surfacing on a lathe, or by grinding on an optical surfacing machine (Fig. 13.1). Excellent results are obtained by the last method, using cast iron laps and a speed of about 250 r.p.m. starting with No. 150 carborundum grain and working down through No. 240,400,600. The plate is then ready to be polished on the same machine with a cloth covering the lap and rouge as the polisher. In some laboratories the model surface is machined but not polished. The machining ridges are eliminated from the optical image by immersing the model in a fluid of the same index of refraction, or by coating the surface with oil, or by lacquering the surface. Fig. 13.2 shows a comparative study of the image appearance for four kinds of surface treatment.

The plate is cut roughly to shape with a hand or power jig saw, but the final cutting must be done more carefully. The tools used for final cutting vary with the preference of the technician

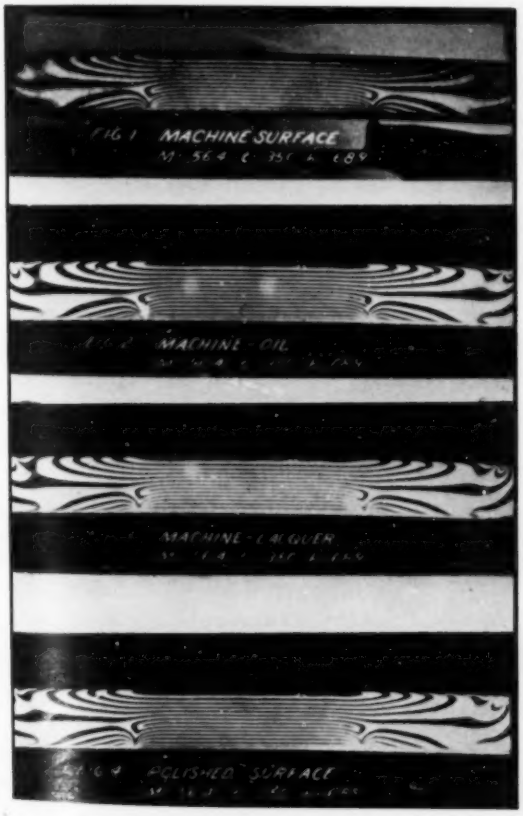


FIG. 13.2. Comparative study of image appearance due to different surface treatments. W. N. Bell and J. K. Bussey, California Institute of Technology.

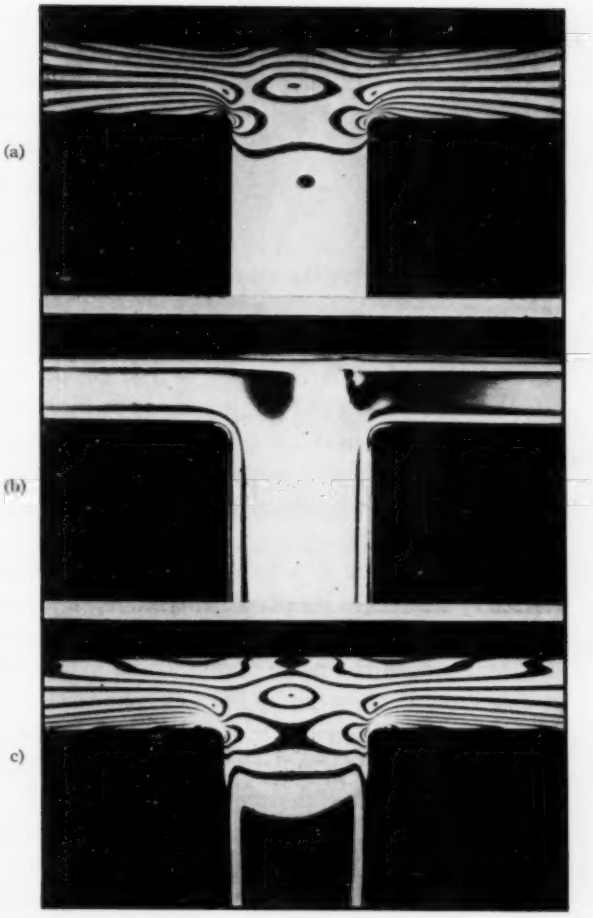


FIG. 13.3(a). Fringe photograph of model with very small "edge effect." D. C. Drucker, Columbia University. (b). Photograph of same model 8 months later, showing "edge effect," with model unloaded. (c). Showing influence of "edge effect" on fringe pattern of loaded model.

and the shape of the model. In any case, it is desirable (a) to avoid heating the material unduly, (b) to form sharp edges and (c) to have the boundary surfaces accurately normal to the faces of the plate. If these precautions are taken, the edges of the model image will be sharp and clear. In many laboratories, straight edges are cut on a milling machine using sharp cutters and lard oil lubrication. Circular holes are cut on a lathe rather than with a twist drill in a drill press. When the shape of the model is irregular, good results may be obtained by careful filing.

The model should be used within a few hours after the edges are cut in order to avoid diffi-

culties with "edge effect." This is a little understood phenomenon which makes its appearance in the form of a considerable amount of double refraction at the edges which increases with time, is accelerated at elevated temperatures, and is retarded by absence of air. According to Hetényi,[78] it may be due to (a) progressive polymerization of the material, (b) evaporation of combined or absorbed water, causing uneven shrinking, or (c) oxidation of the surface layers. The same effect is also found immediately after cutting the edges if the tool is dull or poorly lubricated, or if the cutting speed is too high; all of which tend to heat the material. Photographs of the results obtained in a model with and without edge effect are shown in Figs. 13.3(a), (b) and (c).

If the prototype is a two-dimensional system statically loaded in its plane, the model is made geometrically similar in all its dimensions except the thickness of the plate about which more will be said later. A theorem by Michell* shows that a two-dimensional stress system not involving body forces is independent of the elastic constants of the material except in the case of a multiply connected plate with a resultant force on an internal boundary. In the latter case, Filon† has given a method for making corrections

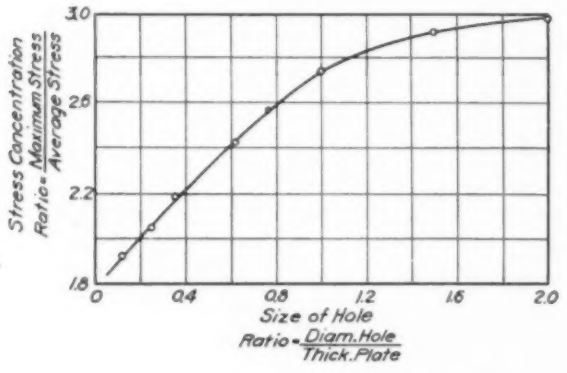


FIG. 13.4. Variation of stress-concentration with size of hole in a tension plate. See R. W. Vose, reference 175.

to the observed stresses involving an auxiliary photoelastic experiment of some difficulty. However, in a particular case which he examined mathematically, Filon found that the correction is small.

Concerning the thickness of the model, we recall (Section 10) that a true state of plane stress is only approximately simulated in a plate; however, the smaller the thickness of the plate in comparison with a representative linear dimension in the plane of the plate, the closer is the similarity. It is also true that the larger the thickness of the plate, in comparison with a representative linear dimension in the plane of the plate, the closer does the stress distribution approach a state of *plane strain*. It is only when the thickness and other dimensions of the plate are of the same order of magnitude that a two-dimensional state of stress is not, in general, realized. In a plate having a hole or fillet, a representative linear dimension in the plane of the plate in the neighborhood of the hole or fillet is its radius of curvature. When the latter is of the same order of magnitude as the plate thickness, neither a state of plane stress nor plane strain is, in general, produced. In such a case it is reasonable to expect that stress concentration factors obtained photoelastically will not coincide with those obtained from the two-dimensional mathematical theory. This has been studied experimentally for the circular hole by Vose[175] and the results are given in Fig. 13.4.**

If the thickness is included in the geometrical similarity relations between prototype and model, it is likely that the photoelastic results will be more reliable than the two-dimensional mathematical theory. No verification of these conclusions, other than for the two limiting cases mentioned, can be drawn from the mathematical theory because a solution has not been found for a hole in a plate of finite thickness.

## 14. Loading Machines

An ideal apparatus for applying forces to the model would include (1) adaptability to a wide variety of loading systems, (2) large, unobstructed passage for the optical field, (3) ade-

* Reference 5, page 518.
† Reference 5, page 521.

** It would seem that the stress concentration factor should approach the value 3 for *both* very large holes (plane stress) and very small holes (plane strain). The discrepancy in Fig. 13.4 is explained by noting that Vose measured the change in thickness of the plate rather than optical double refraction.

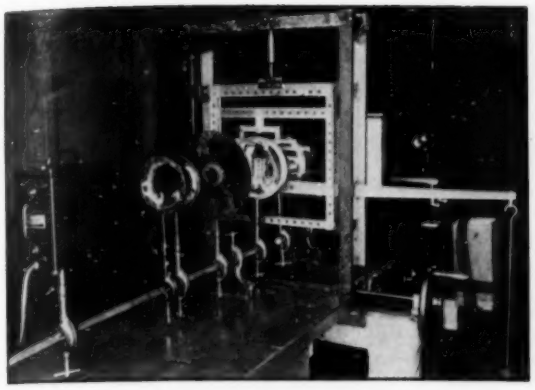

FIG. 14.1. Photoelastic polariscope and loading machine (University of Illinois).

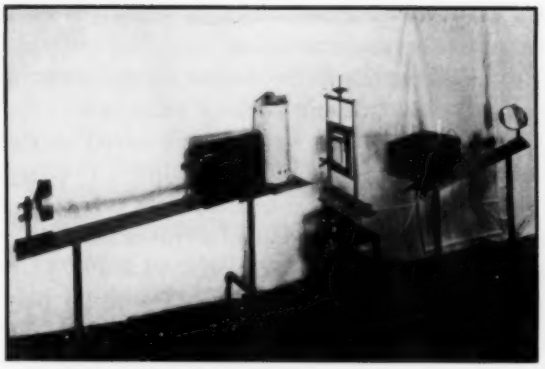

FIG. 14.2. Photoelastic polariscope with reflectors replacing lenses. (U. S. Bureau of Reclamation.)

quate range of load (0 to 1000 pounds), (4) suitable load measuring devices (accurately calibrated springs or lever loading, or both), (5) provision for continuous increase and decrease of loading, (6) provision for remote control of loading so that operator may observe formation of fringes, (7) provision for relative motion of loading machine and optical apparatus for examination of models larger than the optical field.

These requirements have necessitated the design of special loading machines for photoelastic installations. Some typical machines which include many of the desired features are illustrated in Figs. 14.1 to 14.3 and on pages 208 and 223.

## *Part III. Measurement of the Difference Between and the Directions of the Principal Stresses*

### 15. MEASUREMENT OF $\phi$ AND $p-q$

Under this heading are included optical devices and procedures for measuring directions of polarization and relative phase retardation; for, as we have seen in Section 11, the former give the principal stress directions and the latter gives the principal stress difference. The fundamental components of the photoelastic polariscope are as follows.

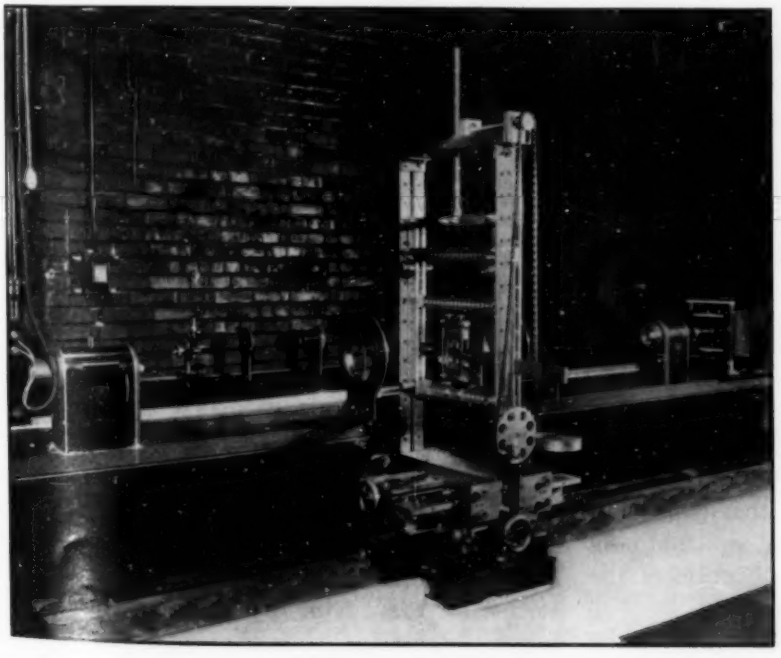

FIG. 14.3. Photoelastic polariscope and loading machine (Timken Roller Bearing Co.).

(a) *Light source.*—Both homogeneous (monochromatic) and nonhomogeneous are required. The mercury vapor lamp with a 5461A filter is widely used as a monochromatic source. For the nonhomogeneous source, the mercury lamp without its filter is sometimes used, but an incandescent filament lamp is preferable.

(b) *Polarizer and analyzer.*—Calcite prisms (Nicol, Glan-Thompson, Halle, etc.), Polaroid plates, and reflec-

tion from or refraction through glass plates at the polarizing angle are used.

(c) *Viewing device.*—Screen (translucent or opaque), photographic plate or telescope.

In addition, a lens system is required so that the model is in a field of parallel light. For large diameter fields, the cost of the lenses is high, and they have been replaced in a few installations[40, 72] by spherical reflectors (see Figs. 14.2 and 15.1).

The usual arrangement of the essential parts is illustrated schematically in Fig. 15.2(a). The intensity of monochromatic light transmitted through such a system with polarizer and

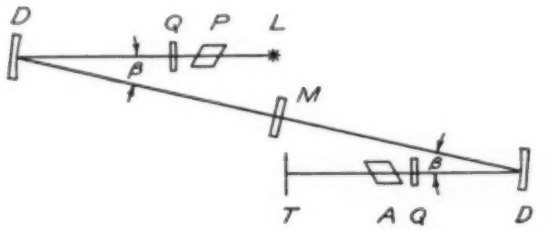


FIG. 15.1. Schematic diagram of photoelastic polariscope with reflectors (California Institute of Technology).

analyzer crossed is (neglecting reflection and absorption losses)

$$I = I_0 \sin^2 2\phi \sin^2 (\Delta/2), \qquad (15.1)$$

in which $\phi$ is the angle which the polarization direction of the faster moving wave in the model makes with the polarization direction of the incident light, and $\Delta$ is the relative phase retardation for a point of the model. Eq. (15.1) is the intensity equation for the *plane polariscope*, so called because the light incident on the model is plane polarized.

Considering any one point of the model, Eq. (15.1) shows that, as the plane of polarization of the light incident on the model is rotated (keeping the Nicols crossed), extinction of light will be observed when $\phi$ is an integral multiple ($m$) of $\pi/2$. These positions determine the directions of the principal stresses $p$ and $q$ at that point; but it is not yet known which of the two mutually perpendicular directions is the direction of the algebraically larger principal stress.

Still confining our attention to one point of the model, we see by Eq. (15.1) that, if we fix the plane of polarization at an angle of 45° with the principal axes of stress, the intensity will be given by

$$I = I_0 \sin^2 (\Delta/2). \qquad (15.2)$$

Since, from Eq. (11.2), $\Delta$ is directly proportional to $p-q$, the intensity of monochromatic light will vary cyclically through dark and light as the load on the model is increased. Knowing the number of cycles, the principal stress difference may be calculated from Eq. (11.2) provided the wave-length ($\lambda$), the thickness ($d$) and the stress optical coefficient ($C$) are known. The last may be determined from an auxiliary simple tension specimen for there we know that $p-q$ is equal to the tensile stress in the bar so that we may solve Eq. (11.2) for $C$. This method, when applied to the simultaneous observation of the entire stress field is known as the *fringe method*.

When $\Delta$ is small, the method of counting intensity cycles lacks precision. Some of the alternative methods which have been used are color comparison, the tension compensator, the quarter-wave plate compensator, the quartz wedge compensator, and the spectroscopic analyzer.

### Color comparison

If we substitute a white light source for the monochromatic source, only certain wave-lengths will be extinguished for a given value of $p-q$, the remainder being partly or completely transmitted. The latter combine to produce a color stimulus to the eye and, for a given light source, polariscope and model material, there is a characteristic color for each value of $p-q$, which may be determined by a simple tension experiment. The value of $p-q$ at a point in the model may then be determined by matching the color at that point with the color scale found with the tension experiment. A detailed analysis of the observed colors is given by Baud and Wright.[27] The method is, again, lacking in precision and is now obsolete, but a white light source is still useful for at least three purposes. First, the only value of $(p-q)$ for which all wave-lengths are extinguished is $p-q=0$, so that we thus have a means for identifying points in the model for which the principal stresses are equal. Second, all wave-lengths are also extinguished when $\phi$ is an integral multiple of $\pi/2$; a feature which is

useful in examining the isoclinic lines (see Section 17). Third, for demonstration purposes, such as projection on a large screen in the classroom or auditorium, the white light source gives a much brighter image than any monochromatic source now available.

### Tension compensator

In a method originated by Wertheim[180] and later developed by Coker,[44] a tension bar is placed in the polariscope between the model and the analyzer (Fig. 15.2(b)). The bar is of the same material and thickness as the model and its axis is oriented so as to be parallel to a principal stress direction of the point in the model under examination. It is also desirable to have the plane of polarization of the incident light at 45° to the principal axes in the model, since, from Eq. (15.1), this position gives maximum intensity. If the axis of the bar is parallel to the direction of the algebraically smaller principal stress, then, as the tension in the bar is gradually increased, the observed colors with white light will progress down the scale of colors until extinction is reached; at which point the tension in the bar is equal to $p-q$ for the point in the model. This procedure serves the double purpose of determining $p-q$ and also determining which polarization direction in the model corresponds to the algebraically larger and which to the algebraically smaller principal stress.

### Quarter-wave plate compensator

The determination of fractional relative phase retardations at a point in the model may be achieved by using a doubly refracting plate of one quarter-phase relative retardation as a compensator (de Senarement compensator). In this method, the Nicols are not maintained in the crossed position, but both the analyzer and the quarter-wave plate are rotated independently to adjust for settings giving maximum and minimum intensity. From these positions the shape and orientation of the elliptical vibration which emerges from the model may be determined.* This information yields the required values of $\phi$ and $\Delta$. The quarter-wave plate is also used to distinguish between the directions of the algebraically larger and smaller principal stresses. This corresponds to the determination of the fast and slow axes of a doubly refracting plate or the determination of the optical character of a crystal.**

### Quartz-wedge compensator

Instead of varying the retardation of the compensator by varying its double refraction (as in the tension compensator), the same effect may be obtained by varying the thickness. This is accomplished by sliding a crystal wedge (usually quartz) across the field by means of a micrometer screw. Again, the compensator (Babinet or Babinet-Soleil) is adjusted so that its phase retardation is equal and opposite that of the

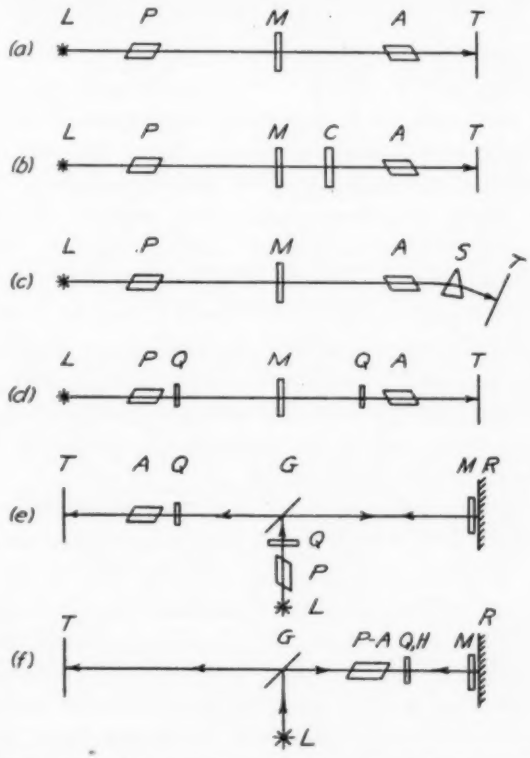


FIG. 15.2. Arrangements of the essential parts of a photoelastic polariscope. (a) Plane polariscope, (b) plane polariscope with compensator, (c) plane polariscope with spectroscopic analyzer, (d) circular polariscope, (e) Nörrenberg doubler, and (f) reflection polariscope.

| | |
|---|---|
| $L$ = Light source | $S$ = Prism |
| $P$ = Polarizer | $Q$ = Quarter-wave plate |
| $A$ = Analyzer | $G$ = Glass plate |
| $M$ = Model | $R$ = Reflector |
| $T$ = Screen | $H$ = Half-wave plate |
| $C$ = Compensator | $D$ = Spherical reflector. |

* G. Szivessy, *Handbuch der Physik* (Julius Springer, Berlin, 1928), p. 936.

** A. Johannsen, *Manual of Petrographic Methods* (McGraw-Hill Book Co., New York, 1918), p. 361.

model. The Babinet-Soleil compensator used with a half-shadow plate† is a very accurate instrument for measuring relative phase difference.

### Spectroscopic analyzer

If we examine Eqs. (8.2) and (11.2), we see that, in addition to varying $(n_1-n_2)$, $(p-q)$ and $d$, we may also vary the wave-length $\lambda$ to obtain variations of relative phase difference $\Delta$ in our compensator device. This is accomplished by placing a spectrometer in the field of the polariscope,* (Fig. 15.2(c)), and observing extinction bands in the white light spectrum.

### Large field polariscopes

We have, so far, considered methods which are mainly suitable for examining the model point by point. In engineering work it is often desirable to obtain a picture of the stress field as a whole. For a particular orientation of the model with respect to the plane of polarization, extinction of light will be observed at all points where the axes of principal stress are parallel or perpendicular to the plane of polarization. These points will be connected by a dark band called an *isoclinic*. In addition, with monochromatic light and crossed Nicols, dark bands will be observed wherever the relative phase retardation is a multiple of $2\pi$. The latter are called *isochromatics* and they are curves of constant difference between principal stresses. The optical field is thus covered by two sets of superimposed dark bands.

In our point-by-point methods with plane-polarized light we were able to avoid the extinction position corresponding to an isoclinic by setting $\phi$ equal to 45°, thus obtaining Eq. (15.2) for the intensity; but in a stress field in which the principal stress directions vary, it is not possible to do this for the entire field at once in the plane polariscope. However, the isoclinics may be eliminated by placing quarter-wave retardation plates on either side of the model with their polarizing axes at 45° to the planes of polarization and analyzation (Fig. 15.2(d)). Such an apparatus is called a *circular polariscope*. The intensity equation for the entire field is then given by Eq. (15.2), and the only curves of constant principal stress difference will appear in the field.

If the two auxiliary retardation plates are not accurately quarter-wave plates for the monochromatic source, Baud[25] has shown that the intensity is given by

$$I = I_0(1-\cos^2 2\phi \cos^2 \Delta_0) \sin^2 (\Delta/2), \quad (15.3)$$

where $\Delta_0$ is the phase retardation for the (identical) retardation plates. Eq. (15.3) shows that the only effect of identically inaccurate retardation plates with monochromatic light is that the isoclinics are not completely removed. Baud[25] has used Eq. (15.3) to show that for *white light* the isochromatics are slightly distorted in a circular polariscope. If the phase retardations $\Delta_0'$ and $\Delta_0''$ of the two auxiliary plates are not only different from $\pi/2$ but are different from each other, the intensity equation is given by[112]

$$I = I_0\Big\{\sin^2\frac{\Delta}{2}[\cos(\Delta_0''-\Delta_0') - \cos^2 2\phi \cos\Delta_0' \cos\Delta_0'']$$
$$+\sin^2\frac{\Delta_0''-\Delta_0'}{2} - \tfrac{1}{2}\sin\Delta\sin 2\phi \times\sin(\Delta_0''-\Delta_0')\Big\}, \quad (15.4)$$

showing that in this case the isochromatics are distorted even with monochromatic light.[113] All of these effects, however, are very small and need only be considered in experiments of extreme precision.

The Nörrenberg doubler (Fig. 15.2(e)) is a useful optical system distinguished by the fact that the polarized light passes through the model twice, thus doubling the retardation. G. Mabboux[98] has taken advantage of the fact that there is only a reflecting surface behind the model in this arrangement so that he was able to embed small photoelastic plates, backed by reflectors, in the surface of a concrete structure, and, by measuring the double refraction in the plates, determine the stresses in the structure. The fact that the relative retardation is doubled in the Nörrenberg system has been used by many experimenters to increase precision in the measurement of weak double refraction.

Another type of doubler known as a reflection polariscope[111] is illustrated in Fig. 15.2(f). In this

† See G. Szivessy, *Handbuch der Physik*, Vol. 19, pp. 935–953, for this and other methods for measuring phase difference.

* Reference 5, page 220.

instrument a single polarizing device is used as both polarizer and analyzer.

## 16. Isochromatics

We have seen that, in the circular polariscope, extinction of monochromatic light occurs when the phase retardation $\Delta$ is an integral multiple, $n$, of $2\pi$. Hence, from Eqs. (10.10) and (11.2), a monochromatic fringe or isochromatic line is the locus

$$(\sigma_x-\sigma_y)^2+4\tau_{xy}^2=(p-q)^2=(n\lambda/dC)^2. \quad (16.1)$$

The number $n$ is called the *fringe order* and is a measure of the relative magnitude of $p-q$. For example, the principal stress difference along the sixth-order fringe is three times the principal stress difference along the second-order fringe. The fringe order at any point is the number of intensity cycles through which the point passes during the gradual loading of the model. Fig. 16.1 shows the fringes around a small hole in a plate under simple tension.

With white light we have seen that all the isochromatics are colored except the zero order, which is black. When $n=0$, that is, when the principal stresses $p$ and $q$ are equal, Eq. (16.1) shows that

$$\sigma_x-\sigma_y=0, \quad (16.2)$$

$$\tau_{xy}=0. \quad (16.3)$$

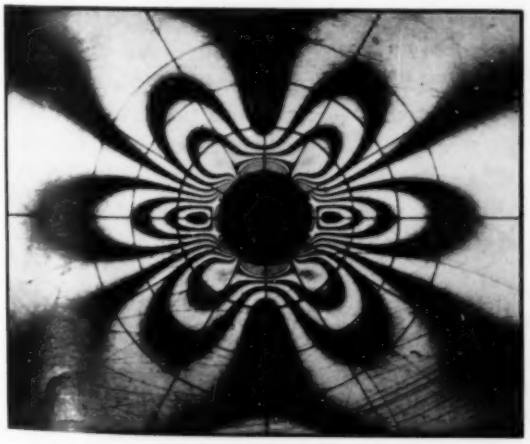

Fig. 16.1. Isochromatics around a small hole in a plate under simple tension. (W. M. Murray, Massachusetts Institute of Technology.)

Each of these is the equation of a curve and in general the two curves will intersect only at isolated points. Hence the zero isochromatic is usually observed as an isolated black spot known

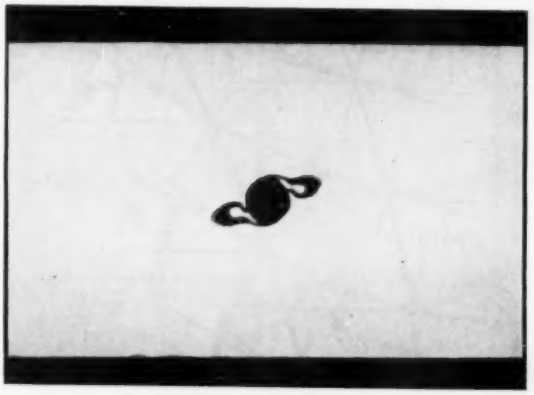

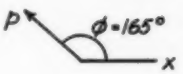


Fig. 17.1. 165° isoclinic for the stress field around a small hole in a tension plate.

as an *isotropic point*. An example of a fringe pattern with four isotropic points is shown in Fig. 13.3(a).

## 17. Isoclinics

We have observed, Eq. (15.1), that in a plane polariscope, extinction of light occurs when $\phi$ is an integral multiple, $m$, of $\pi/2$. Hence the equation of the isoclinic curve along which the angle $\phi$ is a constant, is, from Eqs. (10.6),

$$\tan 2\phi=\frac{2\tau_{xy}}{\sigma_x-\sigma_y}. \quad (17.1)$$

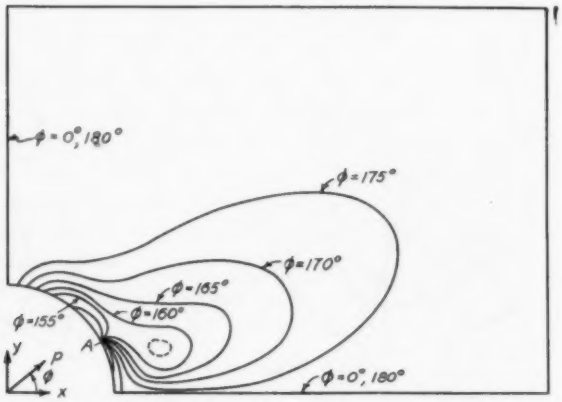


Fig. 17.2. Sketch of isoclinics around a small hole in a tension plate (only one-quarter of the field is shown).

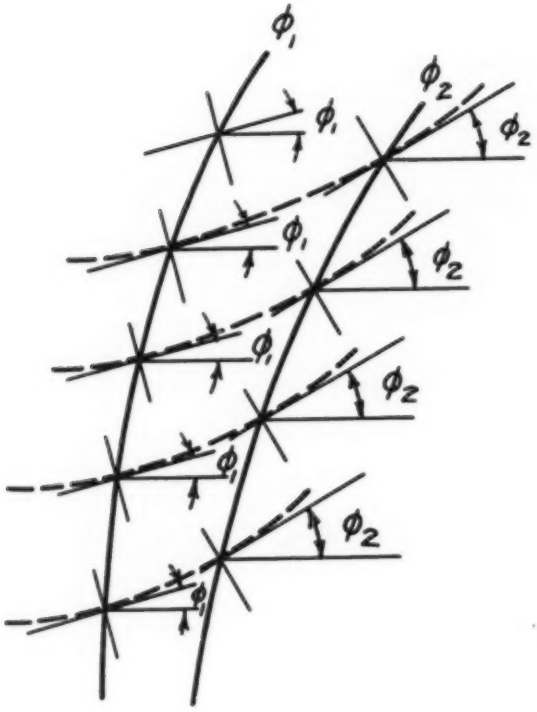


FIG. 18.1. Construction of isostatics from isoclinics.

Thus the isoclinic of parameter $\phi = \phi_1$ is the locus of points in the model for which the direction of $p$ makes an angle $\phi_1$ with the $x$ axis; $\phi_1$ being at the same time the angle which the direction of polarization of the incident light makes with the $x$ axis (Fig. 17.1). When we rotate the plane of polarization to a new orientation $\phi = \phi_2$ (keeping the Nicols crossed), the isoclinic moves to a new locus along which $p$ makes an angle $\phi_2$ with the $x$ axis. By recording the isoclinics for successive increments of $\phi$ between 0 and $\pi/2$, the orientations of the axes of principal stress are determined throughout the model (Fig. 17.2).

## 18. ISOSTATICS

An important set of curves which may be constructed graphically from the isoclinics are the *isostatics* or *stress trajectories*. An isostatic is a curve whose tangent and normal at any point coincide with the principal stress directions at that point. The construction of these curves is illustrated in Fig. 18.1. Crosses are marked along the isoclinics with the arms of the crosses oriented in the respective directions of the principal stresses for each isoclinic. The isostatics are then faired, free hand, through the isoclinics so that each isostatic is tangent to an arm of a cross when passing through an isoclinic.

An ingenious method for obtaining a photograph of the isostatics directly in the polariscope has been described by Biot.[31]

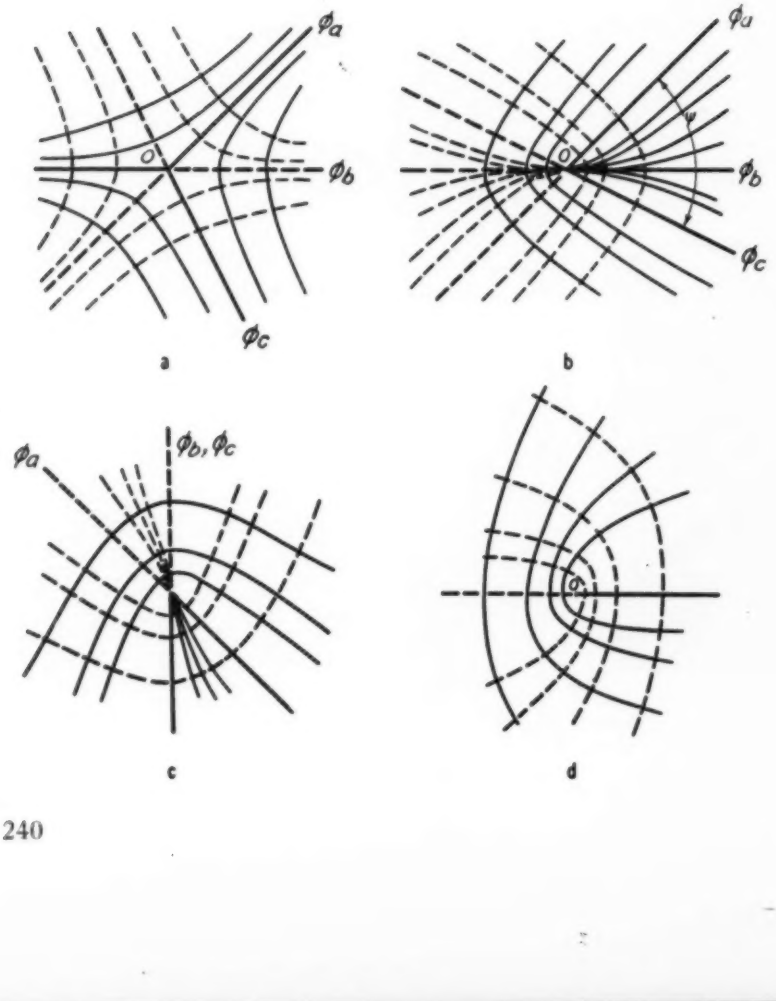


FIG. 19.1. First-order isotropic points. (*a*) Case I(*a*) three asymptotes. (b) Case I(*b*) three asymptotes, $\psi < \pi/2$. (c) Case I(*c*) two asymptotes. (d) Case II, one asymptote.

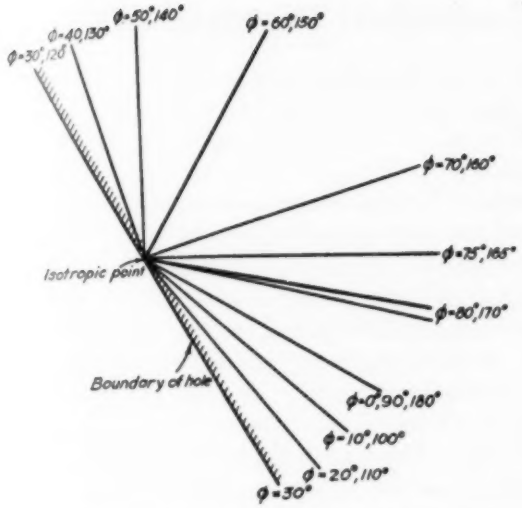


FIG. 19.2. Enlarged view of isoclinics in the neighborhood of point $A$, of Fig. 17.2.

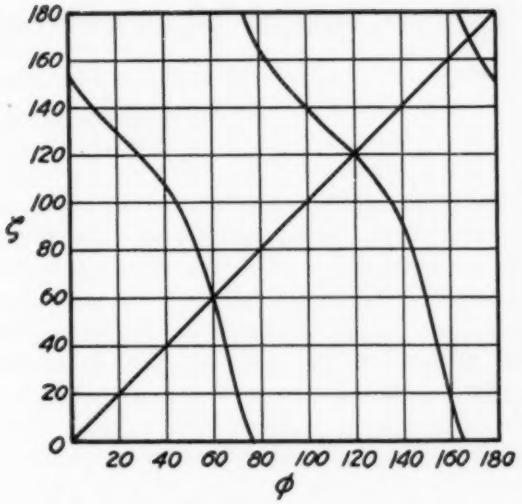


FIG. 19.3. Determination of asymptotic directions for isoclinics of Fig. 19.2.

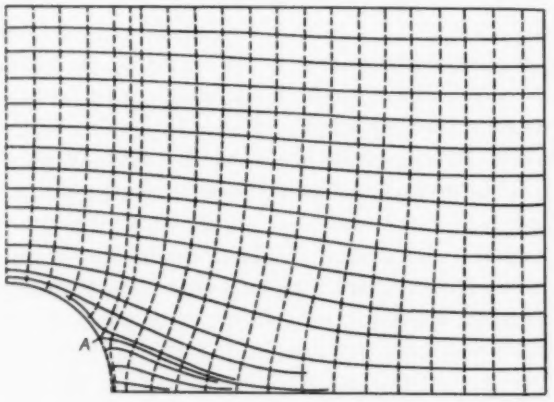


FIG. 19.4. Stress trajectories from isoclinics of Fig. 17.2.

## 19. ISOTROPIC POINTS

At an isotropic point we find, substituting Eqs. (16.2) and (16.3) in Eq. (17.1), that the parameter of the isoclinic is indeterminate. Hence all isoclinics pass through an isotropic point and there is some difficulty in constructing the isostatics in the neighborhood of such a point.

Filon,[59] Föppl and Neuber,[9] and Von Mises[173] have shown that the configuration of the isostatic curves in the neighborhood of an isotropic point depends upon the number and orientation of the directions through the point for which a tangent to the isoclinic makes an angle with the $x$ axis equal to the parameter of the isoclinic. There are one, two or three such *asymptotic directions* in the cases which occur most often. These types, with their corresponding isostatics, are illustrated in Fig. 19.1, in which the asymptotic directions are drawn in heavy lines. The four types are readily distinguished from one another except, perhaps, for Cases I$a$ and I$b$. Case I$b$ differs from case I$a$ in that, in the former, there is an angle $\psi$ less than $\pi/2$ between two asymptotic directions ($\phi_a$ and $\phi_c$) which include a third ($\phi_b$).

To determine to which type a particular isotropic point belongs, it is necessary to find the asymptotic directions. As an illustrative example, we shall consider the isotropic points which occur at the boundary of a circular hole in a wide plate under simple tension. There are four such points, one of them occuring at point $A$ in Fig. 17.2. In Fig. 19.2, the isoclinics through $A$ are drawn to an enlarged scale. Calling $\zeta$ the angle which the isoclinic through $A$ makes with the $x$ axis, we plot a graph for which the parameter $\phi$ of the isoclinic is the abscissa and $\zeta$ is the ordinate (Fig. 19.3). A line $\phi=\zeta$ on this diagram meets the $\phi$ *vs.* $\zeta$ curve at a number of points equal to the number of asymptotic directions, in this case three. The intersections occur at $\phi=60°$, $\phi=120°$ and $\phi=169°7'$. Hence the isotropic point is Type I$a$. The complete system of stress trajectories is shown in Fig. 19.4.

Von Mises[174] and Föppl[9] have, in addition, examined isotropic points having four asymptotic directions.

(Concluded in the May issue.)

# Direct Optical Measurement of Individual Principal Stresses

BY J. H. A. BRAHTZ* AND J. E. SOEHRENS**

*United States Bureau of Reclamation, Denver, Colorado*

PHOTOELASTIC analysis, as it is ordinarily understood, concerns itself with the experimental determination of the differences and directions of principal stresses in a stressed transparent model by means of the polariscope. Photographic fringe patterns called isochromatics are obtained when the model is set in a path of circularly polarized light. These fringes are a measure of the difference of principal stresses at all points. When viewed in a field of plane-polarized light, superimposed fringes called isoclinics are obtained. Isoclinics give the locus of points along which the directions of principal stresses coincide with the plane of polarization of the incident light beam. By rotating the plane of polarization, the directions of principal stresses may be obtained at all points in the model. It can be shown that the differences of principal stresses are equal to twice the maximum shear stresses, and, for many problems that arise, the knowledge of these quantities is sufficient. It frequently happens that the maximum principal stresses that occur in a photoelastic model are known to be at points located on a boundary. If this boundary is free of normal and shear loads, or subjected to a known normal load, the extreme fiber stress may be directly determined from the isochromatic pattern.

The problem of finding the individual principal stresses at interior points is not quite so simple. One common procedure is to employ one of several forms of graphical integration.[1] Another method is to make use of an auxiliary experiment by means of which the sum of the principal stresses is measured at all points. Some common methods are the lateral extensometer,[2] the membrane analogy,[3] and the electric analogy. Each method has its own limitations and sources of error. For example, the application of the membrane and electric analogies presupposes a knowledge of the sum of the principal stresses at all points on the boundary. Moreover, the analogy breaks down when the boundary is subjected to concentrated loads. The lateral extensometer requires delicate manipulation and control of room temperature and cannot be used beyond the elastic limit of the model material. In 1929, Henri Favre[4] brought to the attention of the scientific world a method by means of which the individual stresses could be measured optically. The basic principle of his method was to measure the absolute retardation of a beam of light passing through a transparent model when subjected to a change in stress. His principal optical instrument for measuring the retardation was a rather precise interferometer

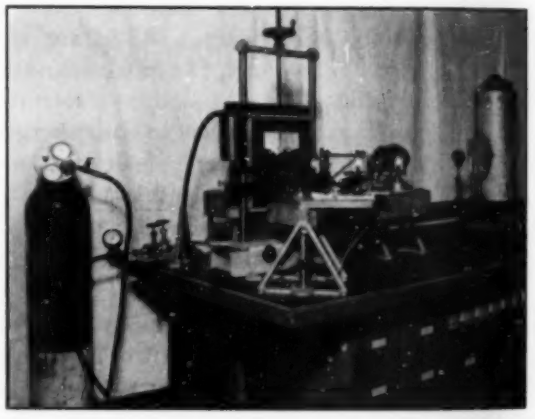

FIG. 1. Complete assembly of the photoelastic interferometer.

of the Mach-Zehnder or Jamin type. The purpose of this paper is to present a description of an instrument patterned after the one used by Henri Favre; to describe its theory and method of operation and to point out certain improvements made possible by recent advances in optics and plastics. The instrument herein described will be referred to as the photoelastic interferometer. It should not be confused with the lateral extensometers that employ the interferometer principle for their operation,[5] and, in no way, is this paper intended to detract from

* Director, Photoelastic Laboratory.
** Assistant Director, Photoelastic Laboratory.

the basic work of Henri Favre. Instead, it is hoped that it may be regarded as supplemental.

In presenting the theory and operation of the photoelastic interferometer, it will be assumed that certain terms and concepts are well understood. Some of these are: Plane-polarized light, monochromatic light and rotation of polarization planes by half-wave plates. Space does not permit a clear presentation of these, and the reader is referred to any good treatise on optics. *College Manual of Optics* by L. W. Taylor is a good example. However, a brief explanation of the fairly well understood phenomenon of interference will be included.

Figures 1 and 2 show photographs of the complete assembly. The straining frame or model holder is in operating position in Fig. 1. Fig. 3 shows a diagrammatic layout of the same assembly and will be frequently referred to in the following discussion. The principal optical parts are the two optical flats $L_3$ and $L_4$, and the four optical parallels $L_1$, $L_2$, $L_5$ and $L_6$. $L_3$ and $L_4$ are given a full first-surface aluminum plating. $L_2$ and $L_5$ are clear glass with no plating. $L_1$ and $L_6$ are given a thin plating of aluminum on one face. The plating is sufficiently thin that light is both reflected and transmitted. Moreover, the depth of coating is gaged so that the intensity of the reflected beam is equal to the intensity of the transmitted beam. The light beam that starts at

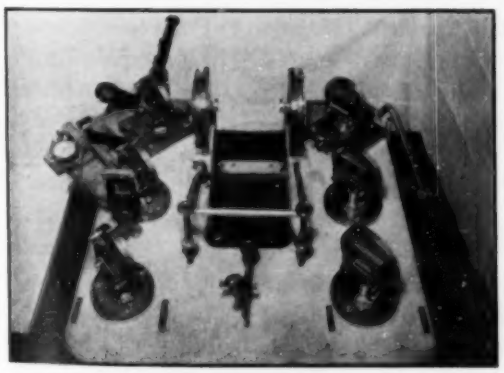

FIG. 2. Detailed view of the photoelastic interferometer.

the point source ($S$) is, therefore, split into a double path starting at $L_1$ and is brought together again at $L_6$. That part of the light referred to as the outside path goes around the model, and the part that goes through the model will be referred to as the inside path. The interference phenomenon is developed at $L_6$, where the two paths converge, and is visible as a series of alternate dark and light bands or interference fringes. The fringes are visible in the telescope and are of a character entirely different from the familiar isochromatic fringes, particularly in that the interference fringes are visible both before and

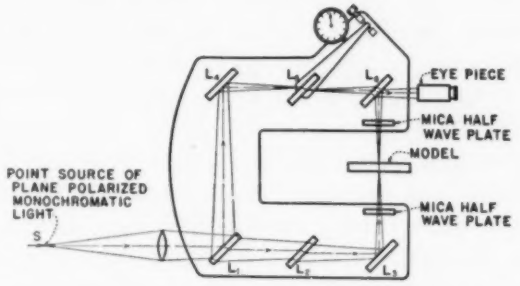


FIG. 3. Diagrammatic sketch of the optical path in the interferometer.

after loading the model. The interference fringes are merely shifted by a change in stress within the model, and the change in stress is linearly related to the number of interference fringes that cross a fixed point in the field of the eyepiece.

In order that the phenomenon may be better understood, let us temporarily lay aside the common concept of regarding a beam of light as a sine curve and instead visualize it, as shown at (A) in Fig. 4, as resembling a corrugated sheet; in other words, a sine curve with an additional dimension, depth, added. Looking downward on this corrugated sheet, we can represent the valleys as dashed lines and the ridges as solid lines. This convention is shown at (B) in Fig. 4. At (C) in Fig. 4, is shown a picture of the conditions at $L_6$, where the inside and outside light paths converge. It is physically impossible to adjust the position of the optical parallel in such a manner that the direction of propagation of the inside path upon reflection from $L_6$ coincides exactly with the direction of the transmitted path. The divergence of the two beams is shown in an extremely exaggerated condition but permits a visualization of the interference phenomenon. With the eye looking in a direction of the two emerging beams, it is evident that, along ray 1 at (C), the valleys for one system coincide with the valleys for the other system. Similarly, the ridges of the two systems

coincide along this line. Therefore, along ray 1, the illumination is built up from both sources. At ray 2, the valley points are nullified by the ridge points, and illumination will, therefore, be extinguished along this line. For sections between ray 1 and ray 2, the intensity will vary from bright to dark. This variation in illumination is visible in the eyepiece as a series of dark and light bands called interference fringes. Their general appearance in the eyepiece is shown at (D) in Fig. 4. The two heavy diagonal lines are fixed cross hairs in the eyepiece. It can be seen from an examination of (C) in Fig. 4 that, if, for any reason, either the inside path or the outside path should undergo a change in length relative to the other path, there would be an accompanying displacement of interference fringes across the field of view in the eyepiece. Furthermore, this change in length would be equal to the product of the number of fringes that passed the cross-hair intersection times the wave-length of the light. Since the wave-length of the light commonly employed, the green line of the mercury spectrum, is 5461 angstrom units, or 0.0000215 inch, and since it is possible to estimate fractional fringe displacements as small as a tenth of a fringe, it follows that the instrument is capable of detecting optical length changes with a precision of about two-millionths of an inch. Because of this extreme sensitivity, the interferometer is ideally suited to the problem of measuring changes in refractive indices of transparent models undergoing a change in stress, and, since each principal stress is a linear function of the change in refractive index in the two principal stress directions, the interferometer may be used to measure individual principal stresses.

Before the interferometer can be applied directly to the problem of stress measurements, several essential requirements must be fulfilled. First of all, since the state of stress in general varies from point to point within the model, it is necessary that the beam of light that traverses the model come to a pin-point focus within the model. This is approximated by starting with as good a point source as possible and choosing the focal length and location of the convex lens on the optical rail in such a manner that a real image of the point source falls within the model as shown in Fig. 3. For most problems, it will be sufficient if the width of the beam within the model is less than a millimeter. The optical measurements can, at best, give the average state of stress over this small illuminated portion of the model.

Another essential feature is that the narrow pencil of light that penetrates the model must

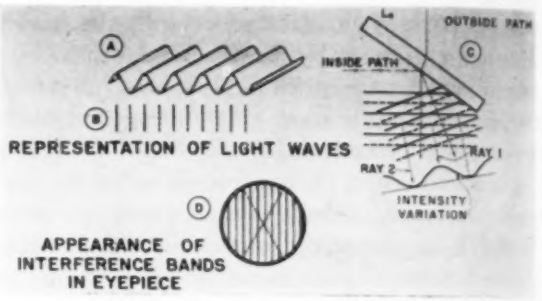


FIG. 4. Representation of light waves and the production of interference bands.

be plane-polarized and vibrating in a principal stress direction. Since there are two principal stress directions at every point, and the directions vary from point to point, there must be some convenient provision made to rotate the plane of polarization into the principal stress directions. In addition, there must be a means of quickly determining when the plane of polarization coincides with a principal stress direction. These conditions are fulfilled by making use of two small polarizing disks ("Polaroids") and two mica half-wave plates. The first polarizing disk is mounted in a fixed position on the optical rail immediately in front of the point source. It is oriented in such a position that the light that is transmitted is polarized in a vertical plane. This insures that the light will be vertically polarized in the remainder of the optical system with the exception of the small interval between the two mica half-wave plates. The half-wave plate mountings are shown in Figs. 2 and 3. The two mica plates are split to be half-wave plates for the green line of mercury and are set in ball-bearing mountings to rotate together. This is accomplished by a device shown in Fig. 2, in which a taut piano-wire loop mechanically links the two plates so that they rotate together. The two plates are cut from the same sheet of mica, but the second plate is set in a reversed position

with respect to the first plate. When the first plate causes a rotation of the plane of polarization into some position other than the vertical, the second plate produces the reverse effect. This insures that the light emerging from the second plate is always polarized in a vertical plane, regardless of the plane of polarization of the light in the interval between the half-wave plates. This fulfills the requirement of rotating the plane of polarization of the light beam that penetrates the model.

In order to ascertain when the plane of polarization of the light beam that penetrates the model coincides with a principal stress direction, an auxiliary polarizing disk or analyzer is placed in front of the eyepiece at the same time that the light in the outside path is cut off. A small horizontal rod equipped with a conveniently located knob is mounted near $L_6$ as shown in Figs. 1 and 2. By turning the knob to the left, the analyzer is brought into a position that extinguishes vertically polarized light at the same time that the outside path is cut off by a black sheet-metal shutter. Since the analyzer passes only light that is horizontally polarized and only vertically polarized light emerges from the second half-wave plate, the light field in the eyepiece will be extinguished. If a stressed double-refractive model is now placed between the mica plates, the light that emerges from the model will not, in general, be plane-polarized. The emerging light vector may, however, be resolved into two components, one coplanar with the incident beam and one perpendicular to it. The second mica half-wave plate will rotate the former into a vertical plane, and the latter into a horizontal plane which will be clearly visible in the eyepiece. As the mica plates are rotated in unison, the intensity of illumination in the eyepiece will vary from extinction to full illumination. The extinction position occurs when the plane of polarization of the light beam incident upon the model coincides with a principal stress direction. The direction of principal stresses is now obtained by doubling the reading on a graduated vertical circle connected with the mica plate holders.

Having the light beam vibrating in a principal stress direction, the analyzing unit is lifted from in front of the eyepiece, the interference fringes are visible, and we are in a position to measure the individual principal stresses. But, first, let us review the laws relating changes in refractive indices to principal stresses, as investigated by such men as Maxwell, Neumann, Favre, Filon and others. For plane stress, these relations are:

$$\left.\begin{aligned}\delta_1 &= C_1\sigma_2 + C_2\sigma_1 \\ \delta_2 &= C_1\sigma_2 + C_2\sigma_2\end{aligned}\right\}, \tag{1}$$

where $\delta$ = change in refractive index, $\sigma$ = principal stress, 1, 2 = subscripts denoting principal stress directions, $C_1$ = transverse stress-optical coefficient, and $C_2$ = direct stress-optical coefficient.

Solving these for the principal stresses, we obtain:

$$\left.\begin{aligned}\sigma_1 &= A\delta_1 + B\delta_2 \\ \sigma_2 &= B\delta_1 + A\delta_2\end{aligned}\right\}, \tag{2}$$

where the original constants are replaced by the constants $A$ and $B$, which bear the relation:

$$A = C_2/(C_2^2 - C_1^2),$$
$$B = C_1/(C_1^2 - C_2^2).$$

Since $A$ and $B$ can be obtained by a simple calibration experiment, the principal stresses $\sigma_1$ and $\sigma_2$ can be determined by Eqs. (2) in terms of the changes in refractive indices, and the latter are measured by the number of interference fringes that pass the cross hairs while the model is undergoing a change of stress. The individual principal stresses are, therefore, linear functions of the fringe displacements.

However, in actual operation of the interferometer, it is not necessary to count the number of fringes that pass the cross hairs. The operation is much more rapid and more accurate if the outside path is changed in length by an amount equal to the refractive change of the inside path. This is accomplished by using the clear glass optical parallel $L_5$. $L_5$ is mounted on a spindle and equipped with a tangent arm and tangent motion. As the tangent screw is turned in, the effective length of glass through which the outside light path must travel increases. The change in length of the outside path may, therefore, be made equal to the change of the inside path. A micrometer dial bears against an agate insert on the tangent arm, and changes in length of the outside path can be read directly on the micrometer dial. In making stress measurements, the procedure is, after having found a principal stress

direction, to gradually remove the load acting on the model. As the load is gradually removed, the fringes in the eyepiece tend to move across the field of vision in the eyepiece. By turning the tangent-motion screw, the fringe displacement can be nullified. The difference in dial readings before and after loading is a measure of the

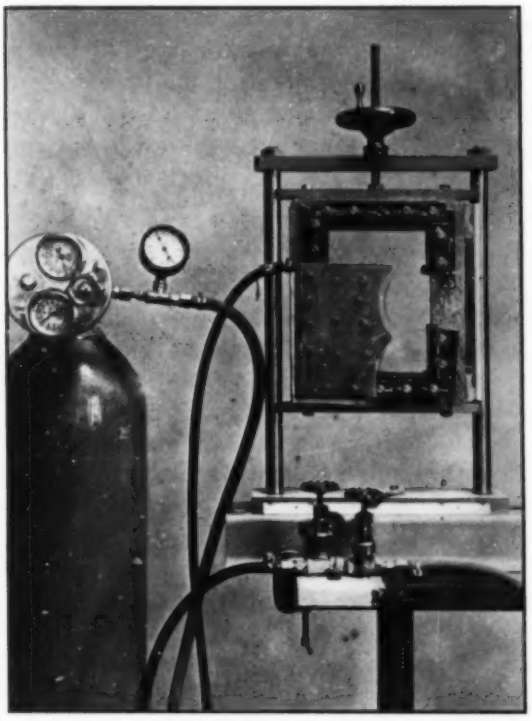

FIG. 5. Loading frame fitted with model ready for testing.

refractive change ($\delta$). This operation is repeated for the other principal stress direction. The magnitudes of the principal stresses are obtained by substituting the differences in dial readings ($\delta$) into Eqs. (2). The constants $A$ and $B$ are so adjusted that, by substituting the actual difference in dial readings into Eqs. (2), the stresses are given in pounds per square inch. To calibrate $A$ and $B$, a simple tensile specimen with cross-sectional area ($a$) is subjected to a known pull ($P$). If the ratio of length to width of model is sufficiently small, the two principal stresses are $P \div a$ and 0. By obtaining the differences in dial readings that accompany these two known principal stresses, the constants $A$ and $B$ may be obtained. It is necessary, of course, that the tensile calibration specimens be made of the same material used for experimental purposes and possess the same thickness.

The instrument herein described was designed and constructed by J. E. Soehrens and has been in successful operation at the United States Bureau of Reclamation's photoelastic laboratory in Denver for about three years. During that time, a number of improvements have been made, not only in the instrument itself and in its operation, but also in the preparation and loading of models.

Since the interferometer provides a means of point-to-point analysis, it is necessary to have the model mounted in a loading frame that can be moved not only in a vertical direction but also in a horizontal direction. Fig. 5 shows a photograph of the loading frame fitted with a model ready for testing, and Fig. 1 shows the loading frame in operating position. The arch model shown in Fig. 5 is loaded on the up-stream face by means of compressed nitrogen applied through a soft rubber tube held against the model. The advantages of using this method of loading are the following: It provides a means of rapidly loading and unloading. When there are many points in the model to examine, this becomes an important advantage. It was further found that, when this system of loading was used, the displacements of the model were negligible, but, when models were loaded with weights and levers, displacements of the model occurred due to strains within the loading frame. These displacements were of the order of a few hundredths of an inch, and, although these would be of no consequence in a polariscope, they are too great for this instrument. The reason for this is that the beam of light that covers a certain small circular area on the model before loading covers an adjacent area after loading if the displacement is too great. If the model were ground and polished with the accuracy and precision of an optical parallel, small displacements would be of little consequence, since displacements of the model would not cause fringe displacements.

For those cases where the forces are applied through levers, an air piston with internal expanding bellows has been constructed to replace weights. This again permits rapid loading and unloading and produces no appreciable displacements of the model. Both of these loading methods necessarily require a well-regulated

source of compressed air or nitrogen. A two-stage regulator has been found to operate satisfactorily.

Although the stresses may be obtained by substituting the dial readings into formulas (2), it has been found more convenient to employ a collinear nomograph for this operation. Such a chart is shown in Fig. 6. The outside scales are graduated in dial readings and the stress scales in pounds per square inch. This permits rapid determination of the principal stresses from the dial readings. An important check is provided by means of the center scale which is graduated to give the differences of principal stresses in terms of the isochromatic fringe orders. This provides an important system of cross-checking between the interferometer and the polariscope. If the model is reasonably well annealed and free of initial stress, the differences of principal stresses obtained by these two optical methods should be in agreement.

In comparing the photoelastic interferometer herein described with the instrument used by

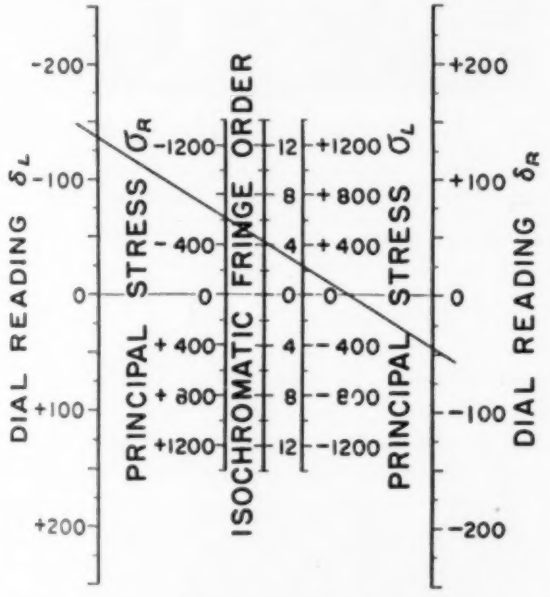


FIG. 6. Nomographic representation for determining the principal stresses $\sigma R$ and $\sigma L$ from the dial readings $\delta R$ and $\delta L$. The equations are $\sigma L = a\delta R + b\delta L$, $\sigma R = a\delta L + b\delta R$, where $a$ and $b$ are to be determined by calibration test. For clear white Bakelite $a = 5.70$ and $b = -3.59$.

Favre, two essential differences should be pointed out. One important difference centers about the method of finding principal stress directions. Favre predetermined these in an auxiliary polariscope along with the differences of principal stresses. Having the principal stress directions, the mica half-wave plates are individually turned into proper orientation as determined by the polariscope. The combination of the two instruments into a single instrument obviously increased the speed of operation.

Another essential difference lies in the fact that the models used in the machine described in this paper were made of water-white Bakelite, a plastic developed since Favre conducted his experiments on glass models. Although Eqs. (2) hold for both glass and Bakelite, they cannot be used successfully for the former. When used on glass, the stresses are obtained as the differences of two large quantities of about the same magnitude. The experimental errors resulting from such measurements are relatively large. Favre eliminated this difficulty by the ingenious device of expressing each individual principal stress as the sum of three quantities, the two absolute retardations or refractive changes, and the relative refractive change, each multiplied by a suitable constant obtained by calibration. The relative refractive change was measured in the polariscope by a Babinet compensator.

The photoelastic laboratory of the Bureau of Reclamation is a branch of the division of dams, which is under the direction of Mr. K. B. Keener, Civil Engineer, Dams. All research and work of the Bureau are under the direction of Mr. J. L. Savage, Chief Designing Engineer. All engineering and construction are under the general direction of Mr. R. F. Walter, Chief Engineer, with headquarters at Denver. All activities are under the general direction of Mr. John C. Page, Commissioner of the Bureau of Reclamation, with headquarters at Washington, D. C.

### *Bibliography*

1. A. Neuber, "New Method of Deriving Stresses Graphically from Photoelastic Observations," Proc. Roy. Soc., London **141**, (1933).
2. L. N. G. Filon, *Photoelasticity for Engineers* (Cambridge University Press, London, 1936), p. 121.
3. J. P. Den Hartog, J. Frank. Inst. **216**, 5 (1933).
4. H. Favre, "Sur Une Nouvelle Méthode Optique de Détermination des Tensions Interieures," Revue d'optique (1929).
5. R. W. Vose, "An Application of the Interferometer Strain Gage in Photoelasticity," J. App. Mechanics, **A99** (1935).

# Isopachic Stress Patterns[1, †]

MAX M. FROCHT*
*Carnegie Institute of Technology, Pittsburgh, Pennsylvania*

## DEFINITIONS: ISOPACHIC STRESS PATTERN AND INHERENT PLANE OF SYMMETRY

THE new stress patterns which give the loci of equal sums of principal stresses will be referred to as isopachic patterns in order to distinguish them from the photoelastic patterns which give the loci of equal differences of principal stresses. The term isopachic is due to Coker and Filon[2] and is derived from the two Greek words *iso*, meaning same, and *pachic*, meaning thickness.

In a two-dimensionally stressed body there is always one plane of symmetry. This plane bisects the body and is free from normal strains. It is the only plane which remains a plane under all loads giving two-dimensional stresses. This plane we will call the *inherent plane of symmetry*. It is obvious that there may be one or two more planes of symmetry perpendicular to the plane just discussed.

A two-dimensionally stressed body which has no plane of symmetry other than the inherent plane will be spoken of as a nonsymmetrical two-dimensional body.

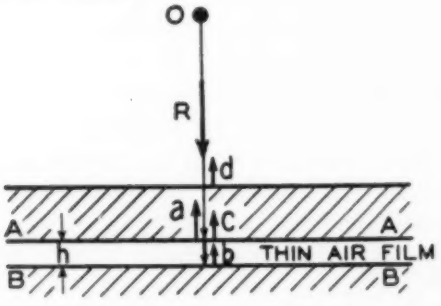


FIG. 1. Sketch showing formation of interference fringes.

## I. THE OPTICAL METHOD FOR ISOPACHIC STRESS PATTERNS

### Brief theory of interference fringes

We review briefly the theory of the simplest case of interference fringes. In Fig. 1, let a ray $R$ from a monochomatic source $O$ be incident normally on the half mirror $A$–$A$, which for concreteness we can take as the polished surface of a glass plate. Upon reaching the surface $A$–$A$ part of the light is reflected upwards and is represented in our figure by vector **a**, and a part is transmitted. The transmitted ray upon reaching the lower surface $B$–$B$ is also partially reflected and the reflected component is designated by vector **b**. Upon reaching surface $A$–$A$ this latter vector **b** is again resolved, a part of it denoted by **c** being transmitted. The rays $a$ and $c$ meet and combine to form a new ray $d$, the nature of which depends on the thickness $h$ of the air film. If the difference in optical path is taken as $2h$, and remembering that upon reflection from a denser to a rarer medium the ray is retarded by $\lambda/2$, we get for the condition of

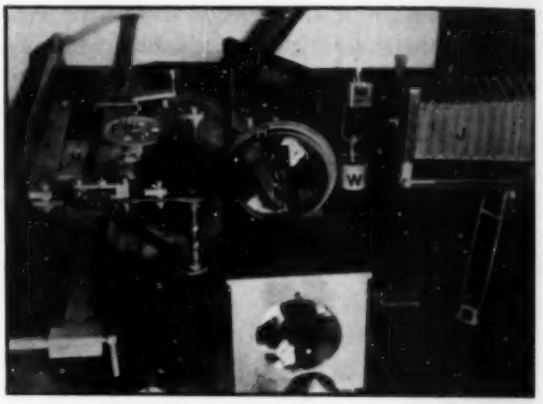


FIG. 2. Photograph of equipment used to obtain isopachic stress patterns. $A$, $B$—cross bars, $C$—loading lever, $D$, $E$—lever bearing and guide, $F$—balancing head of prism, $G$—mercury vapor lamp, $H$—collimating lens, $I$—reflecting glass plate, $J$—camera, $M$—supporting plate, $W$—dead weights for loading.

[1] Presented in part at the Fifth International Congress on Applied Mechanics, held at Cambridge, Massachusetts, September, 1938. This paper is an extension of work described in J. Frank. Inst. **216** (1933) entitled "On the Application of Interference Fringes to Stress Analysis."

† Received in Editor's office for Contributed Original Research section on January 27, 1939.

* Associate Professor of Mechanics, Carnegie Institute of Technology. Member A. S. M. E.

[2] E. G. Coker and L. N. G. Filon, *Treatise on Photoelasticity* (Cambridge University Press, 1931), p. 178.

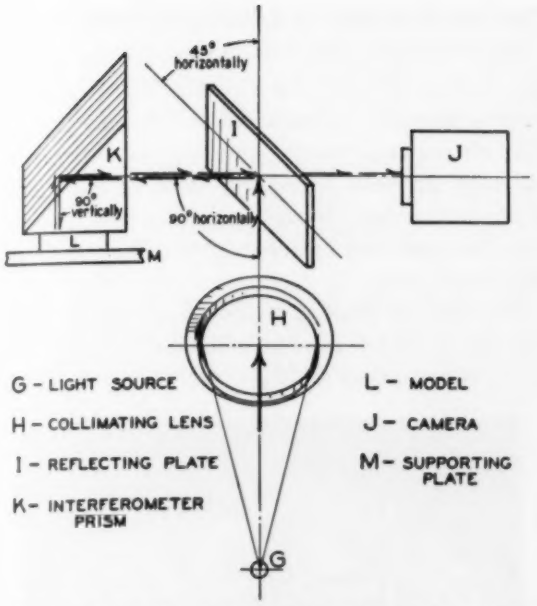


FIG. 3. Schematic diagram of optical path. All axes shown through lens $H$ and reflecting glass plate $I$ lie in one horizontal plane.

interference the well-known equation

$$(2h+\lambda/2)=(2n+1)\lambda/2, \qquad (1)$$

where $n$ is any integer and $\lambda$ the wave-length of the light, since interference takes place if the rays meet with a phase difference equal to an odd number of half-wave-lengths.

Solving for $h$ we get

$$h=n\lambda/2, \qquad (2)$$

which means that for a beam of parallel rays interference fringes will appear for $h$ equal 0, 1/2, 2/2, 3/2, etc. wave-lengths.

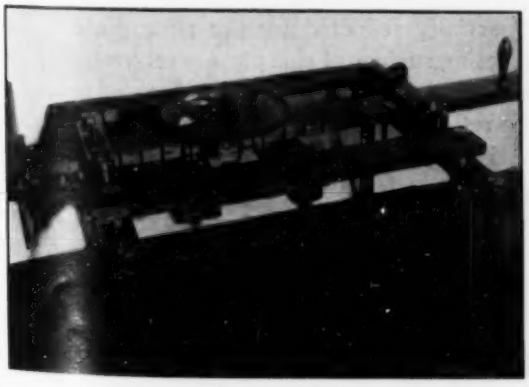

FIG. 4. Photograph showing adjusting head in place on interferometer, and small weights used for balancing.

It also means that no two fringes could cross and that along any one interference fringe the depth or thickness of the film is constant. If one surface, say, $A$–$A$ be considered perfectly flat and

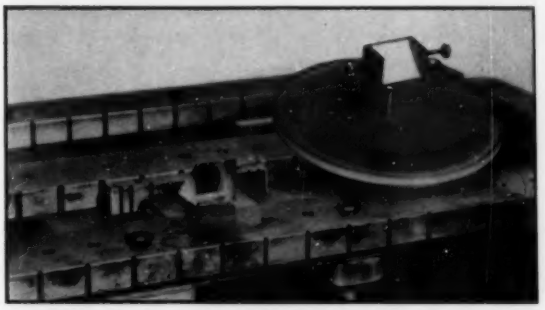

FIG. 5. Photograph showing interferometer prism resting on model and adjusting head removed from prism.

taken as a datum plane then the interference fringes would represent contours of the surface $B$–$B$.

### Deformation of a flat surface in a two-dimensional stress system

If a body which is subjected to a two-dimensional stress system has initially flat surfaces these surfaces will after the application of the loads no longer be flat. They will be deformed. If one of these surfaces be polished and a plate of glass with a good optical surface, a datum plane, be brought close to it so that the two planes are separated by a thin film of air, and if now the model be strained and its polished face illuminated by a normal beam of monochromatic light as shown in Fig. 1, then the interference fringes thus obtained would be paths of constant thickness of the air film between the datum plane and the face of the model.

If we assume that during the application of the loads to the model the positions of the inherent plane of symmetry in the model and that of the datum plane remain parallel relative to one another so that the changes in the thickness of the air film could be attributed to the stresses alone, *then each interference fringe would directly represent a path of constant* $(p+q)$, *which we shall hereafter refer to as an isopachic curve, meaning thereby a curve along which the model has the same thickness*. The above conclusion follows from the

well-known expression

$$\delta = -(\mu t/E)(p+q), \qquad (3)$$

in which $p$ and $q$ are principal stresses, $\mu$ and

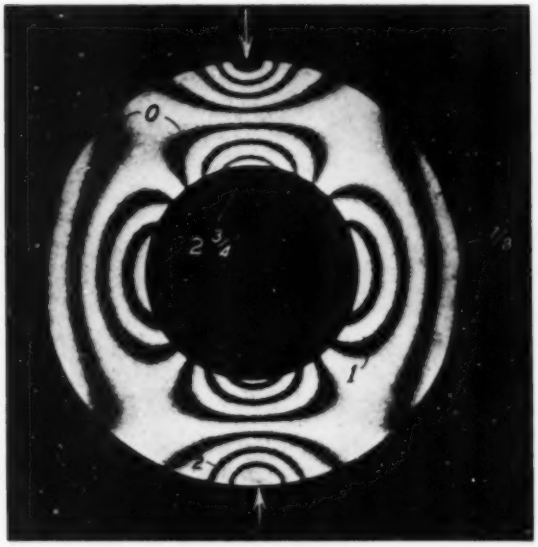


FIG. 6. Isopachic stress pattern from a stainless steel ring subjected to concentrated diametral loads. Dimensions of model: inner diameter = 0.375 in., outer diameter = 0.751 in., thickness = 0.243 in.

$E$ Poisson's ratio and modulus of elasticity, respectively, $t$ thickness, and $\delta$ deformation in a direction normal to the plane determined by $p$ and $q$, or the inherent plane of symmetry.

## Equipment

The main equipment used in the investigation described here consists of: (1) a monochromatic source of light, (2) a collimating lens, (3) a straining frame, (4) an interferometer or datum plane, (5) a balancing or adjusting head, and (6) a camera.

The light source was a mercury vapor lamp from the photoelastic apparatus. The camera and collimating lens were similarly from the same set-up.

The straining frame is shown in Fig. 2. The model is placed on a supporting horizontal plate $M$, fastened to the cross bars $A$ and $B$, and loads are applied by means of dead weights $W$ acting on the lever $C$. The lever $C$, bearing $D$, and guide $E$, Fig. 2, are from the photoelastic testing machine. The applied forces lie in a horizontal plane.

## The interferometer or datum plane. Optical path

After considerable development the author adopted a 45° standard one-inch prism as an interferometer. The main merit of such a prism is that all the equipment including the camera can be kept at desk level and observation can be made in comfort. Such a prism is also inexpensive, the one used by the author costing only five dollars.

The optical path is as shown in the sketch of Fig. 3. A beam of monochromatic light originates at the source $G$, is collimated by lens $H$ and

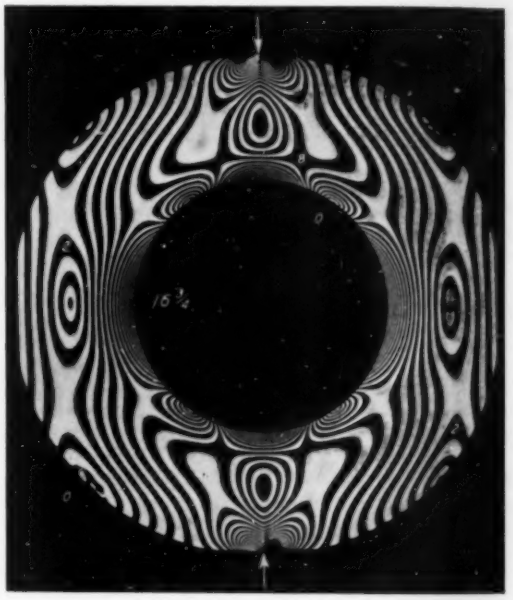


FIG. 7. Photoelastic stress pattern from a Bakelite ring under concentrated diametral loads of 202.6 lb. Dimensions: inner diameter = 0.766 in., outer diameter = 1.532 in., thickness = 0.1795 in. Model fringe value = 500 lb./in.$^2$ in tension or compression.

is partially reflected by the glass plate $I$. The reflecting surface of this plate is set vertically and at 45° to the direction of the collimated beam $HI$. The reflected beam $IK$ meets the inclined plane of the interferometer prism $K$ and is again reflected vertically downward, passes through the air gap between the prism $K$ and model $L$, and retraces its path to the plate $I$ carrying an isopachic stress pattern which can be observed and recorded by the camera $J$.

## The balancing or adjusting head

The interferometer prism rests directly on the polished surface of the model and rides on the

high points developed in it by the loads. Since the weight of the prism is not uniformly distributed and since there may be small differences in the elevations of the high spots in the model itself,

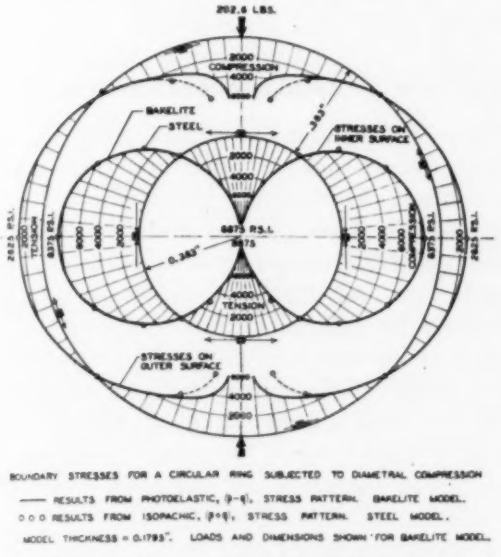


BOUNDARY STRESSES FOR A CIRCULAR RING SUBJECTED TO DIAMETRAL COMPRESSION
—— RESULTS FROM PHOTOELASTIC, (p−q), STRESS PATTERN. BAKELITE MODEL.
o o o RESULTS FROM ISOPACHIC, (p+q), STRESS PATTERN. STEEL MODEL.
MODEL THICKNESS = 0.1795". LOADS AND DIMENSIONS SHOWN FOR BAKELITE MODEL.

FIG. 8. Comparative curves of boundary stresses from photoelastic and isopachic stress patterns.

the interferometer surface may not be parallel to the inherent plane of symmetry. In order to assure that the planes in question are parallel the interferometer prism is set in a light Bakelite disk about five inches in diameter which we call a balancing or adjusting head, as shown in Fig. 4.

This head is fixed to the glass prism by means of two small horizontal screws as shown in Figs. 4 and 5. The balancing or adjusting of the prism for parallelism is attained by means of small weights placed on the horizontal disk at suitable points.

An interference fringe image of the surface of the model can be clearly seen by looking directly into the prism and in cases of symmetrical bodies the prism can be balanced to obtain a symmetrical pattern. This process of balancing or adjusting although delicate in nature, the weights sometimes consisting of small pieces of cardboard, does not call for extraordinary skill nor is it a time-consuming process.

### Loading

As already stated the model is assumed to be subjected to two-dimensional stresses. It is therefore of utmost importance to make sure that the loads are properly applied. All eccentricities, however small, will affect the assumed stress distribution and therefore the isopachic pattern. As a general rule it is decidedly simpler to work with tensile loads than with compressive loads. The main difficulties in the problem discussed in this paper were due to eccentricities in the applied compressive loads.

### The particular problem and model

In our first work[1] we tested the proposed method on a glass block and obtained a satisfactory stress pattern for the case of a concentrated load on a straight edge. For our present problem we chose a circular disk with a concentric hole in which the outside diameter was twice that of the inner. The model was 0.243 in. thick and had outer and inner diameters equal to 0.751 in. and 0.375 in., respectively (see Fig. 13(a)).

Unlike photoelastic models, the models in this method need not be made from transparent material. They can be made from metal or any other substance obeying Hooke's law which can

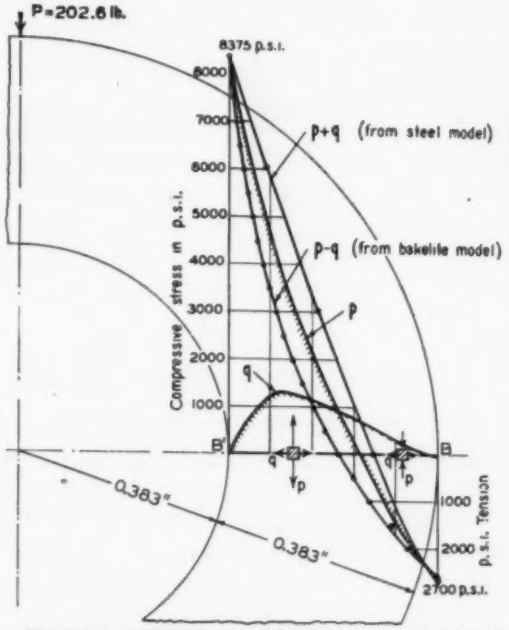


PRINCIPAL STRESSES ACROSS CENTRAL HORIZONTAL SECTION FOR RING IN DIAMETRAL COMPRESSION.
LOADS AND DIMENSIONS SHOWN FOR BAKELITE MODEL OF THICKNESS = 0.1795 INCH

FIG. 9. Principal stresses across horizontal section of symmetry determined from photoelastic and isopachic stress patterns.

be polished to an optical flat. The model under consideration was made of stainless steel.

## Results

After several trials in which the eccentricities in the loading were discovered and eliminated we obtained the stress pattern shown in Figs. 6, in which the fringe orders are indicated by small numerals. As already stated the assumption is that each fringe in the pattern represents the loci of equal sums of principal stresses and that the sums are proportional to the order of the fringes.

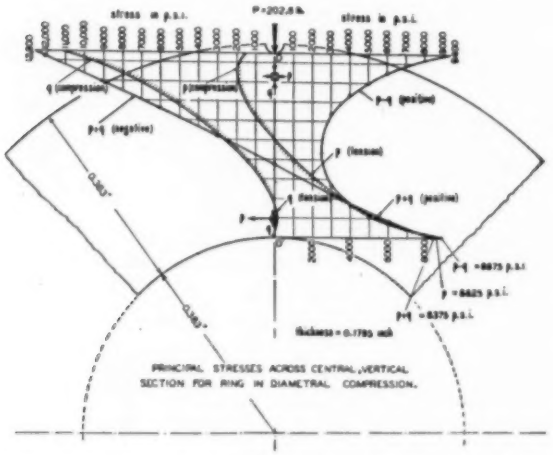


FIG. 10. Principal stresses across vertical section of symmetry determined from photoelastic and isopachic stress patterns.

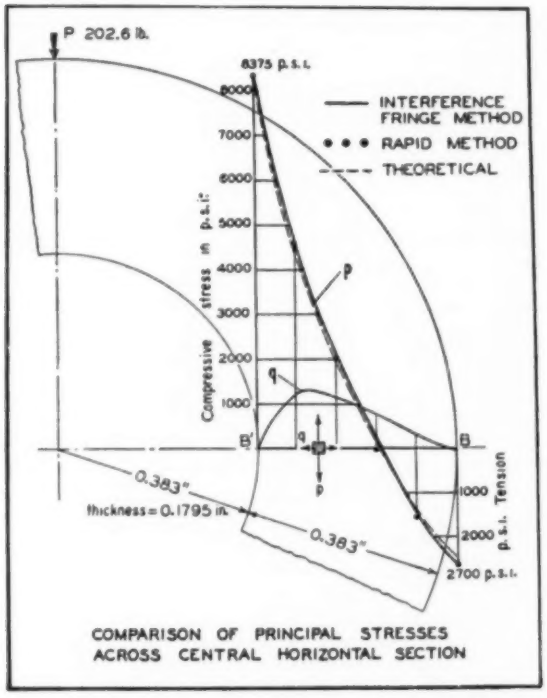


FIG. 11. Comparative curves of normal principal stresses across horizontal section of symmetry obtained by several different methods. See references 5 and 6.

## Analysis of the results. Boundary stresses

Since at free boundaries one principal stress is zero it follows that free boundary stresses can be determined from either the isopachic or the photoelastic stress pattern and that the distribution of these stresses must be the same in both cases. The first check on the present work is obtained by comparing the curves of the free boundary stresses from the two stress patterns of Figs. 6 and 7. This comparison is shown in Fig. 8. The full curve is from the $(p-q)$ pattern from a Bakelite model, while the small circles are from the $(p+q)$ pattern from the steel model. The results are seen to be entirely satisfactory.

It should be noted that the loads on the steel model were not measured and that they were unnecessary in our calculations. The two curves of boundary stresses were compared by arbitrarily assuming the zero points to coincide and by assigning a constant difference between consecutive fringes in the isopachic curves, which

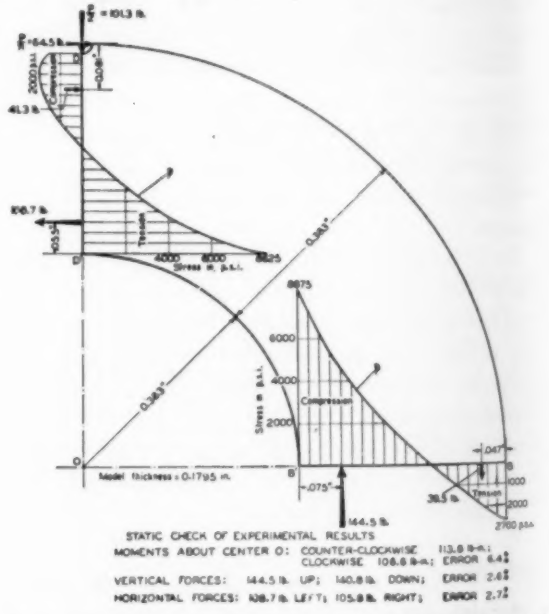
STATIC CHECK OF EXPERIMENTAL RESULTS
MOMENTS ABOUT CENTER O: COUNTER-CLOCKWISE 113.8 lb-in.; CLOCKWISE 108.6 lb-in.; ERROR 6.4%
VERTICAL FORCES: 144.5 lb. UP; 140.8 lb. DOWN; ERROR 2.6%
HORIZONTAL FORCES: 108.7 lb. LEFT; 105.8 lb. RIGHT; ERROR 2.7%

FIG. 12. Normal stresses across horizontal and vertical section of symmetry and static check of same.

was obtained from the photoelastic data. For example, the maximum compressive fringe order in the photoelastic pattern on the inner boundary was found to be 16.75. At the corresponding point of the isopachic pattern the fringe order was found to be 2.75. The ratio is 6.06 photoelastic fringes per isopachic interference fringe.

The above procedure is equivalent to letting two points from the isopachic curve coincide with two points from the photoelastic curve, and letting the position of all other points on the isopachic curve be determined by the law of proportionality which is assumed to govern the fringes in the isopachic pattern.

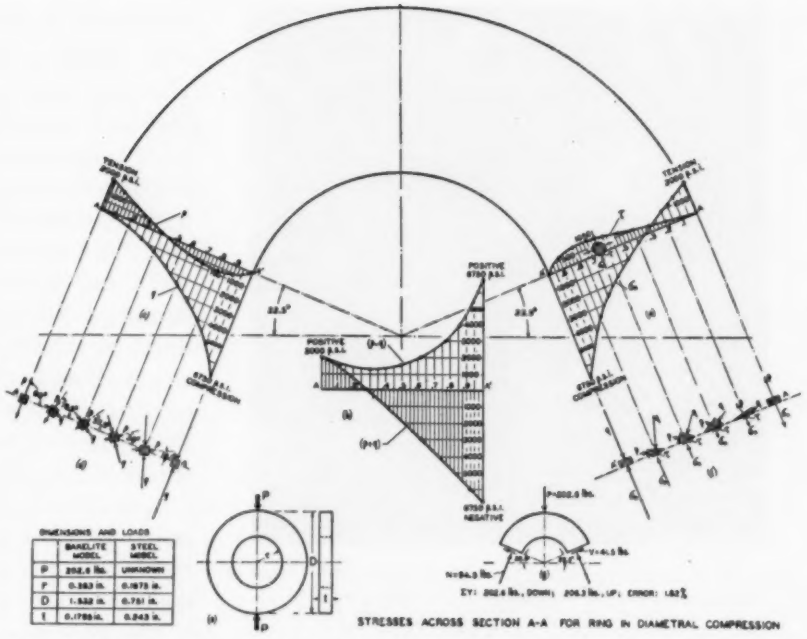


FIG. 13. Distribution of principal stresses, shear and normal stresses across a radial section and static check of results.

## Stresses across sections of symmetry

Figure 9 shows the principal stresses across the section of symmetry $B'B$ which is perpendicular to the plane of the loads, whereas Fig. 10 shows similar results for the plane of symmetry $D'D$ containing the loads. Fig. 11 shows comparative curves of the normal stresses across the first section of symmetry. The results from three methods are compared: the one under discussion, the Rapid-method,[3] and one from the mathematical theory of elasticity.[4] Again the agreement is seen to be completely satisfactory.

The results across the sections of symmetry are further checked from the point of view of equilibrium and the results are shown in Fig. 12. In checking the forces across section $D'D$, Fig. 12, a small semi-circular section was removed and the original load replaced by a horizontal load of $P/\pi = 64.5$ lb. and a vertical load of $P/2 = 101.3$ lb. which enter into the theoretical solution of this problem.[5] As shown in Fig. 12 the error in the summation of moments is 6.4 percent and in the summation of $X$ and $Y$ forces 2.7 percent and 2.6 percent, respectively.

In laying off the $(p-q)$ and $(p+q)$ curves one must note the signs of the stresses at the terminal points. Thus on line $B'B$, Fig. 9, which is a stress trajectory, $q$ is zero at the ends and hence $(p-q)=(p+q)=p$ at both ends.

On the line $D'D$, Fig. 10, point $D$ is not a free point and at that point $(p-q)$ is positive whereas $(p+q)$ is negative since $q$ is a large compressive stress.

## Stresses across arbitrary radial section

Figures 13, (a) to (g) inclusive show the stress system across a radial section making an angle of 22.5° with the horizontal. In Fig. 13(a) we see the sketch of the model and loads. Fig. 13(b) shows the $(p-q)$ and $(p+q)$ curves for the radial section $A'A$. We note that at point $A$

$$(p-q)=(p+q)=p,$$

while at point $A'$

$$(p-q)=-(p+q);$$

[3] See M. M. Frocht, "A Rapid Method for the Determination of Principal Stresses Across Sections of Symmetry from Photoelastic Data," J. App. Mechanics (1938).

[4] See S. Timoshenko, *Theory of Elasticity* (McGraw-Hill Book Co., New York, 1934), p. 119.

[5] Reference 4, pp. 96 and 97.

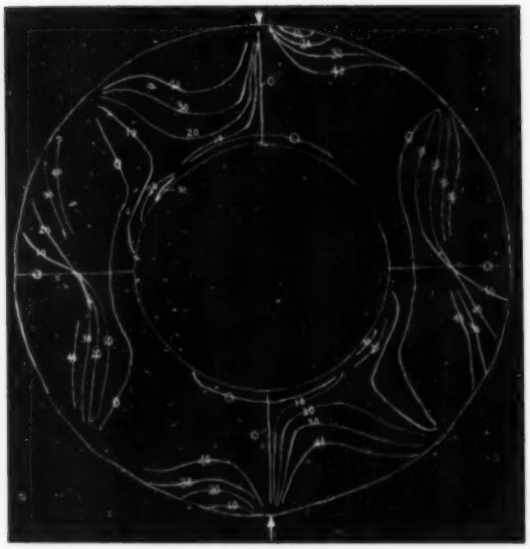

FIG. 14. Laboratory sketch of isoclinics for the Bakelite ring the stress pattern of which is shown in Fig. 7.

that is, if $(p-q)$ is positive then $(p+q)$ is negative, and, as can be seen from Fig. 13(b). This is due to the fact that the direction of stress $p$, which at point $A$ is tangential, has turned through 90° when it reaches point $A'$ as shown in the sketch, Fig. 13(d). The direction of the stresses are taken from the isoclinic sketch shown in Fig. 14. From the principal stresses shown on the left, Fig. 13(c), we next determine the normal and shear stresses, Fig. 13(e), using the well-known equations

$$\sigma_n = p\cos^2\theta + q\sin^2\theta,$$

$$\tau = \left(\frac{p-q}{2}\right)\sin 2\theta.$$

The static check is shown in Fig. 13(g) and as before the errors are relatively small.

We recall that in all these calculations the $(p-q)$ curves were taken from the photoelastic stress pattern shown in Fig. 7 and the $(p+q)$ curves were taken from the isopachic pattern in Fig. 6.

### The solid disk

Figure 15 shows an isopachic stress pattern of a solid glass disk subjected to two diametral loads distributed over an appreciable area.

### Extension of method to nonsymmetrical bodies

It seems to the author that isopachic stress patterns can also be obtained from nonsymmetrical two-dimensionally stressed bodies. In such cases, however, a positive means must be provided to keep the datum plane of the interferometer parallel to the inherent plane of symmetry of the model.

To this end we suggest that the model be equipped with one or two projecting wings or arms, attached at points sufficiently distant from the stressed region under observation, so as not to affect its stress distribution. It follows from St. Venant's principle that such arms, if attached through a single small area, remain free from strains. This is clearly shown in the photoelastic stress pattern of Fig. 16. This figure further shows that the attached arms do not disturb the stresses in the region under investigation.

The interferometer prism can be set in a casing which is equipped with a three-point adjustable

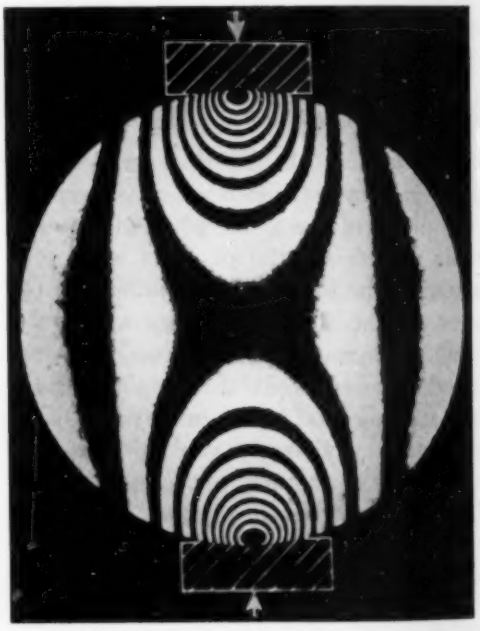

FIG. 15. Isopachic stress pattern of a glass disk subjected to diametral loads distributed over an appreciable area. Dimensions: diameter = 0.751 in., thickness = 0.392 in.

support which in turn rests on the strain-free arm. Before the loads are applied the interferometer datum plane is adjusted until it is parallel to the polished face of the model. Since the supports on which the adjusting screws rest

remain by assumption free from strain it follows that in two-dimensionally stressed systems the interferometer datum plane must remain parallel to the inherent plane of symmetry of the model during and after the application of the loads.

It may be found possible and perhaps desirable to make removable arms and to fasten them to the model at a suitable point. The wings may also be provided with a flat polished surface and in that way used to verify the assumption that the interferometer plane remains parallel to the inherent plane of symmetry, and at the same time furnish a level for adjustment.

The model and the interferometer supports can be tied together by means of a spring to act as a unit and in this way difficulties caused by vibration and relative motion can be eliminated. Further, the interferometer can be adjusted so that it does not rest on the model but is separated from it by a thin air space in order to provide room for possible expansion of the model. It is believed that such arrangements will give correct isopachic curves in nonsymmetrical cases. Work along these lines is now in progress in the Photoelastic Laboratory at the Carnegie Institute of Technology.

### Significance of isopachic patterns

The significance of the isopachic stress patterns at the present time is mainly of a scientific character. They complete the *optical solution* of two-dimensional problems by providing complete stress patterns of loci of constant sums analogous to the photoelastic stress patterns of constant difference of the principal stresses, thereby eliminating the need for point-by-point exploration of the $(p+q)$ values.

There is, however, another and, perhaps, more important aspect. All teachers of strength of materials are familiar with the natural and inevitable skepticism which practical engineers evince when they are asked to apply stress data obtained from materials such as Bakelite, Celluloid, and other plastics to structural materials. The agreement between boundary stresses from isopachic patterns obtained from steel or other metallic materials with those from photoelastic materials should result in greater coordination between laboratory findings of research workers and design practise.

Further, in those cases where the stress distributions are affected by the constants of the material, such as the modulus of elasticity and Poisson's ratio, the isopachic pattern obtained from models cut from the actual structural material would give correct results.

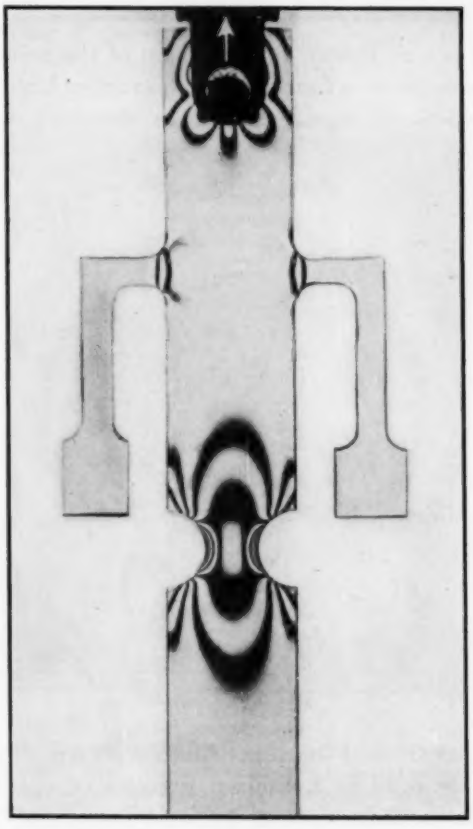

FIG. 16. Photoelastic stress pattern of model with strain-free arms showing that the arms do not affect the stress distribution at regions far from the points of attachment.

It should also be noted that numerical values of the boundary stresses can be obtained from the isopachic stress pattern just as from the photoelastic stress pattern with this difference that at points of stress concentration the gradient of the isopachic curves is always gentle, almost linear in character, in contrast to the steep gradient of the $(p-q)$ curves at similar points. With the perfection of the technique for isopachic patterns, it may be found desirable to study the phenomena of stress concentration from isopachic patterns from metal models.

It is also conceivable that isopachic patterns

may prove useful in the study of surface stresses on actual structures in service.

## II. Isopachic Curves from Boundary Stresses and the Numerical Solution of Laplace's Equation

It is well known that the sum of the principal stresses forms a function which satisfies Laplace's equation. Thus, if $\phi$ denotes the Airy stress function then

$$\frac{\partial^2\phi}{\partial y^2}=\sigma_x, \quad \frac{\partial^2\phi}{\partial x^2}=\sigma_y,$$

$$\sigma_x+\sigma_y=\frac{\partial^2\phi}{\partial x^2}+\frac{\partial^2\phi}{\partial y^2}.$$

But $$\sigma_x+\sigma_y=p+q.$$

Hence $$p+q=\frac{\partial^2\phi}{\partial x^2}+\frac{\partial^2\phi}{\partial y^2}.$$

Combining this with the continuity equation

$$\left(\frac{\partial^2}{\partial x^2}+\frac{\partial^2}{\partial y^2}\right)\left(\frac{\partial^2\phi}{\partial x^2}+\frac{\partial^2\phi}{\partial y^2}\right)=0$$

we obtain $$\frac{\partial^2(p+q)}{\partial x^2}+\frac{\partial^2(p+q)}{\partial y^2}=0.$$

An analytical solution of Laplace's equation is possible only in a limited number of cases of simple boundaries and boundary stresses. Research workers having need to solve this problem are compelled to resort to numerical methods of successive approximations, which are based on the principle that the value of an harmonic function at any point is equal to the average of the values at four equidistant points located on two mutually perpendicular lines. Such methods were used by the author in connection with photoelastic researches as far back as 1932. The procedure was the same as that suggested by Liebman.[6]

An important contribution to the solution of this problem was recently made by G. H. Shortley and R. Weller.[7] Their procedure shortens measurably the path toward convergence and reduces materially the time and labor. They also developed useful correction factors to take care of cases in which the influencing points are not equidistant from the origin. Their published results confine themselves, however, entirely to rectilinear coordinates.

This has certain disadvantages. It necessitates the use of correction factors for points on curved boundaries, which are generally sources of stress concentrations, and calls for a preliminary solution with a coarse network to be followed by a closer approximation with a finer network.

The use of polar coordinates eliminates the need for correction factors on circular boundaries, gives from the start as large a number of points on curved boundaries as conditions require and automatically results in a finer network in the region surrounding the circular boundaries, the sources of stress concentrations, and a progressively coarser network in the regions removed from the origin.

The theoretical justification for this procedure rests on the possibility for a conformal transformation of rectangles into circles and vice versa for which the necessary equations are

$$x=\log r, \quad y=\theta.$$

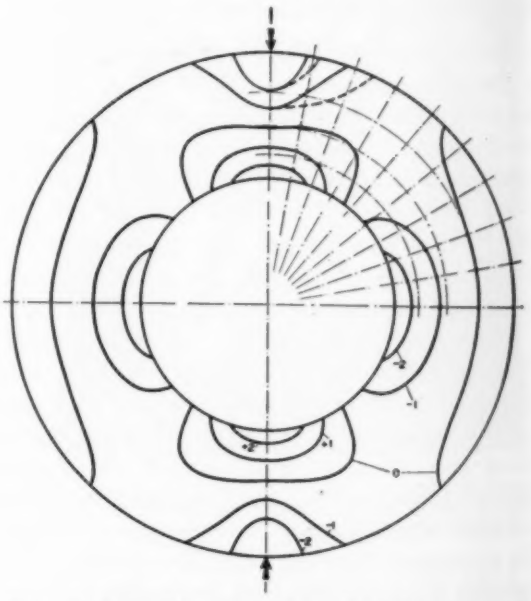

Fig. 17. Isopachic curves determined by a numerical solution of Laplace's equation using polar coordinates. The boundary stresses were taken from the Bakelite model shown in Fig. 7 and the concentrated loads were replaced by theoretical distributions of stresses as given by Boussinesq-Flamant.

[6] H. Liebman, Sitz. Math. Phys. Klassen d. Bayer Akad. München 385 (1918).

[7] G. H. Shortley and R. Weller, "The Numerical Solution of Laplace's Equation," J. App. Phys. 9, 334 (1938).

It can be shown that for analytic functions all the essential relations between points in cartesian coordinates are also valid in the corresponding points of the polar coordinates, such as the nine-block procedure suggested by Shortley and Weller.

For problems involving circular boundaries it is obvious that the use of polar coordinates would result in increased accuracy and a saving of effort. Moreover, even in some cases where the boundaries are not all circular, as for example in the case of a hole in a rectangular bar the same advantages can be obtained. In such cases the origin is again taken at the center of the hole, and instead of making corrections at the straight boundaries the network is stopped at the points closest to the boundaries and values of $(p+q)$ are approximated directly from the values of $(p-q)$ given by the photoelastic stress pattern. Such a procedure, while not absolutely rigorous, is warranted because of the fact that at free, straight boundaries the vanishing principal stresses remain negligible quantities in regions close to the free, straight edges.

The author has investigated a large number of problems by means of both cartesian and polar coordinates and found the proposed procedure of polar coordinates to give satisfactory results. Limitations of space do not permit more than one illustration.

Figure 17 shows computed contours, or isopachic curves, for the same disk with the hole which was treated optically and described in the preceding part of the paper. In the numerical solution the boundary values were taken from the photoelastic stress pattern of Fig. 7, in which the concentrated loads were replaced by theoretical stress distributions on small semicircles as given by the Boussinesq-Flamant stress function.[8]

$$\phi = Ar\theta \sin \theta.$$

Figure 18 shows a composite photograph of the isopachic stress pattern obtained optically (Fig. 6), and the contours obtained from the numerical solution of Laplace's equation (Fig. 17).

The composite photograph shows good agreement between the two solutions in all regions except in the immediate vicinity of the concentrated loads. It must be remembered that the numerical solution is based on boundary values from a Bakelite model in which the state of stress near the loads is obviously somewhat different from that in the steel model, due to local plastic flow. The assumed distributions replacing the concentrated loads are probably another factor contributing to the local discrepancies.

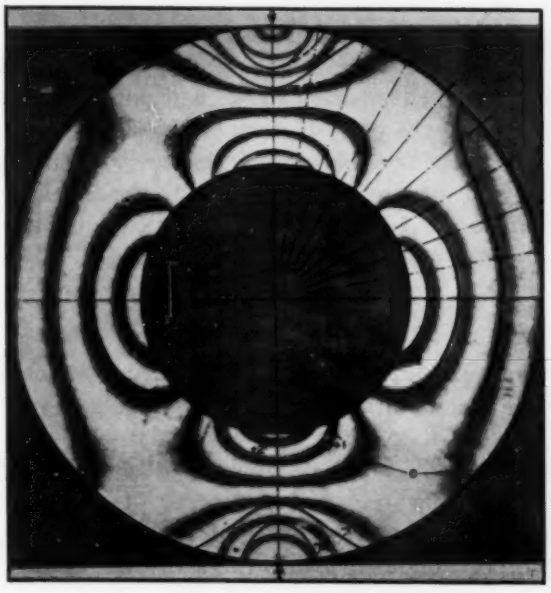

FIG. 18. Composite photograph of $(p+q)$ contours obtained from numerical solution of Laplace's equation superimposed upon the isopachic stress pattern obtained by means of interference fringes from the surface of a steel model. Numerical solution is based upon the boundary stresses from the Bakelite model shown in Fig. 7.

The results shown in the composite photograph represent, in our judgement, a satisfactory corroboration of both methods.


## ACKNOWLEDGMENTS

The author expresses his appreciation to the administration of the Carnegie Institute of Technology, especially to Dr. Robert E. Doherty, President of the Carnegie Institute of Technology; Dr. Webster N. Jones, Director, College of Engineering; Professor N. C. Riggs, Head of Mechanics Department, for their interest in and support of this work. Special acknowledgment is made to M. M. Leven, mechanician in the photoelastic laboratory for his cooperation and assistance.


[8] See Flamant, Comptes rendus **114**, 1465 (1892). See also paper by J. H. Michell, Proc. Math. Soc. London **32**, 35 (1900).

# The Operational Calculus. II*

By Louis A. Pipes**

*Electrical Engineering Department, The University of Wisconsin, Madison, Wisconsin*

### *III. Development of Heaviside's Rules*

The development of certain transforms which are known in the literature of operational calculus as "Heaviside's rules" will now be undertaken. In the early history of the subject, there appears to have been much controversy over the subject, but when viewed from the Laplacian transform point of view, the proof of these powerful rules is seen to be most simple.

#### A. Heaviside's First Rule

Heaviside's first rule is commonly known as "the partial fraction rule." This rule may be stated as follows:

If $g(p)=f(p)/F(p)$, where $f(p)$ and $F(p)$ are polynomials in $p$ and the order of $F(p)$ is at least as high as the order of $f(p)$ and, further, the polynomial $F(p)$ has the $n$ distinct zeros $p_1$, $p_2$, $\cdots$ $p_n$. Then we have

$$f(p)/F(p)\doteqdot f(0)/F(0)+\sum_{r=1}^{n}\frac{F(p_r)\epsilon^{p_r t}}{p_r(dF/dp)_{p=p_r}}. \quad (59)$$

*Proof*:

By our general formula (1), we have, by the theory of residues,

$$\frac{f(p)}{F(p)}\doteqdot \sum \text{ residues of } \frac{f(p)}{pF(p)}\epsilon^{pt}. \quad (60)$$

Now if $p_1$, $p_2$, $\cdots p_n$ are the $n$ distinct zeros of $F(p)$, then we may write $F(p)=a(p-p_1)(p-p_2)\cdots(p-p_n)$, where $a$ is the coefficient of $p^n$.

The residue at $p=0$ is

$$\text{Limit}_{p\to 0}\frac{pf(p)\epsilon^{pt}}{pF(p)}=\frac{f(0)}{F(0)}, \quad (61)$$

and the residue at $p=p_i$ is

$$\text{Limit}_{p\to p_i}\frac{(p-p_i)f(p)\epsilon^{pt}}{pa(p-p_1)(p-p_2)\cdots(p-p_i)\cdots(p-p_n)}=\frac{f(p_i)\epsilon^{p_i t}}{p_i(dF/dp)_{p=p_i}}. \quad (62)$$

Hence, we have the Heaviside expansion theorem:

$$\frac{f(p)}{F(p)}\doteqdot\frac{f(0)}{F(0)}+\sum_{r=1}^{n}\frac{f(p_r)\epsilon^{p_r t}}{p_r(dF/dp)_{p=p_r}}. \quad (59)$$

#### B. Heaviside's Second Rule

If $$g(p)=\sum_{n=0}^{\infty}\frac{a_n}{p^n},$$

where the series on the right is a convergent series of negative powers of $p$, then

$$g(p)\doteqdot\sum_{n=0}^{\infty}a_n t^n/n! \quad (63)$$

This result is obtained by the term by term substitution of $t^n/n!\doteqdot 1/p^n$.

#### C. Heaviside's Third Rule

Heaviside's third rule concerns the transform of the series

$$g(p)=\sum_{0}^{\infty}a_n p^n+p^{\frac{1}{2}}\sum_{0}^{\infty}b_n p^n,$$

where both series are convergent series in $p$.

By making use of the direct term by term application of the transform

$$1/p^r\doteqdot t^r/\Gamma(r+1) \quad (53)$$

and the facts that $\Gamma(1/2)=\sqrt{\pi}$ and $p^s\doteqdot 0$ when $s$ is a positive integer, the transform

$$g(p)=a_0+\frac{1}{(\pi t)^{\frac{1}{2}}}\left(b_0-\frac{b_1}{2t}+\frac{1\cdot 3b_2}{(2t)^2}-\frac{1\cdot 3\cdot 5b_3}{(2t)^3}+\cdots\right) \text{ for } t>0. \quad (64)$$

* This paper is the second of a series of three. The final part will appear in the May issue.

** Now at Harvard University, Graduate School of Engineering, Pierce Hall, Cambridge, Massachusetts.

## IV. Solution of Linear Integro-Differential Equations with Constant Coefficients

### A. Applications to Linear Lumped Electrical Networks

Consider a series circuit containing linear lumped constant parameters of resistance, capacitance and inductance and let an electromotive force $e(t)=E\sin(wt)$ be impressed on the circuit at $t=0$. If the initial charge on the condenser is $Q_0$, $i_0$ is the initial current, and $R$, $L$, $C$, are the coefficients of resistance, inductance and capacitance, respectively, then the equation of the circuit valid for $t>0$ is

$$L\frac{di}{dt}+Ri+\frac{1}{C}\int_{-\infty}^{t} idt=E\sin\omega t. \tag{65}$$

Now let $I(p)$ be the transform of $i(t)$; that is, $i(t)\doteqdot I(p)$. Then by our fundamental theorem for the transform of an integral *Th. II* we have

$$\int_{-\infty}^{t} idt=\frac{I}{p}+Q_0, \tag{7a}$$

and for the transform of a derivative, we have

$$\frac{di}{dt}\doteqdot pI-pi_0. \tag{6a}$$

Making use of the transform,

$$\sin(\omega t)\doteqdot \omega p/(p^2+\omega^2), \tag{38}$$

and the above transforms for the integral and derivative of $i(t)$, we obtain the equation to be satisfied by $I(p)$, the transform of $i(t)$ in the form

$$L(pI-pi_0)+RI+\frac{1}{C}\left(\frac{I}{p}+Q_0\right)=\frac{E\omega p}{p^2+\omega^2} \tag{66}$$

or

$$I(p)=\frac{1}{LCp^2+RCp+1}\times\left\{i_0LCp^2-pQ_0+\frac{E\omega Cp^2}{p^2+\omega^2}\right\}. \tag{67}$$

Now to determine the current we have the general expression

$$i(t)=\sum \text{ residues of } \frac{I(p)}{p}\epsilon^{pt} \tag{68}$$

in the $p$ plane.

We must hence calculate the position of the poles of the function $I(p)e^{pt}/p$. These poles are determined from

$$LCp^2+RCp+1=0 \quad \text{and} \quad p^2+\omega^2=0 \tag{69}$$

and are given explicitly by

$$p=-\frac{R}{2L}\pm\left(\frac{R^2}{4L^2}-\frac{1}{LC}\right)^{\frac{1}{2}} \quad \text{and} \quad p=\pm i\omega. \tag{70}$$

If we let

$$\alpha=\frac{R}{2L}, \quad \beta=\left(\frac{R^2}{4L^2}-\frac{1}{LC}\right)^{\frac{1}{2}},$$

$$p_1=-\alpha+B, \quad p_2=-\alpha-\beta,$$

we may therefore write

$$I(p)=\frac{1}{(p-p_1)(p-p_2)}\times\left\{p^2i_0-\frac{pQ_0}{LC}+\frac{E\omega}{L}\frac{p^2}{p^2+\omega^2}\right\}. \tag{71}$$

There are the following three cases to be considered:

a. $R^2/4L^2>1/LC$; in this case $p_1$ and $p_2$ are real and distinct.
b. $R^2/4L^2=1/LC$, giving $p_1$ and $p_2$ real and equal.
c. $1/LC>R^2/4L^2$; $p_1$ and $p_2$ are conjugate complex.

The evaluation of the residues for the case of distinct roots $p_1$ and $p_2$, gives the solution

$$i(t)=i_0/(p_2-p_1)\{p_1\epsilon^{p_1t}-p_2\epsilon^{p_2t}\}$$
$$-Q_0/LC(p_1-p_2)\{\epsilon^{p_1t}-\epsilon^{p_2t}\}$$
$$+\frac{E\omega}{L}\left\{\frac{p_1\epsilon^{p_1t}}{(p_1-p_2)(p_1^2+\omega^2)}+\frac{p_2\epsilon^{p_2t}}{(p_1-p_2)(p_2^2+\omega^2)}\right\}$$
$$+\frac{E}{|Z|}\sin(\omega t-\theta), \tag{72}$$

where $Z(iw)=R+i(\omega L-(1/\omega c))$

and $$\theta=\tan^{-1}\left\{\frac{\omega L-(1/\omega c)}{R}\right\},$$

it may be noted that the steady-state term

$$\frac{E}{|Z|}\sin(\omega t-\theta)$$

is obtained by evaluating the residues of the transform of the function $E\sin(\omega t)$. The transient terms, on the other hand, depend on the poles of the impedance function.

We see quite clearly the effect of the original charge $Q_0$, and the original current $i_0$, as well as the steady-state term produced by the electromotive force $E\sin(\omega t)$, which persists after the exponentially damped or transient terms have subsided.

The case of equal roots may be handled in a similar manner by making use of the transforms (34) to (37) of the list given in Section II.

*The most general linear lumped network.*—Let us now consider the most general linear lumped network with constant parameters. Let the network have $n$ meshes and have initial charges and currents. Let electromotive forces be applied to the network at $t=0$.

The well-known canonical equations of such a network are:

$$\begin{aligned} &Z_{11}i_1+\cdots Z_{1n}i_n=e_1(t)\\ &\cdot\quad\cdot\quad\cdot\quad\cdot\quad\cdot\quad\cdot\quad\cdot\quad\cdot\\ &Z_{n1}i_1+\cdots Z_{nn}i_n=e_n(t), \end{aligned} \tag{73}$$

where $(i_1\cdots i_n)$ are the $n$ mesh currents,
$(e_1\cdots e_n)$ are the $n$ mesh voltages.

The $Z_{ij}$ quantities are impedance operators of the form

$$Z_{ij}=L_{ij}d/dt+R_{ij}+S_{ij}\int_{-\infty}^{t}(\quad)dt \tag{74}$$

and

$L_{ij}$ are coefficients of inductance,
$R_{ij}$ are coefficients of resistance,
$S_{ij}$ are coefficients of elastance.

If we now introduce the following matrices,

$$[Z]=\begin{Vmatrix} Z_{11} & \cdots & Z_{1n}\\ \cdot & \cdot & \cdot\\ Z_{n1} & \cdots & Z_{nn}\end{Vmatrix},$$

$$[e]=\begin{Vmatrix} e_1\\ -\\ -\\ e_n\end{Vmatrix},\quad [i]=\begin{Vmatrix} i_1\\ -\\ -\\ i_n\end{Vmatrix}. \tag{75}$$

We may write the above set of equations in the convenient matrix form

$$[Z][i]=[e]. \tag{76}$$

Let us now introduce the matrix $[I(p)]$, a column matrix whose elements are the transforms of the elements of the matrix $[i(t)]$. That is, we write

$$[I(p)]\doteqdot[i(t)]. \tag{77}$$

In terms of this notation, the transform of the matrix equation (76) may be written in the form

$$[Z(p)][I]=[E(p)]+p[L][i^0]-[S][q^0]. \tag{78}$$

Where we have assumed the initial values at $t=0$ of the charges and currents in the $n$ meshes to be, respectively, $(q_1^0,\cdots q_n^0)$ and $(i_1^0,\cdots i_n^0)$, and we have introduced the matrices:

$$[i^0]=\begin{Vmatrix} i_1^0\\ -\\ -\\ i_n^0\end{Vmatrix},\quad [q^0]=\begin{Vmatrix} q_1^0\\ -\\ -\\ q_n^0\end{Vmatrix},$$

$$[Z(p)]=\begin{Vmatrix} Z_{11} & \cdots & Z_{1n}\\ - & - & -\\ - & - & -\\ Z_{n1} & \cdots & Z_{nn}\end{Vmatrix},$$

where $Z_{ij}(p)=L_{ij}p+R_{ij}+S_{ij}/p$ and

$$[L]=\begin{Vmatrix} L_{11} & \cdots & L_{1n}\\ - & - & -\\ - & - & -\\ L_{n1} & \cdots & L_{nn}\end{Vmatrix},\quad [S]=\begin{Vmatrix} S_{11} & \cdots & S_{1n}\\ - & - & -\\ - & - & -\\ S_{n1} & \cdots & S_{nn}\end{Vmatrix},$$

and the matrix $[E(p)]$ is the transform of $[e(t)]$. If we multiply (78) by the inverse of $[Z(p)]$, we obtain an explicit solution for the transform matrix $[I]$.

$$[I(p)]=[Z(p)]^{-1}([E(p)]+p[L][i^0]-[S][q^0]). \tag{79}$$

The currents are given explicitly by the matrix equation

$$[i(t)]=\frac{1}{2\pi i}\int_{c-i\infty}^{c+i\infty} e^{pt}[I(p)]dp/p. \qquad (80)$$

We see from this equation the advantages of the operational method over the classical procedure. In the classical method we have to find a complementary function and a particular integral separately. To find the former, we assume a solution of the form $i_s=a_se^{\mu t}$, and we substitute this into the differential equation with the driving forces omitted. We then find an equation to determine the $2n$ possible values of $\mu$ and the ratios of the $a$'s corresponding to each. The particular integral is then found by some method. The actual values of the amplitudes are still undetermined, and the value associated with each $\mu$ must be found by substituting in the initial conditions and again solving a set of $n$ simultaneous equations. The labor of finding the equation for the $\mu$'s and the ratios of the $a$'s corresponding to one of them is about the same as finding the operational solution. The rest of the work is avoided by the operational method.

If some of the $\mu$'s are equal or zero, a considerable complication is introduced in the classical method but not in the operational one.

### B. Applications to Mechanical Vibrations

The Lagrangian equations of motion for a general mechanical system defined by $n$ parameters $(x_1, x_2, \cdots x_n)$ that is executing small motions about a position of equilibrium may be written in the form

$$\begin{aligned} &Z_{11}(x_1)+Z_{12}(x_2)+\cdots+Z_{1n}(x_n)=F_1(t)\\ &\quad\cdots\cdots\cdots\cdots\cdots\cdots\\ &Z_{n1}(x_1)+Z_{n2}(x_2)+\cdots+Z_{nn}(x_n)=F_n(t) \end{aligned} \qquad (81)$$

where $Z_{ij}$ is a differential operator of the form

$$Z_{ij}=A_{ij}d^2/dt+B_{ij}d/dt+C_{ij} \qquad (82)$$

and $F_i(t)$ are the forces impressed on the various component parts of the system.

Let us introduce the notation:

$$[x]=\begin{Vmatrix} x_1 \\ \cdots \\ x_n \end{Vmatrix} \text{ the coordinate matrix,} \qquad (83)$$

$$[A]=\begin{Vmatrix} A_{11} & \cdots & A_{1n} \\ \cdots & \cdots & \cdots \\ A_{n1} & \cdots & A_{nn} \end{Vmatrix} \text{ the inertia matrix,} \qquad (84)$$

and two additional matrices, similarly defined,

$$[B], \text{ the damping matrix,} \qquad (85)$$

$$[C], \text{ the stiffness matrix,} \qquad (86)$$

and a columnar matrix whose elements are the applied forces

$$[F(t)], \text{ the force matrix.} \qquad (87)$$

By means of this notation, the equation of motion (70) may be conveniently written in the form

$$[A][\ddot{x}]+[B][\dot{x}]+[C][x]=[F(t)], \qquad (88)$$

where the dots indicate differentiation of the elements of the matrices with respect to time.

If we introduce a columnar matrix $[y(p)]$, whose elements are the transforms of the elements of the coordinate matrix $[x(t)]$, we may write symbolically

$$[y(p)]\doteqdot[x(t)]. \qquad (89)$$

Similarly, let us introduce the matrix $[G(p)]$, whose elements are the transforms of the force matrix $[F(t)]$, or symbolically

$$[G(p)]\doteqdot[F(t)]. \qquad (90)$$

Let us also introduce the following two columnar matrices:

$$[x^0], \text{ the matrix giving the initial displacements at } t=0, \qquad (91)$$

$$[x^1], \text{ the matrix giving the initial velocities at } t=0. \qquad (92)$$

If we now make use of (6) for the transform of the first and second derivatives of a function then Eq. (77) transforms to

$$[Z(p)][y]=[G(p)]+(p^2[A]+p[B])[x^0]+p[A][x^1], \qquad (93)$$

where $Z_{ij}(p)=p^2A_{ij}+pB_{ij}+C_{ij}$.

Multiplying (82) by the inverse of $[Z(p)]$, $[Z(p)]^{-1}$, we obtain:

$$[y]=[Z(p)]^{-1}\{[G]+(p^2[A]+p[B])[x^0]+p[A][x^1]\}. \qquad (94)$$

The explicit solution for the coordinate matrix $[x]$ is then given by

$$[x]=\frac{1}{2\pi i}\int_{c-i\infty}^{c+i\infty} e^{pt}[y]dp/p, \qquad (95)$$

where in the contour integral expression, the constant $c$ is such that all the singularities of the integrand lie to the left of the path of integration.

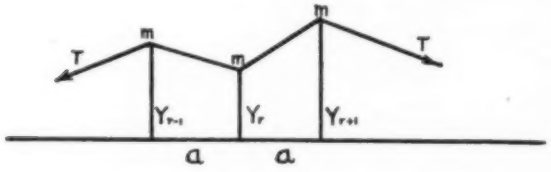


FIG. 3.

The above formula for $[y]$, which is the operational equivalent of the coordinate matrix, $[x]$, contains a great deal of information in that the effect of the impressed forces, the initial displacements, and the initial velocities is clearly evident. In the absence of impressed forces, $[G(p)]=[0]$, and we have the case of free vibrations. The procedure of obtaining the explicit solution is that of calculating the sum of the residues of the integrand at its poles. Since the poles of the integrand depend on the poles of $[Z(p)]^{-1}$, the zeros of the determinantal equation must be located. This equation may be written in the form

$$|Z(p)|=0. \qquad (96)$$

When numerical values are given, this may be solved by the usual methods and the residues computed.

*Resonance of a simple pendulum.*—To give a simple illustration of the theory, let us consider the effect on a simple pendulum of a disturbing force varying harmonically with a period equal to the free period of the pendulum. The differential equation of motion of such an arrangement may be conveniently written in the form

$$\ddot{x}+n^2x=A\sin(nt). \qquad (97)$$

Now let $y\doteqdot x$ and use the boundary conditions that at $t=0$, $x=0$ and $dx/dt=0$, and the known relation that $A\sin(nt)\doteqdot Anp/(p^2+n^2)$. Then the transformed equation becomes

$$y=Anp/(p^2+n^2)^2. \qquad (98)$$

The evaluation of this equation to obtain the inverse transform is a simple matter if we note that from our table of direct transforms

$$p/(p^2+n^2)\doteqdot\sin(nt)/n. \qquad (38c)$$

Hence,

$$\frac{\partial}{\partial n}\frac{p}{p^2+n^2}\doteqdot\frac{\partial}{\partial n}\frac{\sin(nt)}{n}$$

and, therefore,

$$x=A[\sin(nt)-nt\cos(nt)]/2n^2. \qquad (99)$$

The amplitude $x$ increases with passage of time until the motion becomes so large that it can no longer be represented by the simple differential equation under consideration.

*Vibration of a string of beads.*—Before passing to the discussion of continuous systems leading to partial differential equations, let us consider the interesting mechanical problem of the vibration of a string of beads. The motion which we shall consider is that of a massless string on which are fastened a number of massive equal and equidistantly spaced beads. Let $n$ be the number of beads and the mass of each bead be $m$. Let $L$ be the length of the string. Let the ends be fastened and the distance of each bead from the next be

$$a=L/(n+1). \qquad (100)$$

Let $y_1, y_2, \cdots y_n$ be the lateral displacements of the beads considered all to be in the same plane. If we assume that the displacements are so small that the tension may be considered as a constant $T$, and that we may neglect the action of the force of gravity, then the force on any particle parallel to the $y$ axis is seen from Fig. 3, to be

$$T\left\{\frac{-y_r-y_{r-1}}{a}+\frac{y_{r+1}-y_r}{a}\right\}.$$

The equations of motion, are

$$\begin{aligned} m\ddot{y}_1+\frac{T}{a}(y_1-0+y_1-y_2)&=0, \qquad (102)\\ m\ddot{y}_2+\frac{T}{a}(y_2-y_1+y_2-y_3)&=0,\\ -\ -\ -\ -\ -\ -\ -\ -\ -\ -&,\\ m\ddot{y}_n+\frac{T}{a}(y_n-y_{n-1}+y_n-0)&=0. \end{aligned}$$

Let $g_i\doteqdot y_i$ and make use of the transforms of

a derivative by means of Eq. (6). We then have the equations to be satisfied by the transforms as

$$\begin{aligned}
&m\{p^2g_1-y_1(0)p-y_1'(0)\}+\frac{T}{a}(2g_1-g_2)=0,\\
&m\{p^2g_2-y_2(0)p-y_2'(0)\}+\frac{T}{a}(2g_2-g_1-g_3)=0,\\
&\quad\cdots\cdots\cdots

the residues at the poles given by (118) may be computed.

The problem of a vibrating string of beads occupies a key position in oscillation mechanics.

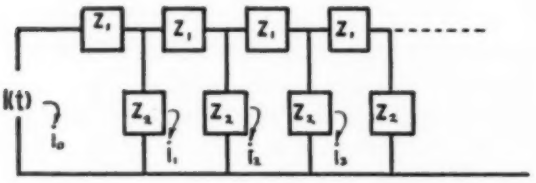


FIG. 4.

The general theory of discrete systems reaches a climax in this problem and from it have come most important technical applications such as the periodic electric structures or filters which are indispensible in telephony.

*The electric wave filter.*—Before considering continuous systems, let us consider the problem of the artificial line or wave filter. This is a periodic structure composed of a series of sections as shown in Fig. 4.

Each section consists of a lumped impedance $Z_1$ in series with the line and a lumped impedance $Z_2$ in parallel across the line. We will consider that the voltage is applied at the middle of the initial or zeroth section. This termination is chosen because of its practical importance and because it simplifies the mathematical analysis. Any other termination may be dealt with by adding an additional terminal impedance. If we let $i_n$ denote the mesh current in the $n$th section, $i_{n-1}$, the mesh current in the $(n-1)$th section, etc., then we may write the expression for the voltage in the $n$th section by Kirchhoff's law in the form

$$(Z_1+2Z_2)i_n-Z_2(i_{n-1}+i_{n+1})=0, \quad (121)$$

where the impedance operators have their usual significance. Now if we let

$$i_n(t)\doteqdot I_n(p) \quad (122)$$

and assume the network without initial currents or charges, we have

$$(Z_1+2Z_2)I_n-Z_2(I_{n-1}+I_{n+1})=0. \quad (123)$$

The solution of this difference equation is of the form

$$I_n=Ae^{-nb}+Be^{nb}, \quad (124)$$

where $A$, $B$ and $b$ are constants independent of $n$. Substituting this solution into (123) we obtain

$$[(Z_1+2Z_2)-2Z_2\cosh(b)]\times[Ae^{-nb}+Be^{nb}]=0. \quad (125)$$

Now if we choose $b$ so that

$$\cosh(b)=(Z_1+2Z_2)/2Z_2 \quad (126)$$

then the constants $A$ and $B$ are left at our disposal and the equation is satisfied by the assumed form of the solution. $b$ is called the operational propagation constant of the line.

The constants $A$ and $B$ are determined from the terminal conditions that is, the circuit equations of the first and last sections. For the zero section we obtain

$$Z_1I_0/2+Z_2(I_0-I_1)=E(p), \quad (127)$$

where $E(p)$ is the transform of the impressed electromotive force. The circuit equation of the last or $r$th section is

$$Z_1I_r/2-Z_2(I_{r-1}-I_r)=0. \quad (128)$$

If we substitute (124) into (127) and (128), we obtain two equations involving $A$ and $B$. Solving these equations for $A$ and $B$ and substituting the constants back into the equation for $I_n$ we obtain

$$I_n=\frac{E(p)\cosh(r-n)b}{Z_2\sinh(b)\sinh(rb)}. \quad (129)$$

For the last section, $r=n$, we have

$$I_r(p)=\frac{E(p)}{Z_2\sinh(b)\sinh(rb)}. \quad (130)$$

The transform of the current in the $n$th mesh is then given explicitly by the evaluation of the basic integral

$$i_n(t)=\frac{1}{2\pi i}\int_{c-i\infty}^{c+i\infty}e^{pt}I_n(p)dp/p. \quad (131)$$

The poles of the integrand depend on the zeros of $Z_2\sinh(b)\sinh(rb)$ which are determined by the character of the impedances $Z_1$ and $Z_2$.

Many interesting special cases will be found discussed in *Heaviside's Electrical Circuit Theory* by Louis Cohen.[D6]

# Resumés of Recent Research

**Theory of Reversible Magnetization in Ferromagnetics** A demagnetized ferromagnetic crystal consists of "domains" magnetically saturated along different but crystallographically equivalent directions. In a gradually increasing field, the whole crystal first becomes magnetized along the one of these directions nearest the field; then the magnetization rotates toward the field direction. The latter process is controlled by regular, easily describable crystalline forces. The former is less well understood. There is evidence that it consists of a growth of some domains at the expense of others by electron spin transitions in the interdomain boundaries; but the internal forces opposing this boundary displacement are local stresses and fields of largely accidental origin, difficult to describe quantitatively. By a statistical method, formulas have been obtained for the magnetostriction and the reversible susceptibility, and the agreement with experiment is fairly good in polycrystalline specimens. The assumptions of the statistical theory, however, are easily stated only in terms of a simplified model. It is difficult to interpret them in terms of boundary displacement, or to modify them so as to take account of forces that are not entirely random.

Considerable progress toward a mathematical analysis of the boundary displacement process was recently made by Kondorsky, who obtained formulas for the reversible susceptibility of crystals. But to evaluate some of the quantities in his equations, Kondorsky had to use formulas borrowed from the statistical theory. It has now been shown* that with very few additional assumptions Kondorsky's theory can be made complete in itself. The new theory leads to the formulas of the statistical theory when there is no regular dependence of the internal forces upon the type of boundary or its position. Deviations of the experimental results from these formulas would therefore indicate such dependence, and measurements of the reversible susceptibility of crystals should give information about the internal forces opposing magnetization.

* W. F. Brown, Jr., Phys. Rev. **55**, 568 (1939).

**Origin of Terrestrial Magnetism** A new solution of this much debated problem has been proposed by W. M. Elsasser.* According to his theory the interior of the earth is not at rest, but is in a state of perpetual convective motion maintained by radioactive heat development. The magnetic field is induced by thermoelectric currents accompanying the mechanical motions.

Our knowledge of the mechanical properties of the earth's interior is derived from seismic observations. The existence of a surface of discontinuity at a depth of 2900 km is well established and this surface is usually identified with the boundary between the metallic core (iron-nickel) and the nonmetallic exterior. Transversal seismic waves are reflected at the boundary, but are not transmitted through the core. From this fact and from some other evidence Jeffreys was able to estimate the viscosity of the core. He found that a value of $2 \cdot 10^{10}$ c.g.s. units should represent an upper limit for the coefficient of viscosity of the core. (For comparison we might notice that the viscosity of the rocks in the earth's crust is of the order of $10^{22}$.) Elsasser demonstrates that with this low value of the viscosity we must almost certainly have convective motions, the heat developed by even an extremely small fraction of the earth's total radioactivity being sufficient to maintain such motions against internal friction.

It is then assumed that the motions are accompanied by irregular temperature fluctuations. The material being a metallic conductor, these temperature differences will give rise to a system of thermoelectric currents. It has been possible to estimate roughly the order of magnitude of these currents by extrapolating the properties of iron to a state of high temperature and pressure. In the extrapolation one has been guided by the principles of the electronic theory of conductivity; the result is that the thermoelectric currents should be somewhat larger than currents produced by the same temperature differences would be under ordinary conditions of temperature and pressure.

* W. M. Elsasser, Phys. Rev. **55**, 486 (1939).

The main problem of the theory lies now in the explanation of the fact that the thermoelectric currents do not cancel in the average, but yield a resultant magnetic momentum which is approximately parallel to the earth's axis. To understand this one has to study the mechanical motions more closely. From the equations of motion one sees that the Coriolis force acting upon the moving masses is vastly larger than all other mechanical forces. This produces a particular asymmetry of the motions with regard to the east-west direction; if we picture the motions as a system of vortices, the Coriolis force will tilt each vortex in the same sense. This results in an east-west asymmetry of the temperature distribution in each vortex. It can be shown however that temperature variations in an otherwise homogeneous medium produce a current system whose resultant magnetic momentum vanishes. Just as in ordinary thermoelectricity there must also be a variation of the thermoelectric constant (there must at least be two different conductors in contact). We know from Bridgman's investigations that phase transformations are extremely frequent at high pressures and it is now furthermore necessary to assume that phase changes occur induced by the vertical component of the convective motions. The theory necessitates therefore two fundamental independent assumptions, first the existence of convective motions and secondly the existence of phase changes connected with them. The rest follows by considering the dominant influence of the Coriolis force upon this type of motion.

It is clear that the observed magnetic moment can only be caused by a small one-sided excess of an otherwise rather irregular current distribution. Therefore the actual current densities must be considerably larger than the calculated density of a straight flow which would be parallel to the circles of latitude and which would produce the earth's magnetic moment. Taking this into account and using the estimate of the electric properties mentioned above, it is found that temperature fluctuations of the order of 10° can produce a magnetic moment of the right order of magnitude.

## Letter to the Editor

### A New Method for Photoelasticity in Three Dimensions

It is possible to use the polarization caused by the scattering of light within a cloudy model in place of the usual analyzer in photoelastic investigations. This enables one to make analyses of three-dimensional stress systems very conveniently.

One makes a model from a suitable transparent plastic which contains enough scattering particles to analyze satisfactorily a beam of polarized light. The model is then loaded and placed in a beam of plane-polarized light which has been collimated and passed through a slit. This beam illuminates a plane section through the model. Interference fringes appear in this section when it is viewed normal to the direction of the beam and also to the plane of polarization of the beam. One may place the model in any desired position with respect to the beam and thus observe all possible sections. One may also immerse the model in a liquid of the same index, if desired, to eliminate unwanted refraction.

This method has many advantages over the one proposed by Opel in which the model is cooled under load from an elevated temperature and subsequently analyzed after slicing it into plates. The number of slices which one may make in the latter method is limited and one may disturb the stress pattern somewhat by the slicing operation unless considerable care is exercised. With the proposed method one may search for the directions of the maximum and minimum shears at any desired point by illuminating successive planes and observing the fringe patterns in them and no necessity arises for destroying the model in this process. One may determine the maximum and minimum shears at any interior point and also separate the principal stresses at a free edge with ease and determine their directions without the complex manipulations necessary in handling the sliced model. There is no necessity for heating the model and thereby changing its optical and elastic constants. Large deformations do not take place with accompanying loss of exactness in applying the usual assumptions of the theory of elasticity. The accuracy at interior points seems better than that obtainable by the slicing method.

FIG. 1.

The accompanying photograph shows the fringes resulting from illuminating the central section of a rectangular block in which stresses exist because of rapid cooling. It is to be noted that the interpretation of these fringes is not that of the usual photoelastic analysis in two dimensions. Here the stress is a function of the spacing of the fringes rather than of the fringe order.

Complete details will be published when theory and technique are more fully developed.

R. WELLER

Mendenhall Laboratory of Physics,
Ohio State University,
Columbus, Ohio,
March 10, 1939.

# Here and There

### New Appointments

It is announced in *Nature* that Dr. Erwin Schrödinger, Professor of Theoretical Physics at the University of Graz, Austria, has been appointed by the Foundation Francqui as a visiting professor for the next six months to a "Chaire Francqui" in the University of Ghent.

★

Dr. Frederick Seitz has been appointed to an assistant professorship at the University of Pennsylvania.

★

Dr. Benedict Cassen has joined the staff of the Westinghouse Research Laboratories in East Pittsburgh, Pennsylvania, to conduct research on means of producing high voltage x-rays for therapeutic uses. He has been engaged in x-ray and neutron research at the Harper Memorial Hospital in Detroit.

★

Dr. A. R. Olpin has been appointed Research Director of the Ohio State University Research Foundation at Columbus, Ohio.

★

Dr. George E. Uhlenbeck, Professor of Theoretical Physics at the University of Utrecht, who is this year visiting Professor of Theoretical Physics at Columbia University, will return to the University of Michigan as Professor of Physics, the appointment to take effect at the beginning of the next academic year. Professor Uhlenbeck was a member of the faculty of the University of Michigan from 1927 to 1935.

★

### Awards

The Oersted Medal of the American Association of Physics Teachers, established through the generosity of an anonymous donor, was awarded for 1938 to Professor Alexander Wilmer Duff, Professor Emeritus of Physics at the Worcester Polytechnic Institute. The award was made at the annual meeting of the American Association of Physics Teachers in Washington, D. C., on December 30.

★

Dr. William D. Coolidge, Director of General Electric's research laboratory, has been awarded the Faraday Medal for 1938 by the council of the Institution of Electrical Engineers of England. The Faraday Medal, founded in 1921 to commemorate the fiftieth anniversary of the first meeting of the institution, is awarded each year for notable scientific and industrial achievement in electrical engineering or for conspicuous service rendered to the advancement of electrical science.

★

The Institute of Metals Division Award for 1939 was presented to Assistant Professor Frederick N. Rhines and Robert F. Mehl, Director of the Metal Research Laboratory, both of the Carnegie Institute of Technology, Pittsburgh. The award was for their paper on "Rates of Diffusion in Alpha Solid Solutions of Copper."

★

Harold Jeffreys, M.A., D.Sc., F.R.S., received the Murchison Medal in recognition of the value of his researches on the constitution and physics of the earth's interior, and, in particular, of the deductions he has drawn from the analysis of records of distant earthquakes.

★

The degree of Doctor of Science was conferred on Sir Arthur Stanley Eddington on the occasion of the installation of the Duke of Devonshire as Chancellor of the University of Leeds.

★

### Biophysics Symposium

A Biophysics Symposium will be held in connection with the Annual Meeting of the Southeastern Section of the American Physical Society at the University of Georgia, Athens, Georgia, March 31 and April 1, 1939. Dr. Detlev W. Bronk, Director of the Johnson Foundation for Medical Physics, University of Pennsylvania, has been invited to give a paper on the subject: "The Physical Basis of Biological Organization." A series of shorter invited papers also included on the program are: "Applications of Nuclear Physics to Biology," J. B. Fisk, University of North Carolina; "The Present Status of the Electron Microscope," Otto Stuhlman, Jr., University of North Carolina; "Applications of Photography to Medical and Biophysical Problems," Gilford G. Quarles, University of Alabama; "Purification of Biological Materials by Centrifuging," J. W. Beams, University of Virginia. In addition there will be a program of contributed papers. Dr. Clyde B. Crawley, University of Alabama is Chairman of the Biophysics Symposium.

### Commemoration Meeting

A meeting in commemoration of the life and work of Professor Elihu Thomson was held in the halls of the American Philosophical Society and the Franklin Institute of Philadelphia on Thursday, February 16. Nine papers, each dealing with a different phase of his life, were read by men who were closely associated with Professor Thomson during his lifetime.

The papers presented at the afternoon meeting in the Philosophical Society hall were:

Elihu Thomson, the Educator, by Vannevar Bush, President of the Carnegie Institution of Washington.

Elihu Thomson, His Interest in Research, by Dr. William D. Coolidge, Director of the research laboratory of the General Electric Company.

Elihu Thomson, the Electrical Engineer, by Professor Dugald C. Jackson, Professor Emeritus of Electrical Engineering, Massachusetts Institute of Technology.

Elihu Thomson, Inventor of 700 Patents, by Albert G. Davis, retired Vice President of General Electric and former manager of its patent department.

Elihu Thomson, His Interest in Astronomy, by Harlan T. Stetson, research associate, Massachusetts Institute of Technology.

Elihu Thomson, His Love of Nature, by Albert L. Rohrer, retired advisory engineer and close associate of Professor Thomson.

At the evening session in the Franklin Institute halls, the following papers were read:

The Philadelphia Period in the Life of Professor Thomson, by John L. Haney, President of the Boys Central High School in Philadelphia, where Professor Thomson as an instructor at the early age of 23 began his work of discovery and invention.

Elihu Thomson and the American Philosophical Society, by Roland S. Morris, President of the American Philosophical Society.

Elihu Thomson, the Scientist, by Dr. Karl T. Compton, President of Massachusetts Institute of Technology.

Following the papers a talking motion picture in which Professor Thomson was interviewed on some of his more important accomplishments by the late E. Wilbur Rice, Jr., former President of the General Electric Company, was shown. This picture was made on the lawn of Dr. Rice's home in Schenectady two or three years before Professor Thomson died.

★

### Detroit Physics Club

Dr. Charles Sheard, Director of the Physics Department of the Mayo Clinic, spoke at a joint meeting of the Detroit Physics Club and the Detroit Roentgen Ray and Radium Society on January 27, 1939, at Harper Hospital. His topic was "Some Applications of Physics to Biological and Medical Problems."

### Photoelasticity Conference

The ninth semi-annual Eastern Photoelasticity Conference will be held at Cornell University, Ithaca, N. Y., on Saturday, May 13. The Committee on local arrangements, of which Professor F. G. Switzer of the College of Engineering at Cornell is chairman, expects an attendance of approximately 100 scientific workers in this field, both from college faculties and from the research staffs of various industries. The program of technical papers will be supplemented by an exhibit of the latest equipment for photoelastic research, and demonstrations in the Cornell laboratories. A special program is being prepared for wives of those who attend the conference.

★

### Ohio Physics Club

The Ohio Academy of Science meets this year at Cincinnati, Ohio, on April 14 and 15. At that time The Ohio Physics Club will hold its customary joint session with The Academy.

★

### Necrology

Dr. Albert Sauveur, Emeritus Professor of Metallurgy and Metallography at Harvard University, died on January 26 at the age of seventy-five years.

★

### Calendar of Meetings

| | |
|---|---|
| **March** | |
| 31–April 1 | Pennsylvania Conference of College Physics Teachers, Gettysburg, Pa. |
| 31–April 1 | Southeastern Section, American Physical Society, Athens, Ga. |
| **April** | |
| 1 | New York State Section, American Physical Society, Clinton, N. Y. |
| 3–7 | American Chemical Society, Baltimore, Md. |
| 16–22 | American Ceramic Society, Chicago, Ill. |
| 19–22 | American Society of Civil Engineers, Chattanooga, Tenn. |
| 26–29 | Electrochemical Society, Columbus, Ohio. |
| 27–29 | American Physical Society, Washington, D. C. |
| **May** | |
| 15–17 | American Institute of Chemical Engineers, Akron, Ohio. |
| 16–17 | Acoustical Society of America, New York, N. Y. |
| 22–June 8 | World Automotive Engineering Congress, New York, Indianapolis, Detroit, San Francisco. |
| **June** | |
| 19–24 | American Association for the Advancement of Science, Milwaukee, Wis. |
| 23–24 | American Physical Society, Princeton, N. J. |
| 26–30 | American Society of Testing Materials, Atlantic City, N. J. |
| 28–30 | American Physical Society, Stanford University, Cal. |
| **July** | |
| 6–8 | Sixteenth Colloid Symposium, Stanford University, Calif. |
| 10–14 | American Society of Mechanical Engineers, San Francisco, Cal. |
| **September** | |
| 4–12 | International Congress of Mathematicians, Cambridge, Mass. |
| 4–15 | International Union of Geodesy and Geophysics, Washington, D. C. |
| 11–15 | American Chemical Society, Boston, Mass. |
| **December** | |
| 1–2 | American Physical Society, Chicago, Ill. |
| 27–Jan. 2 | American Association for the Advancement of Science, Columbus, Ohio. |

# New Books

**Modern Plastics.** Edited by E. F. LOUGEE. Pp. 304, 22×30 cm. Breskin and Charlton Publishing Corporation, New York City, 1938. Price $2.00.

The purpose of this volume is to review the progress made in all major branches of the plastics industry during the year preceding October, 1938. The principal sections are: (1) A foreword in which a statement as to the advances in plastics in Australia, England, France, Germany, Italy and the United States is given; (2) materials and methods in which specific processes are described; (3) machinery and equipment in which various molding machines and ovens are described; (4) laminated plastics; (5) bibliography and nomenclature; and (6) directory of manufacturers of material, equipment and molds, and also of industrial designers. A very useful chart is given of the physical properties of nearly all the common plastics in use. It seems as though the chart is by far the most useful part of this volume. The pages of the volume are interspersed throughout with advertising.

❧

**Elementary Survey of Physics.** ARTHUR E. HAAS and IRA M. FREEMAN. Pp. 203+x, Figs. 75, 13×20 cm. E. P. Dutton and Co., New York City, 1938. Price $1.90.

Those who believe that colleges should give cultural courses in physics will welcome the publication of this very brief and somewhat condensed textbook because of the daring that is exhibited in omitting a great deal of material that makes most books too involved for the nontechnical student. The problem as to what topics to omit is indeed perplexing and few will agree as to the solution. It seems to the writer that the authors have presented too many topics so that the treatment of important concepts is much to sketchy. For example, the distinction between mass and weight is dealt with in ten lines, Newton's first law of motion in six lines, momentum in two lines. As instances of the brief treatment often afforded to an important concept, the following references to kinetic energy are cited:

> "One-half the product of the mass by the square of the velocity is called the *kinetic energy* . . .
> Physicists use the *erg* as a unit of energy. It is the kinetic energy of a mass of two grams, moving with a velocity of one centimeter per second."

Would it not be better to treat this important topic more expansively, even if one omitted the discussion of the Coriolus force, Kepler's laws, lamellar flow and the vena cava?

The work is commendable in that the physics is generally reliable. However, one encounters again the oft-repeated statement that centrifugal force urges a body away from the center of the circle on which it moves. All of us will agree that a reaction force does not act *on* a body.

The nine-page supplement for pre-medical students gives a good discussion of topics such as the energy requirements of the body, sight and x-ray therapy. The material is not difficult to understand and is of sufficient general interest to merit inclusion in the body of the text.

This tightly-packed little book, free of mathematical equations and difficulties, may prove to be a useful tool in the hands of a skillful teacher.

OSWALD BLACKWOOD
*University of Pittsburgh*

❧

**A Text-Book on Crystal Physics.** W. A. WOOSTER. Pp. 295+xxii, Figs. 108, 13½×21½ cm. Macmillan, New York, 1938. Price $4.00.

As the first textbook in the English language that makes any pretense of developing the subject in a manner similar to that of Voigt's *Lehrbuch*, this small volume was examined apprehensively by the reviewer, but the succinctness detracts little from the lucidity. In attaining his objectives, "to present the classical treatment of the physical properties of crystals in terms of tensor notation and also to indicate the lines of development of modern theroetical and experimental research," the author chooses most of his material with commendable judgment. In addition to a condensed treatment of subjects to be found in Voigt, there are brief surveys of: plastic deformation and mechanical properties after the manner of the treatises of Houwink, Schmid and Boas, and Joffé; molecular susceptibilities of aromatic hydrocarbon crystals; Bridgman's analysis of thermoelectric effects; and problems in crystal optics. Numerous tables, appendixes and examples clarify the text.

The author's desire to point out errors in the literature is occasionally so insistent that the continuity suffers; e.g., the first half of the chapter on problems of crystal optics so lacks coherence and purpose that the reviewer questions its value.

It is unfortunate that the author did not examine some of his data more critically; the elastic modulus $s_{23}$ for Rochelle salt is given as $-5.0$, a value quite different from $s_{23}=16.5$ found by Mandell.* Tyndall's choice of elastic moduli for Zn are given without specific acknowledgment and discussion. Physicists will notice the omission of thermodynamics and temperature effects. The omission of Debye's treatment of specific heats is unwarranted in view of the importance of Grüneisen and Goen's work on the temperature variation of specific heats of crystals. The reviewer was surprised to find no mention of Kapitza's extensive studies on magnetic induction in crystals.

The book is one that can be read profitably by anyone desiring an introduction to the subject. Many instructors will feel the need of supplementing the text with additional reading or lectures for graduate students.

R. B. DOW
*The Pennsylvania State College*

* Mandell, Proc. Roy. Soc. **A116** (1927).

# Contributors to This Issue

Joseph Valasek received his Ph.D. degree in 1921 from the University of Minnesota where he is now Associate Professor of Physics. He is the author of an optics textbook and various articles on the electrical properties of crystals and in the field of x-ray spectroscopy.

Raymond D. Mindlin received his B.A. degree from Columbia University in 1928, his B.S. degree in engineering in 1931, his C.E. degree in 1932, and his Ph.D. degree in 1936. He was Research Assistant in the Department of Civil Engineering at Columbia University from 1932 to 1936, and has been Instructor in Civil Engineering since 1937.

John Euler Soehrens received his B.S. in Civil Engineering from Yale University in 1931 and his M.S. from the University of Colorado in 1938. He has been associated with the Connecticut State Highway Department and is at present with the Bureau of Reclamation where he has been directly connected with the construction of Boulder Dam.

*J. E. Soehrens*

J. H. A. Brahtz was born in Denmark and received his technical training at Royal Technical College, Copenhagen. He came to the United States in 1914 and became bridge engineer with the Minnesota Highway Department. From 1917 to 1929 he was consulting engineer on concrete and steel structures. From 1929 to 1933 he was research fellow at the California Institute of Technology where he received his Ph.D. Since 1933 he has been connected with the U. S. Bureau of Reclamation, establishing and directing the photoelastic laboratory and in charge of design studies.

Max M. Frocht took his B.S. in M.E. at the University of Michigan in 1922; M.S. in physics at the University of Pittsburgh in 1926 and Ph.D. at the University of Michigan in 1931. Dr. Frocht has been connected with the faculty of the Carnegie Institute of Technology since 1922 where he now holds the rank of Associate Professor of Mechanics. He is the co-author of a book on strength of materials with Professor N. C. Riggs and author of numerous papers dealing with researches in photoelasticity and strength of materials.

*J. Valasek*

*R. Mindlin*

*M. Frocht*

*J. Brahtz*

# KODACHROME PROFESSIONAL FILM

## *FULL-COLOR FILM IN CUT-SHEET FORM*

### TYPE B—for artificial illumination; and DAYLIGHT TYPE

KODACHROME PROFESSIONAL FILM combines the advantages of full-color photography with the simplicity in exposure of black-and-white film. The transparencies have neither screen pattern nor grain.

This new Kodachrome Film is particularly suitable for photomicrography. . .for full-color lantern slides. . .for all forms of reproduction in color for scientific purposes. It is available in the common sizes of cut-sheet film, and may be readily used in apparatus designed for black-and-white photography.

**EASTMAN KODAK COMPANY, ROCHESTER, N. Y.**

# THE WESTON

**Model 525**

## Projection Instrument

Here is the ideal instrument for lecture and demonstration work, and for industrial test and production applications. Inserted in a *lantern slide projector the scale and pointer can be projected to any desired size, and readily seen from any position in the room. It can be obtained with standard or special scales as an ammeter, voltmeter, decibel meter, foot-candle meter and others. » » » Full particulars on this new instrument are available and will gladly be sent on request. Weston Electrical Instrument Corp., 603 Frelinghuysen Ave., Newark, N. J.

**Other WESTON Instruments for laboratory and classroom use:*

Laboratory Standards
Portable Indicating Instruments
Panel Mounting Instruments
Instrument Transformers
Relays (sensitive and power)
Electric Tachometers
Standard Cells
Photoelectric Cells
Light Measuring Devices
Temperature Indicating Instruments
AC Clamp Ammeter

*The size of the instrument is 4-3/8" high, 1-5/64" thick, and 9-3/4" overall length.

# Innovations in Instruments

### Ultraviolet Arc

The General Electric Vapor Lamp Company announces a portable a.c. ultraviolet outfit which consists of a UA-26A2 tubular a.c. Uviarc, a special matte aluminum reflector, a stand and the special auxiliary transformer.

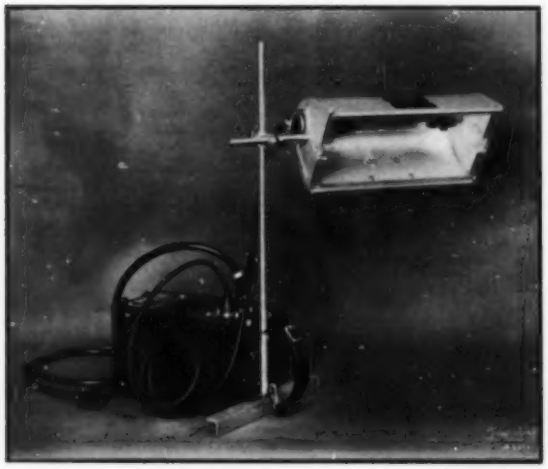

The Uviarc tube fits into clip contacts within the hood. The auxiliary transformer is equipped with brackets to support the stand on which the reflector hood is easily fastened with the clamp supplied. The hood may also be supported on a conventional laboratory ring stand. The reflector hood is designed to accommodate selective filters for fluorescence investigation or other special requirements. The outfit is completely wired with plug-in cords, and can be attached to standard 60-cycle a.c. convenience outlets.

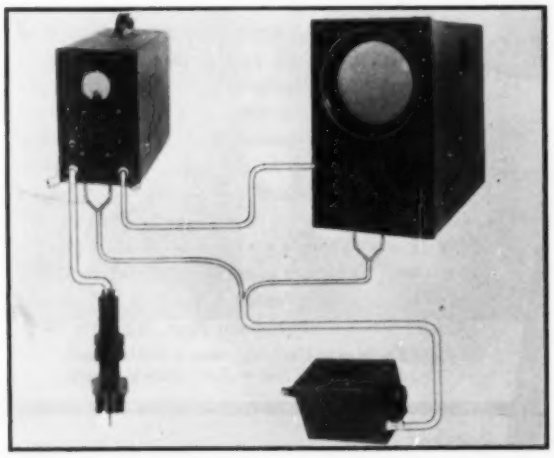

As a source of ultraviolet radiation this portable a.c. Uviarc combines unusual convenience and efficiency. The sealed mercury arc starts and operates without mechanical adjustments, and without the operating problems inherent to open arcs. On a regulated supply line, radiation output can be held constant to better than ±2 percent. The Uviarc retains high output characteristics throughout its rated average operating life of 2000 hours.

Ultraviolet radiation of fused Quartz mercury arcs per watt of electrical input exceeds that of other types of ultraviolet sources. Operating at 360 watts (out of an over-all input of 410 watts supplied to the transformer) the 6-in. Uviarc has an output made up as shown in Table I.

TABLE I. *Spectral analysis.*

| REGIONS (WAVE-LENGTH—A) | APPROXIMATE MICROWATTS PER SQ. CM AT 1 METER DISTANCE FROM LAMP. |
|---|---|
| 25,000–14,000 Far infra-red | 47 |
| 14,000–7,000 Near infra-red | 95 |
| 7,000–4,000 Visible | 299 (approx. 25 lumens per watt over-all) |
| 4,000–3,100 Near ultraviolet | 237 |
| 3,100–2,800 Middle ultraviolet | 91 |
| 2,800–1,850 Far ultraviolet | 193 |

### RCA Develops Electric Engine-Indicator Unit

For designers and manufacturers of high speed internal combustion engines the RCA Manufacturing Company has developed an electrically operated engine-indicator diagram equipment for accurate and dependable measurement of rapidly changing cylinder pressures.

Eliminating inaccuracies due to friction and inertia of mechanical indicating instruments, the RCA equipment assures instant sensitivity and ease of operation. It is composed of a pressure unit of revolutionary design, a cathode-ray oscillograph, an amplifier and a synchronizer unit.

The pressure unit, converts rapidly changing pressures into electrical impulses which are amplified and pictured on the screen of a cathode-ray tube. This is accomplished by transmitting these pressures to quartz crystals which, through their "piezoelectric" properties, generate on their surfaces electrical charges directly proportional to the pressures applied to them.

The unit, unaffected by temperatures up to 350°C and built to withstand pressures up to 5000 pounds per square

# FINE WIRES
## TAYLOR PROCESS

THE TAYLOR PROCESS is a method for making wires from substances which lack ductility. The elements or alloys, because the drawing is done in glass or quartz, are in a very pure state. Lengths of more than a few feet cannot be obtained. The wires may be had with or without the glass insulation. We make Taylor Process wire of Pt, Pd, Rh, Au, Ag, Cu, Fe, Co, Zn, Cd, Pb, Sb, Bi, Sn, Se, Te, Tl, Ga, and In, Constantan, Bi-Sn, Cd-Sb (used where large E.M.F. is desired) and many other alloys. Our wires are packed in containers holding one foot and, with few exceptions, the sizes are from one *mm* to one micron. We manufacture, too, fine wire by the Wollaston Method, by extrusion and by bare drawing.

*WE ARE SPECIALISTS IN PLATINUM AND CAN SUPPLY IT IN WHATEVER FORM YOU REQUIRE*

**BAKER & CO., INC.**

113 Astor Street, Newark, New Jersey

# STABILIZED A-C VOLTAGE

INPUT 95-130 volts
Instantaneous action
A magnetic unit

OUTPUT
115 volts ±1%
Stabilizes at any load within rating

No moving parts. Nothing to wear out.

*RAYTHEON Voltage Regulator*

**APPLICATIONS** Broadly it insures stable operation of all precision apparatus obtaining its power from an A.C. source, for example:—

- Insures constant brilliancy from all types of lamps.
- Improves the operation of X-ray equipment.
- Stabilizes all electronic apparatus.

*Write for Bulletin 48-71G4P.*

**RAYTHEON MFG. CO.** WALTHAM, MASS.

# EPPLEY THERMOPILES *for* RADIANT ENERGY MEASUREMENTS

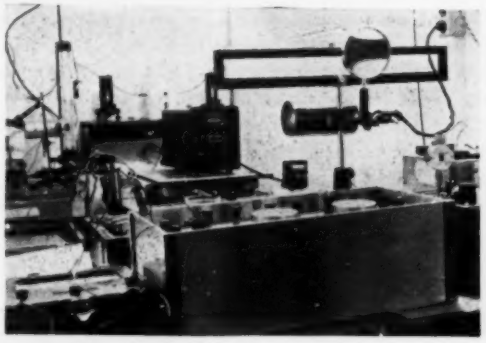

*A view of some of the apparatus used for calibrating thermopiles at the Eppley Laboratory, Inc.*

Adequate manufacturing, testing and calibrating equipment in the hands of our skilled and experienced technicians insures satisfaction to the users of Eppley Thermopiles.

We are prepared to furnish thermopiles of either bismuth-silver or copper-constantan, mounted in vacuum or air type cases. We also furnish thermopiles and mountings especially designed to meet individual needs. A card will bring you our Bulletin R–3 which contains illustrations, sample curves, complete descriptive matter, prices, references, etc., with regard to Eppley Thermopiles.

EPLAB

THE EPPLEY LABORATORY, INC.
SCIENTIFIC INSTRUMENTS
NEWPORT, R.I.
U.S.A.

**Innovations in Instruments (continued)**

inch, consists of two quartz crystals mounted in a stainless-steel holder designed for insertion into a threaded hole in the cylinder head. A piston at the lower end of the holder receives pressures within the cylinder and transmits them directly to the crystals. A diaphragm holds the piston in place, at the same time permitting it to transmit pressure variations to the crystals.

Electrical charges exactly proportional to the pressures are imparted to an electrode between the crystals and then conducted to an output cable. The charges, besides being in exact proportion to the pressures, vary instantly with pressure variations. Accuracy of the unit is high at engine speeds of over 1000 r.p.m. on four-cycle engines. For engine speeds under 500 r.p.m., the unit is not recommended.

Outstanding features of the engine-indicator diagram equipment include; easy tracing of pressure curves of any form of dynamic pressure; simple and accurate orientation of any point on the diagram with respect to the crank-shaft angle; simple electrical calibration of pressure at any point in the pressure diagram; and flexibility of the system, permitting observation of complete engine-cycles in a single curve, or detailed study of any portion of a cycle.

### New Permanent Magnet

A magnet that will lift nearly 1500 times its own weight has been developed in the Research Laboratory of the General Electric Company by W. E. McKibben. The magnet weighs 1.85 grams, 1/250th of a pound, and has been made to lift 2750 grams in tests. About half the size of an eraser on the end of a pencil, it will lift a five-pound flatiron with ease. The new magnet is several times as strong as those previously made. The magnet is made of material known as Alnico, an alloy of aluminum, nickel, cobalt and iron. It was first developed as a heat-resisting alloy which resisted scaling and deterioration at high temperatures. Research on the magnetic properties of alloys of this type was later carried on by Professor T. Mishima of the Imperial University, Tokyo, and General Electric perfected a process of heat treating by which the magnetic properties were more fully developed. The new magnet employs the same alloy as previously used, but utilizes a steel sheath around the Alnico pellet to direct the magnetic flux against the keeper or object being attracted. The steel jacket also protects the magnet against demagnetization when not in use.

### New Temperature Indicator

Ample space for toggle-type switches, for connecting any one of a number of couples to the measuring circuit, is provided in a new temperature indicator made by the Leeds & Northrup Company, 4934 Stenton Avenue, Philadelphia, Pennsylvania. Installed wherever convenient, it enables an operator to measure temperatures of near or distant couples with equal reliability, by simply turning a knob, until a pointer comes to zero, and reading a temperature scale.

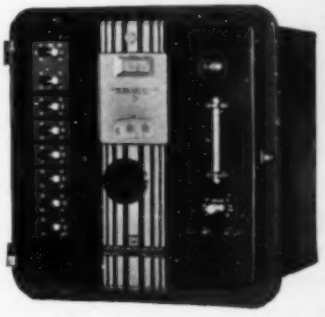

Use of a potentiometer measuring circuit—hand-standardized, but with automatic reference-junction compensation—eliminates uncertainties due to circuit-resistance variables. Scale is practically uniform and equally accurate throughout, and can be calibrated for single or double range, the latter for use with similar or different couples. Built-in terminals, check key and mercury thermometer can be included for checking with a portable indicator.

"APIEZON"
OILS, GREASES and WAXES
*for high vacuum work*
*have vapor pressures as low as $10^{-6}$ mm. of Hg, and even unmeasurable at room temperature.*

THE Apiezon products which we now carry in our Philadelphia stock, include special oils for oil-diffusion vacuum pumps, and a variety of oils, greases and waxes for sealing joints and stop-cocks in high vacuum systems. Bulletin 1565-R listing physical characteristics and prices will be forwarded upon request.

JAMES G. BIDDLE CO.
ELECTRICAL AND SCIENTIFIC INSTRUMENTS
1211-13 ARCH STREET. PHILADELPHIA, PA.

# HARSHAW SYNTHETIC CRYSTAL OPTICS

. . . open new fields in ultraviolet and infrared spectroscopy. . . . Single crystals are synthetically grown from pure molten salts. . . . Harshaw's unique process makes available large crystals of Lithium Fluoride, Sodium Chloride (Rock Salt), and Potassium Bromide—and for polarizing optics, Sodium Nitrate. . . . Write for information.

**THE HARSHAW CHEMICAL CO.**
SPECIAL PRODUCTS DIVISION
CLEVELAND, OHIO

## GRID-CONTROL RECTIFIER

Type EL C6J
Xenon gas filled

| | |
|---|---|
| Amperes Output | |
| Average ..... | 6.4 |
| Peak ..... | 77 |
| Peak Forward Volts | 750 |
| Peak Inverse Volts. | 1250 |
| Average Arc Drop. | 9 |
| Filament | |
| Volts ..... | 2.5 |
| Amperes ..... | 18 |
| Overall Dimensions. | 2 x 9" |
| Price ..... | $23.50 |

ELECTRONS, INC.
127 SUSSEX AVENUE
NEWARK, N. J.

MEETING SPECIAL REQUIREMENTS
BELLOWS WITH SILVER SOLDERED JOINTS FOR HIGH-TEMPERATURE WORK

## Metallic Bellows

HYDRON Metallic Bellows are used as control elements in temperature-and-pressure-control devices, and for liquid or gas seals of compressors and pumps. We are specialists in the design and production of complete thermostatic and pressure units for temperature and pressure controls. We are, therefore, prepared to extend the fullest co-operation to engineering departments of control manufacturers in the solution of design and engineering problems.

Write for 44 page ENGINEERS' DATA BOOK

**CLIFFORD MANUFACTURING CO.**
564 E. FIRST STREET, BOSTON
BOSTON CHICAGO DETROIT LOS ANGELES
PRODUCERS OF BELLOWS EXCLUSIVELY
SERVING AUTOMATIC CONTROL MANUFACTURERS

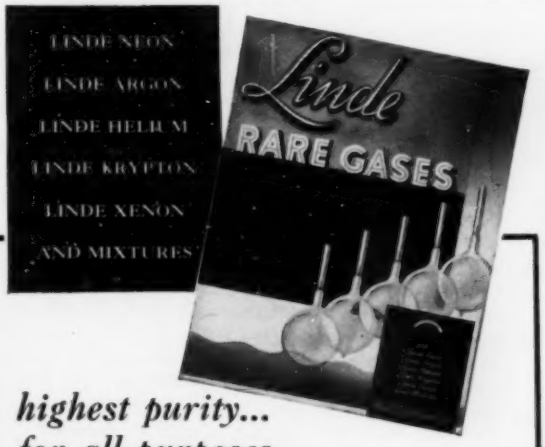


*highest purity... for all purposes*

Linde Rare Gases and Linde Rare Gas Mixtures are available for the study of electrical discharges, for use in rectifying and stroboscopic devices, and in inert atmospheres where heat conduction must be reduced. Additionally, the facilities of Linde laboratories are available for the preparation of special mixtures for experimental uses. Write any Linde office for folder and full information about Linde Rare Gases.

The word "Linde" used herein is a registered trade-mark.

**THE LINDE AIR PRODUCTS COMPANY**
*Unit of Union Carbide and Carbon Corporation*
NEW YORK AND UCC PRINCIPAL CITIES
THE WORLD'S LARGEST PRODUCER OF OXYGEN AND OTHER GASES OBTAINABLE FROM AIR

# RECENT BOOKLETS ON INSTRUMENTS AND MATERIALS

For the convenience of our readers we list these booklets with a key number for each publication. A coupon is supplied at the bottom of the page. If you wish several booklets, jot down the key numbers on the coupon or a postcard, together with your full business address, and mail to this journal and we will have them sent to you.

**81. Laboratory Instruments—Chemical & Biological.** AMERICAN INSTRUMENT COMPANY, *8010 Georgia Avenue, Silver Spring, Md.* Catalog 39. Pp. 108, illustrated, 21¼×28 cm.

**82. Cenco News Chats, No. 22, February, 1939.** CENTRAL SCIENTIFIC COMPANY, *1700 Irving Park Boulevard, Chicago, Ill.* An illustrated bi-monthly publication showing new developments in laboratory apparatus. Pp. 24, 19½×27¼ cm.

**83. Elliot Stencil File No. 960.** HENRY W. ELLIOT, *2067 Broadway, New York, N. Y.* (Describes unique file for preserving technical data mimeograph stencils.) Leaflet. P. 1, illustrated, 34×21½ cm.

**84. The General Radio Experimenter,** Vol. XXII, No. 9. GENERAL RADIO COMPANY, *30 State Street, Cambridge, Mass.* This issue describes "A-C Operated Direct-Current Amplifier for Industrial Use", also "An Analyzer for Noise Measurement." Pp. 12, illustrated, 15×28 cm.

**85. Uviarc Portable A. C. Ultra-Violet Outfit.** GENERAL ELECTRIC VAPOR LAMP COMPANY, *Hoboken, N. J.* (Portable, self starting fused quartz mercury arc.) Bulletin No. 112. Pp. 4, illustrated, 21×28 cm.

**86. Fluorescence with the NiCo Lamp.** GENERAL ELECTRIC VAPOR LAMP COMPANY, *Hoboken, N. J.* (Applications of Fluorescence.) Booklet. Pp. 12, illustrated, 21½×28 cm.

**87. Inco, Vol. 16, No. 2. Winter Edition 1938-1939.** INTERNATIONAL NICKEL COMPANY, Inc., *67 Wall Street, New York, N. Y.* (A quarterly magazine devoted to the uses of nickel and nickel alloy.) Pp. 36, illustrated, 22×29½ cm.

**88. Linde Rare Gases.** THE LINDE AIR PRODUCTS COMPANY, *205 East 42nd Street, New York, N. Y.* Booklet. Pp. 4, illustrated in full color, 21½×28 cm.

**89. Panel Instruments.** ROLLER-SMITH COMPANY, *Bethlehem, Pa.* Catalog 48-a. (On ammeters, voltmeters and pyrometers, etc.) Pp. 8, illustrated, 21½×28 cm.

**90. Weston Photoelectric Cells.** WESTON ELECTRICAL INSTRUMENT CORP., *Newark, N. J.* Circular B-2-B. Pp. 4, illustrations and charts, 21½×28 cm.

## Photoelasticity

**The following booklets and leaflets are available on the subject of this issue, for instruments and publications.**

**91. Photoelasticity Polariscopes.** THE GAERTNER SCIENTIFIC CORPORATION, *1212 Wrightwood Avenue, Chicago, Ill.* Bulletin 143. Pp. 4, illustrated, 21½×28 cm.

**92. Polaroid—for Stress Determination.** THE POLARIZING INSTRUMENT COMPANY, *632 Fifth Avenue, New York, N. Y.* (Large aperture photoelastic polariscope and straining frame for photoelastic analysis.) Leaflet. Pp. 2, illustrated, 21×28 cm.

**93. The Place of Photoelasticity in Engineering Instruction—Engineering Bulletin by Carnegie Institute of Technology.** Supplied by THE POLARIZING INSTRUMENT COMPANY, *632 Fifth Avenue, New York, N. Y.* Pp. 16, illustrated, 15×28 cm.

**94.** Contents and description of Book—**Contributions to the Mechanics of Solids.** THE MACMILLAN COMPANY, *60 Fifth Avenue, New York, N. Y.* Leaflet. Pp. 2, illustrated, 21½×28 cm.

**95.** Contents and description of Book—**Strength of Materials by Riggs and Frocht.** THE RONALD PRESS COMPANY, *15 East 26th Street, New York, N. Y.* Leaflet. Pp. 2, 20×25 cm.

**96.** Contents and description of Book—**A Treatise on Photo-Elasticity by Coker and Filon.** CAMBRIDGE UNIVERSITY PRESS, *60 Fifth Avenue, New York, N. Y.* Leaflet. Pp. 2, 21×28 cm.

**97. Applied Elasticity by John Prescott.** LONGMANS, GREEN AND COMPANY, *114 Fifth Avenue, New York, N. Y.* (Described in Catalog "Science Textbooks and Reference Works—1939.") Pp. 100, 13½×20½ cm.

JOURNAL OF APPLIED PHYSICS
175 FIFTH AVENUE, NEW YORK, N. Y.

*Please send me the booklets listed by key numbers below:*

..... ..... ..... ..... ..... ..... ..... ..... ..... ..... ..... ..... ..... ..... ..... ..... ..... ..... ..... .....

**Name**..... **Title**.....

**Business connection**.....

**Address**..... **Place**.....

## POLAROID*
### *for* Stress Determination

**Large Aperture Photoelastic Polariscope**

Large aperture Polaroid and quarter wave plates make possible this apparatus designed primarily for photoelastic investigation. Simplicity of construction brings this type of apparatus down to a reasonable price level. Send for bulletin.

**Polarizing Instrument Co.**
632 FIFTH AVENUE
NEW YORK

*T.M. Reg. U. S. Pat. Off. by Polaroid Corp.

***FREE***
Send for Interesting Literature

## *IMPROVED "SPOTLIGHT" GALVANOMETERS*

**Rubicon MULTIPLE REFLECTION galvanometers have recently been improved through a redesign of the optical system. The definition of the line-image is now so sharp that readings can be estimated to .1 of a millimeter division.**

**These sturdy, self-contained galvanometers are available with sensitivities as high as .0006 microampere per millimeter. The scales, which are 100 mm. long, are remarkably proportional. Send for Bulletin 320.**

**RUBICON COMPANY**
*ELECTRICAL INSTRUMENT MAKERS*
29 North Sixth Street Philadelphia, Pa.

# JOURNAL OF SCIENTIFIC INSTRUMENTS

**A MONTHLY PUBLICATION DEALING WITH THEIR PRINCIPLES, CONSTRUCTION AND USE AND THE APPLICATION OF PHYSICS IN INDUSTRY**

**Produced by the Institute of Physics with the Co-operation of the National Physical Laboratory**

CONTENTS

Special Articles dealing with the Trend of Development of various classes of Instruments, Working Processes, and with Matters of General Interest to Manufacturers.
*By Recognised Authorities.*

Contributed Papers on New Methods and Apparatus.
*By Workers in every Branch of Science and Manufacture.*

New Instruments Section: the scope includes
Physics and Chemistry
Optics and Surveying
Meteorology and Metrology
Electrical and Mechanical Engineering
Physiology and Medicine.

Laboratory and Workshop Notes, Correspondence, New Books, Catalogues, Notes and Comments, and Institute Notes are also included.

**The subscription rate for a yearly volume is £ 1.10.0 net (post free) payable in advance. Separate parts 2s.8d. (post free). Subscriptions should be sent to the publishers.**

**THE INSTITUTE OF PHYSICS**
1 LOWTHER GARDENS, EXHIBITION ROAD, LONDON, S.W.7 ENGLAND

# Associates

THE American Institute of Physics gratefully acknowledges the continuing support in 1939 of the following Associates of the Institute:

*Agfa Ansco Corporation*
*Allegheny Steel Company*
*Aluminum Company of America*
*American Telephone and Telegraph Company*
*Bausch & Lomb Optical Company*
*Bell Telephone Laboratories*
*Crane Company*
*Dow Chemical Company*
*E. I. du Pont de Nemours & Company*
*Eastman Kodak Company*
*General Electric Company*
*General Motors Corporation*
*Gulf Research & Development Company*
*Libbey-Owens-Ford Glass Company*
*Loomis Laboratory*
*Massachusetts Institute of Technology, Department of Physics*
*Massachusetts Institute of Technology, Division of Industrial Cooperation*
*Research Corporation*
*Shell Development Company*
*Sperry Gyroscope Company, Inc.*
*Westinghouse Electric & Manufacturing Company*

These Associates are contributing materially to the vigorous advance of pure and applied physics. A large part of their corporate dues is used to provide more pages for the recording of the results of research in the periodicals published by the Institute for the Founder Societies. Another part is devoted to the Institute's efforts to improve the opportunities and facilities for physical research in America through better public appreciation of the nature and importance of the science. The remainder helps provide for general work and special projects undertaken for the Founder Societies acting in cooperation through the Institute and designed to further those objects which the Societies have in common.

The American Institute of Physics cordially invites other interested corporations to become its Associates and will welcome their inquiries addressed to

The Director
American Institute of Physics
175 Fifth Avenue, New York, New York

# S. S. WHITE
MOLDED
# RESISTORS
1,000 Ohms
to
1,000,000 Megohms

**NOISE TESTED** At slight additional cost, resistors will be supplied individually "noise-tested" to this specification: "For the complete audio frequency range, resistors shall have less noise than corresponds to 1 part in 1,000,000." (For values up to 10 megohms.)

NOISELESS in operation
NON-HYGROSCOPIC Material
STRONG and DURABLE
DESCRIPTIVE CIRCULAR mailed on request

**S. S. WHITE**
The S. S. White Dental Mfg. Co.
**INDUSTRIAL DIVISION**
Department B, 10 East 40th St., New York, N. Y.

# NEW RCA BEAT FREQUENCY OSCILLATOR

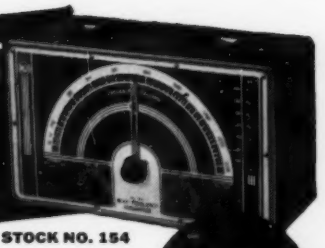

STOCK NO. 154

**$49.95 NET**

**Provides a variable frequency source of alternating current from 30 to 15,000 C. P. S.**

For fidelity checking of audio amplifiers and radio receivers, this fine audio oscillator will be found unexcelled. It also may be used as a source of a-c for making bridge measurements where low distortion is required and several frequencies desirable. In conjunction with a stroboscope, it is useful for checking speeds of moving mechanical parts. As a sweep frequency for a Cathode Ray Oscillograph, it gives accurate measurements of vibration frequencies when used with the RCA Vibration Pickup. There are many other diversified applications.

**SPECIFICATIONS**

*Output Frequency*
30-15,000 cycles (1 db from 30 to 10,000 cycles, down 2 db at 15,000 cycles)
*Output Voltage*
Open circuit, 37.5 volts; 5000 ohm load, 25 volts; 500 ohm load, 7.5 volts; 250 ohm load, 5.2 volts.
*Power Output* . . . . . 125 milliwatts
*Distortion*
less than 5% rms over entire range

Full information may be obtained from all RCA Parts Distributors or by writing to the address below.

*Listen to the Magic Key of RCA every Sunday, 2 to 3 P.M., E.S.T., on NBC Blue Network.*
For finer radio performance . . . RCA Radio Tubes.

RCA *Test Equipment*
RCA MANUFACTURING COMPANY, INC., CAMDEN, NEW JERSEY
A SERVICE OF THE RADIO CORPORATION OF AMERICA

# REPORTS ON
# PROGRESS IN PHYSICS
## VOLUME V (1938)

*445 pages: Illustrated* *$5.00 post free* *Bound in cloth*

A COMPREHENSIVE REVIEW
by leading physicists and under the general editorship of Prof. Allan Ferguson

THE CONTENTS INCLUDE CHAPTERS ON

ABSOLUTE ELECTRICAL MEASUREMENTS
PLASTICS IN INDUSTRIAL PHYSICS
AIDS FOR DEFECTIVE HEARING
TEACHING OF PHYSICS IN SCHOOLS
X-RAYS AND γ-RAYS IN MEDICINE
ELECTRIC WAVE FILTERS
THE GEIGER COUNTER
QUANTUM MECHANICS
THE LIQUID STATE
SOFT X-RAY SPECTROSCOPY OF THE SOLID STATE
ATOMIC PHYSICS
SOUND
ASTRONOMY
METEOROLOGY
HEAT
OPTICS
SPECTROSCOPY
ELASTICITY
SURFACE TENSION
VISCOSITY

*Orders, with remittance, to*
**The Physical Society, 1 Lowther Gardens, Exhibition Road, London, S.W.7, England.**

# INDEX TO ADVERTISERS


| Name | Page |
|---|---|
| AJAX ELECTROTHERMIC CORP. — Ajax-Northrup high frequency electric furnaces from laboratory to plant sizes. | iii |
| BAKER & CO., INC. — Platinum crucibles, dishes, triangles, filter cones, anodes, cathodes, electrodes, platinum tipped crucible tongs, fine wires and bismuth foil. | ix |
| JAMES G. BIDDLE COMPANY — "Jagabi" Rheostats; Adam Hilger and Kipp & Zonen Optical Instruments; "Pointolite" Lamps; Electrical Testing and Speed-measuring Instruments. | x |
| P. BLAKISTON'S SON & CO., INC. | ii |
| CENTRAL SCIENTIFIC COMPANY — Manufacturers of Cenco Physical Apparatus and Instruments to meet all requirements of University, College and High School Physics Laboratories. Specializing in high vacuum pumps and development of instruments and apparatus for various sciences. | Cover 4 |
| CLIFFORD MFG. CO. — Hydron metallic bellows for temperature and pressure control devices. Data for engineers. | xi |
| EASTMAN KODAK COMPANY — Purified Organic Chemicals for research purposes; Plates for Photography, Photomicrography, Spectroscopy, Photometry, Astronomy; Wratten Light Filters; Cameras and Films. | vii |
| ELECTRONS, INC. — Gas-filled rectifier and grid-control rectifier tubes. 0.15 to 50 amperes, 12 to 1500 volts. | xi |
| THE EPPLEY LABORATORY, INC. — Standards of e.m.f. (standard cells). Precision electrical instruments; potentiometers, bridges, temperature bridges, volt boxes. Thermopiles and pyrheliometers. | ix |
| GAERTNER SCIENTIFIC CORP. — Spectroscopes, Spectrometers, Spectrographs, Spectrophotometers, Heliostats, Measuring Microscopes, Comparators, Cathetometers, Reading Telescopes, Interferometers, Chronographs, Dividing Machines, etc. | ii |
| GENERAL ELECTRIC VAPOR LAMP CO. — Uviarc lamp for ultraviolet radiation. Sodium Lab-Arc Lamp. | vi |
| GENERAL RADIO COMPANY — Manufacturers of electronic measuring instruments; vacuum-tube voltmeters, amplifiers and oscillators; wave analyzers, noise meters and analyzers, stroboscopes; laboratory standards of capacitance, inductance and frequency; impedance bridges, decade resistors and condensers; air condensers and variable inductors; rheostats, Variacs, transformers; other laboratory accessories. | Cover 3 |
| HARSHAW CHEMICAL CO. — Optical Lithium Fluoride grown in single crystal to predetermined size. Industrial Chemicals. | xi |
| INTERNATIONAL RESISTANCE COMPANY — Manufacturers of metallized and wirewound fixed and variable Resistors including high voltage and high frequency types. | iv |
| JOURNAL OF SCIENTIFIC INSTRUMENTS | xiii |
| LEEDS & NORTHRUP COMPANY — Manufacturers of Galvanometers, Resistors, Bridges, Condensers, Inductances, Potentiometers, Testing Sets; Temperature Measuring, Recording and Controlling Apparatus; Instruments for Measuring and Controlling Conductivity of Electrolytes and Hydrogen Ion Concentrations. | i |
| LINDE AIR PRODUCTS CO. — Oxygen, Argon, Helium, Krypton, Neon, Xenon, Rare Gas Mixtures, Nitrogen, Hydrogen, Calcium Carbide, Acetylene, equipment for Oxy-Acetylene welding and cutting. | xi |
| MCGRAW-HILL BOOK CO., INC. | v |
| PHYSICAL SOCIETY (LONDON) | xv |
| POLARIZING INSTRUMENT COMPANY — Polaroid Desk Lamp. Polarizing Microscope Attachment, Polarizing Projection Equipment. Polaroid Film. | xiii |


## INDEX—*Continued*


| Name | Page |
|---|---|
| RAYTHEON MFG. CO. — Voltage stabilizers and regulators. Electrical measurement and control instruments. | ix |
| RCA MANUFACTURING CO., INC. — RCA Oscillators and Oscillographs, RCA Test Equipment, RCA Ultra-Sensitive DC Meter. | xv |
| RUBICON COMPANY — Galvanometers, electrometers, potentiometers, Wheatstone and Kelvin bridges, resistance boxes, hydrogen ion and conductivity apparatus. | xiii |
| W. M. WELCH SCIENTIFIC CO. — Scientific instruments—laboratory apparatus. Catalog lists 10,000 items. | iv |
| WESTON ELECTRICAL INSTRUMENT CO. — Industrial temperature gauges, photographic exposure meters, electrical measurement instruments. | vii |
| S. S. WHITE DENTAL MFG. CO. — Resistors, 1000 ohms to 1,000,000 megohms. | xv |


# POSITION WANTED

Young man, single, Anglo-Saxon, age 24. B.S., M.S., Ph.D. Physics. Trained in Physical Chemistry. Research experience. Spectroscopy. Address Box L3-6. Rm. 1502, 175 Fifth Ave., New York, N. Y.

Classified advertisements are accepted under these three headings: Employment, Want to Purchase and Educational Institutions. The rate is 75c per line (six words average) and minimum is three lines.


# *Back Issues*

of these journals are available.

| | Single Copy |
|---|---|
| **Journal of Applied Physics** | $ .70 |
| **Review of Scientific Instruments** | .50 |
| **Physical Review (from July 1929)** | .75 |
| **Same (before July 1929)** | 1.50 |
| **Reviews of Modern Physics** | 1.20 |
| **Same April 1936** | 1.75 |
| **Journal of Chemical Physics** | 1.00 |
| **Journal of the Optical Society** | .60 |
| **Journal of the Acoustical Society** | 1.80 |
| **American Physics Teacher (from 1937)** | 1.00 |
| **Same (before 1937)** | 1.50 |

***Special prices for complete back volumes and complete sets.***

Orders may be sent to

**American Institute of Physics**

175 Fifth Avenue
New York, N. Y.